Instant Foam Physics

Formation and Stability of Aerosol Whipped Cream

M.E. Wijnen

Instant Foam Physics

Formation and Stability of Aerosol Whipped Cream

Proefschrift
ter verkrijging van de graad van doctor
op gezag van de rector magnificus
van de Landbouwuniversiteit Wageningen
dr. C.M. Karssen,
in het openbaar te verdedigen
op woensdag 11 juni 1997
des namiddags te 13.30 uur in de aula

BIBLIOTHEEK
LANDBOUWUNIVERSITEIT
WAGENINGEN

Cover: Bert Groeneveld

Stellingen

---

1   De populariteit van instant producten, zoals spuitroom, geeft aan dat consumenten soms bereid zijn het gemak boven de kwaliteit te stellen.

2   De beginopslag van spuitroom wordt bepaald door de hoeveelheid gas die in de room is opgelost voor het product het ventiel instroomt.
    Dit proefschrift.

3   Spuitroom dankt zijn stevigheid aan de hoge volumefractie gas in het schuim.
    Dit proefschrift.

4   Het botert niet goed tussen de vetbolletjes in spuitroom.

5   Het stromingsproces van spuitroom uit de spuitbus wordt voor een belangrijk deel gereguleerd door "choking" condities in het ventiel.
    Dit proefschrift.

6   De oppervlaktereologische eigenschappen van spuitroom zijn niet in staat om disproportionering, welke wordt bevorderd door de hoge oplosbaarheid van lachgas in de room, te stoppen. Dit verklaart de slechte schuimstabiliteit van spuitroom.
    Dit proefschrift.

7   Om tot een beter vergelijkbare beoordeling van het werk van AIO's te komen hoort, naast de totale aanstellingsduur, ook de verhouding tussen de onderwijsbelasting en onderzoeksbelasting voor alle AIO's gelijk te zijn.

8   Het invoeren van probleemgestuurd onderwijs aan universiteiten versoepelt de overgang naar het probleemgeoriënteerd werken van AIO's.

9   Het belang van de toepassing van wiskunde in andere vakgebieden wordt vaak onderschat.

10 De toename van het aantal luchtige toetjes in de winkel bewijst dat er met handel in lucht nog steeds geld te verdienen is.

11   Voorgeverfde staalplaat wordt gebruikt in bijvoorbeeld omkastingen van koelkasten, kroonkurken en jampotdeksels. Wanneer een coating van kunststoffolie zou worden gebruikt in plaats van verf, zou het voorbeklede product niet alleen milieuvriendelijker zijn maar kan het bovendien gemakkelijker worden gevormd tot een eindproduct zonder dat de 'verf' scheurt.

12   Het ontwikkelen van alternatieven voor dierproeven mag niet meer dieren kosten dan de uitvoering van de (klassieke) dierproef zou doen gedurende vele jaren.
M.D.O. van der Kamp, Ways of Replacing, Reducing or Refining the Use of Animals in the Quality Control of Veterinary Vaccines, ID-DLO rapport, Lelystad, 1994.

13   Het enige product waarvan men zeker kan zijn dat het dagvers in de supermarkt ligt, is een dagblad.

14   De slechte schuimstabiliteit van spuitroom is een luxe probleem.

Stellingen behorende bij het proefschrift "Instant Foam Physics; Formation and Stability of Aerosol Whipped Cream" door M.E. Wijnen. Wageningen, 11 juni 1997.

voor mijn ouders

Abstract

The formation and stability of aerosol whipped cream, as an example of an instant foam, were studied from a physical point of view. Instant foam production out of an aerosol can is based on the principle that a soluble gas (laughing gas) is dissolved under elevated pressure (5-10 bar) in the product (cream). By opening the nozzle of the can the product is allowed to leave the can. The resulting decrease in pressure causes the gas to come out of the cream and a foam is formed.
Formation of the foam occurs in the smallest opening of the nozzle. Here, the velocity is limited to the speed of sound in the foam, which indicates that the flow through the nozzle is controlled by choking conditions. These conditions determine apart from the velocity also the density and pressure of the aerated cream in the nozzle. The whole process of instant foam formation is therefore regulated by the physics of choking.
Aerosol whipped cream is characterised by a high overrun (400-600%) which provides firmness to the close-packed foam. The overrun is determined by the amount of laughing gas (nitrous oxide) dissolved in the cream. Since the pressure in an aerosol can knows practical limits, a high solubility of the gas in the cream is required to ensure that a sufficient amount of gas is dissolved. However, this high solubility enhances the process of disproportionation. Disproportionation involves gas diffusion from smaller to larger bubbles and out of the foam, which negatively affects the foam stability. Cream showed not to have the surface rheological properties that are required to stop this destabilisation process. This explains the fast deterioration of the product. Obviously, optimising the foam properties of aerosol whipped cream involves several compromises.

Contents

Chapter 1

General introduction

1.1 Introduction

Over the past few years consumers show an increasing interest in instant food products. The term instant is used in relation to products which, compared to an analogous product, are prepared relatively quick and easy. Among these food products are some instant foams. This thesis presents a search for physical knowledge about instant foam behaviour. The study mainly focuses on aerosol whipped cream, as an example of an instant foam. It is however important to note that the various phenomena that are discussed in this thesis are more broadly applicable.

In the present chapter several methods to make an instant foam are first described. Because the study applies to aerosol whipped cream, some general information about the foam properties of this product is also given. Aerosol whipped cream can be seen as an instant substitute for whipped fresh cream. Of these two, the former is more convenient to use because relatively small portions can be produced at a time. Moreover, aerosol whipped cream can be formed within a few seconds, whereas whipped fresh cream takes a few minutes to prepare. Since these two products are often compared, some aspects of foam behaviour of whipped fresh cream are described in more detail and the most important differences from aerosol whipped cream are discussed. Finally, the aim and outline of this thesis are given.

1.2 Process of instant foam formation

A foam is a dispersion of gas bubbles in a liquid. In general, there are several methods to make a foam (Dickinson, 1992; Prins, 1988; Walstra, 1989). Firstly, foams can be produced by agitation of a mixture of a given amount of liquid and an unlimited amount of available gas. A commonly used form of this method is whipping a liquid. Here, gas is entrapped in the liquid as large bubbles which are successively broken down into smaller ones by mechanical forces. Instant foams produced in this way are for example desserts which are aerated by whipping a powder mix, after addition of an indicated amount of liquid, during a few minutes (Mansvelt, 1976). Some toppings, spray-dried whippable emulsions, are prepared

analogously to the instant desserts and can be used as a substitute for whipped fresh cream. More information about these toppings can be found in the literature (Barford and Krog, 1987; Buchheim et al., 1985; Kieseker et al., 1979; Knightly, 1968; Krog et al., 1987; Tanaka et al., 1973).

A second method to make a foam also involves agitation. Contrary to the first method, in this case the required amount of gas can be dosed. An example of this method, which is frequently used in continuous processes in industry, is injection of gas into a liquid, often through orifices. The bubbles can be reduced in size later in the process by means of, for example, a dasher or a static mixer. Kikuchi et al. (1995) described a continuous whipping system for the production of whipped cream which works according to this principle.

Thirdly, foam can be produced by generation of gas bubbles in a liquid. These bubbles can be formed in situ when the liquid is saturated with gas and additional gas is generated, for example by yeast cells during the bread making process. Bubbles can also be formed out of with gas supersaturated liquid by means of heterogeneous nucleation. This occurs during the foam formation of carbonated beverages and aerosol whipped cream, where gas has been dissolved under pressure in the liquid, when the pressure is released.

In the present study the physics of instant foam behaviour of aerosol whipped cream is extensively studied. Besides the aerosol can, a newly developed apparatus, the Aerosol Can Simulator (ACS), is used to produce an instant foam under standardised conditions. This continuous method is a combination of the second and the third method of foam formation described before. Analogous to the second method, gas is injected into the cream after which the mixture passes through a static mixer. Due to the elevated pressure in the apparatus, in combination with the agitation in the mixer, the gas dissolves in the cream. Similar to the third method of foam formation mentioned before, the foam results from a decrease in pressure as the product leaves the apparatus. The working principle of the ACS is described in more detail in chapter 3.

1.3   Aerosol whipped cream

The term aerosol *whipped* cream refers to a foamed cream that is produced by means of an aerosol can. It is the most important food product that is retailed from an aerosol can (Peter, 1971; Werner, 1970). The production of instant whipped cream was already described in 1936 (Getz et al.). Besides an aerosol can, a repeatedly used syphon, with gas recharged from cartridges, can be used to produce a foam analogous to aerosol whipped cream (Lang and Lang, 1975).

Although some information on aerosol whipped cream is given in the general dairy literature (Graf and Bauer, 1976; Mulder and Walstra, 1974; Varnam and Sutherland, 1994), hardly any fundamental research concerning the foaming process of aerosol cream was found to be published so far.

In practice, both products are made from dairy (natural) cream and non-dairy cream. Non-dairy whipped creams, also called toppings, generally contain vegetable fats (Anon, 1970; Pader and Gershon, 1965; Takada and Kanda, 1984). In the present study only dairy creams are considered. This section describes the stages from unwhipped cream in the aerosol can to the resulting foamed product.

Aerosol whipping cream

The unfoamed cream present in an aerosol can is called aerosol *whipping* cream. Before the cream, which may vary in fat content, enters the aerosol can, it undergoes some treatment. Firstly, it is UHT (Ultra High Temperature) processed, which allows sterilisation of the cream with minimum heat damage (Kieseker and Zadow, 1973b). This heat treatment extends the shelf life of the product.

After the heating process, the cream is slightly homogenised. Homogenisation reduces the size of the fat globules in the cream and consequently diminishes creaming (Graf and Bauer, 1976; Mulder and Walstra, 1974). Furthermore, the homogenisation process largely prevents the so called 'rebodying'. 'Rebodying' is a strong increase in viscosity with time caused by temperature effects which can occur during the transport and storage of the aerosol cans (Mulder and Walstra, 1974). This process results from a limited degree of partial coalescence of fat globules (§ 1.4), induced by temperature cycling (Boode et al., 1991; Walstra and Jennes, 1984).

Finally, the cream is aseptically fed into tinplate or aluminium cans, which are then closed with a valve. The propellant, usually laughing gas (food grade), is added to the cans via this valve while the cans are shaken. The purpose of this shaking is to speed up the dissolution of the gas in the cream and thereby prevent development of an excessive pressure in the cans.

Several components are added to the cream during its production. Emulsifiers, for example monoglycerides, are added to help stabilise the fat globules during homogenisation. Homogenisation considerably enlarges the total surface area of the fat globules, thus creating clean fat surface. The denuded fat will be covered with surface-active proteins present in the skim milk phase (Walstra and Jennes, 1984). In cream with a fat content larger than 20 % the size reduction of the fat globules is limited by the amount of natural surfactant present in the cream to provide coverage of the fat surface (Graf and Bauer, 1976). Furthermore, if not enough protein is available in the cream to cover the denuded globules, clusters of

fat globules may be formed during homogenisation. In these homogenisation clusters the globules are stuck together by sharing one or more casein micelles (milk protein) (Mulder and Walstra, 1974). Addition of extra surfactant (emulsifier) enables further reduction of the globule size. Moreover, the adsorption of the emulsifiers on the fat globules protects the globules from agglomeration (Precht et al., 1988). These effects reduce the creaming process during storage.

Besides emulsifiers, some stabiliser, in practice often carrageenan, is present in the cream. Stabilisers help to slow down the process of creaming by increasing the viscosity or by formation of some kind of network structure in the cream (Kieseker and Zadow, 1973b; Precht et al., 1988). Finally, to improve the flavour of the cream, sugar and sometimes additional flavourings can be added (Vanrusselt, 1992).

Foam formation

An aerosol can contains besides the cream a propellant which is usually nitrous oxide, better known as laughing gas. This gas has a solubility in cream that is approximately 50 times that of air. Due to the high pressure in an aerosol can (5-10 bar) the nitrous oxide is for the larger part dissolved in the cream. It is recommended to shake the can before the spraying process to disperse possible inhomogenities, such as fat globule aggregates, that might be present in the cream. The aerosol can is closed by a valve. Figure 1.1.a shows a schematic drawing of a closed valve as used in the present study. The inside gasket (3) blocks the holes (7) in the valve cone (5), thereby preventing the cream to leave the can.

Opening of the aerosol can occurs by pressing the valve in the direction of the arrow (figure 1.1.b). A direct contact is now created between the inner and outside of the can via the holes (7), resulting in a local pressure drop. This causes the cream to flow out of the can from the higher to the lower pressure. Moreover, the pressure drop will effect supersaturation of the cream with gas. The nitrous oxide will come out of solution, inducing formation and growth of bubbles. Additionally, the pressure drop will cause expansion of the formed bubbles. The spout (8) of the valve (figure 1.1.a) ensures a decorative 'rose' shape of the produced foam. More information about the foam formation process out of an aerosol can will be given in chapter 2.

The instant foam formation process and thereby the foam properties of aerosol whipped cream are greatly affected by the amount of gas dissolved in the cream in the can. A sufficient amount of gas has to be dissolved to obtain satisfactory foam properties. This amount of gas is related to the pressure in the can; the higher the pressure, the larger the amount of gas dissolved in the cream. To prevent the explosion of the can, the pressure inside the aerosol can is however not allowed to

exceed 15-20 bar. Thus, the high solubility of nitrous oxide in cream is a necessity to ensure a sufficient amount of dissolved gas in conjunction with an acceptable pressure in the aerosol can.
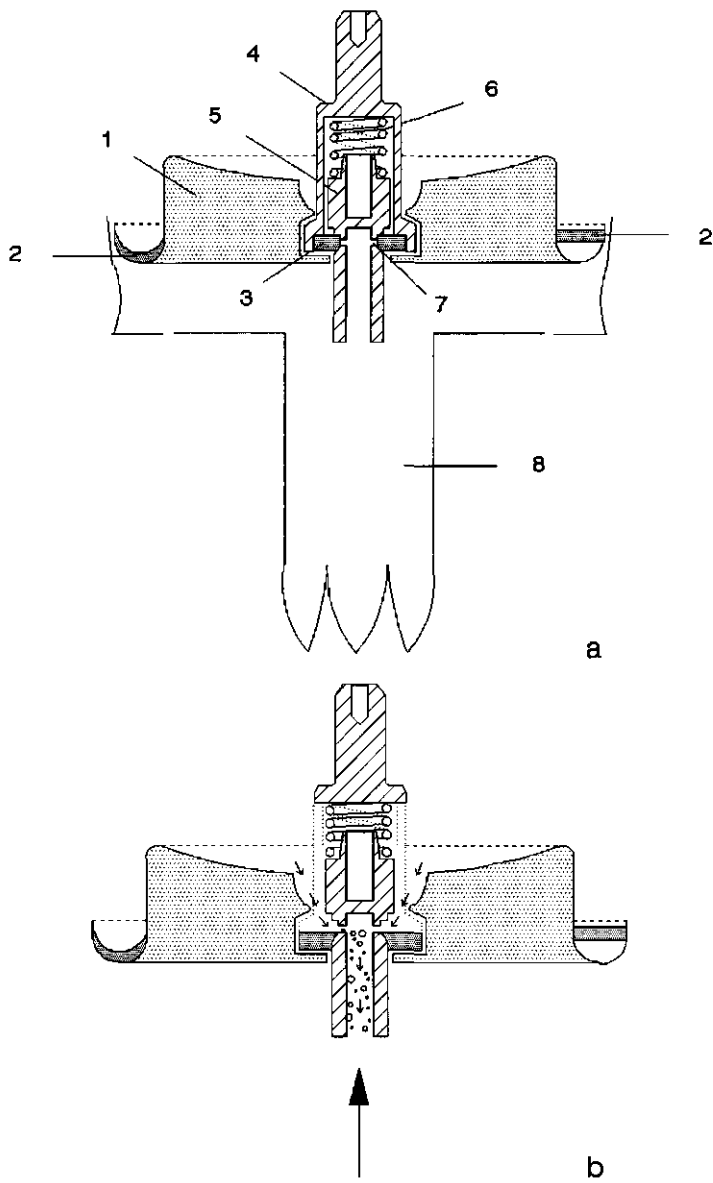
Figure 1.1   Schematic drawing of an aerosol valve (a) closed and (b) open. (1) valve holder, (2) outside gasket, (3) inside gasket, (4) valve casing, (5) valve cone, (6) spring, (7) hole, (8) spout.

Foam properties

Obvious advantages of aerosol whipped cream are in the speed and ease of producing a foam in controllable portions. The foam is characterised by a high overrun of approximately 400-600 %. The overrun relates to the volume fraction of gas in the foam (chapter 2). The initial picture of aerosol whipped cream shows a dry foam with sharp edges at the 'rose' blob (figure 1.2.a). Aerosol whipped cream gives a satisfactory mouthfeel, although on this point it cannot compete with 'ordinary' whipped cream.

a   b

Figure 1.2   Aerosol whipped cream, (a) immediately after foam formation, (b) after 15 minutes.

Unfortunately, aerosol whipped cream is not very stable. Within 15 minutes after the foam formation the foam collapses, which follows from the decrease in blob height. The appearance alters, becoming more shiny and showing degeneration of the 'rose' shape of the blob (figure 1.2.b). Furthermore, the mouthfeel of the aged foam deteriorates into something like a mouthful of air.

Although the high solubility of the nitrous oxide in the cream is, as mentioned, necessary to obtain the required foam properties using an aerosol can, the high

solubility seems to negatively affect the foam stability. It is expected that the deterioration of aerosol whipped cream is mainly caused by a process called disproportionation, which is strongly promoted by a high solubility of the dispersed gas in the surrounding liquid (Wijnen and Prins, 1995). The foam stability of aerosol whipped cream will be discussed in more detail in chapter 4.

1.4   Comparison with whipped fresh cream

Whipped fresh cream refers to 'ordinary' unhomogenised dairy cream, which is mechanically whipped into a foam by means of, for example, a mixer. Describing this topic may seem strange in the present thesis. However, whipped fresh cream and aerosol whipped cream are often compared to each other and there appears to be some lack of clarity concerning the differences between the two products.

Whipped fresh cream

The foam formation of whipped fresh cream is extensively studied and described in literature. Reviews on this topic are given by Mulder and Walstra (1974) and later by Anderson and Brooker (1988) and Brooker (1993). In the whipping process air bubbles are mechanically beaten into the cream. As whipping proceeds, the bubbles become smaller (Noda and Shiinoki, 1986; Schmidt and van Hooydonk, 1980; Sone et al., 1986).

When air is initially incorporated, the bubbles are somehow stabilised by milk proteins (Brooker et al., 1986; Needs and Huitson, 1991). During the whipping, fat globules, containing both solid and liquid fat, adsorb on the bubble surface. This adsorption involves the partial loss of fat globule membrane and so a portion of the fat comes into contact with the air and slightly protrudes into the bubble (Anderson et al., 1987; Buchheim, 1978; Brooker et al., 1986). Some liquid fat may spread over the bubble surface (Anderson and Brooker, 1988). Subsequently, clumping of the fat globules takes place. This is also called partial coalescence because the presence of solid fat in the globules prevents them to coalesce completely (Boode, 1992; Walstra and Jennes, 1984). Clumps of fat become attached to bubbles and to other clumps (Mulder and Walstra, 1974).

Temperature strongly affects the whipping process because effective whipping of the cream requires that part of the fat in the globules is solid (Mulder and Walstra, 1974). The rigidity of the globules prevents complete spreading of the liq id fat around the bubble surface and additionally provides structure to the fat neu ork (Darling, 1982). In fully whipped cream the air bubbles are primarily surrounded oy a network of partially coalesced fat globules, which is clearly visualised by a

number of authors (Anderson et al, 1988; Brooker et al., 1986; Darling, 1982; Graf and Müller, 1965; Schmidt and van Hooydonk, 1980; Stanley et al.; 1996). This network helps to stabilise the foam against disproportionation. The firmness of whipped fresh cream is provided by bridges of aggregated globules connected to adjoining air bubbles and by the adsorption of single globules or groups of globules onto more than one bubble (Anderson and Brooker, 1988). The overrun of the foam is 100-150 %.

Comparison of whipped fresh cream and aerosol whipped cream

Important differences between whipped fresh cream and aerosol whipped cream are the overrun, the firmness and the stability of the foams. The overrun of aerosol whipped cream is 4 times that of whipped fresh cream. This high overrun supplies the aerosol whipped cream with a certain firmness (chapter 2), which is however less than the firmness of whipped fresh cream. The latter is provided by the presence of a fat globule network. The main difference between the two products is the foam stability. Aerosol whipped cream deteriorates within several minutes, whereas whipped fresh cream remains stable for several hours. The fast deterioration of aerosol whipped cream is mainly the result of two factors. Firstly, the gas present in the foam has a high solubility in the cream and thus makes the foam susceptible to the destabilising process of disproportionation. Additionally, there is no fat globule network to stabilise the bubbles against disproportionation or to withstand the collapse of the foam. Unfortunately, because of a number of reasons, it is not possible to easily solve these problems in order to improve the stability of aerosol whipped cream.

Disproportionation of aerosol whipped cream would be much slower if the foam could be produced with a less soluble gas, for example air instead of nitrous oxide. However, in order to obtain a foam with a comparable overrun and bubble size distribution, a certain amount of gas has to be dissolved in the cream in the can. Using a gas with a solubility 50 times lower than the solubility of laughing gas would require a pressure 50 times as high to obtain a similar amount of gas dissolved in the cream. Although machines exist for the production of foams in this manner, such a pressure is obviously not feasible in aerosol cans for domestic use. The presence of a fat globule network in aerosol whipped cream could slow down disproportionation and collapse of the foam. The fat globule network in whipped fresh cream is induced by mechanical forces that cause partial coalescence of the fat globules and thus formation of a network. Aerosol whipping cream is homogenised to prevent physical destabilisation of the emulsion during storage of the cans. Due to the homogenisation the resulting fat globules are smaller and, more important, the membrane of the globules is altered. These factors impair the

clumping tendency of the globules and thus the whipping properties of the cream (Mulder and Walstra, 1974). Consequently, if aerosol cream is mechanically whipped into a foam no fat globule network as in unhomogenised whipped cream is formed.

Graf and Müller (1965) showed that a kind of network in homogenised whipped cream can be formed by homogenisation clusters gathering around the air bubbles and forming agglomerates. However, the presence of these clusters in the cream can result in a rapid creaming during storage in the can (Kieseker and Zadow, 1973a). Darling (1982) stated that the globule membrane structure may be more important in the whipping process than the degree of clustering. Nevertheless, it is clear that there is a link between the whipping properties and the emulsion stability of homogenised cream (Anderson and Brooker, 1988; Streuper and van Hooydonk, 1986). Aerosol whipping cream is processed to be stable during storage and unfortunately the physical stability of the cream seems to be negatively related to its whipping quality.

Even if it would be possible to form some kind of network in aerosol whipping cream, the structure would have to be established within the short time that the mechanical forces act upon the fat globules during the foam formation process out of an aerosol can. The network formation in whipped fresh cream takes on the order of minutes whereas the foam formation of aerosol whipped cream occurs within less than a second. Creating a network within this short time seems not feasible. Obviously, it will not be easy to improve the stability of aerosol whipped cream by inducing the formation of a fat globule network.

1.5   Aim and outline of this thesis

Aerosol whipped cream is a well known convenience product nowadays. The production of aerosol whipped cream has developed more or less empirically instead of being based on fundamental knowledge of the process. Therefore, the present work was started. The aim of this study was to obtain more physical knowledge about the production and stability of aerosol whipped cream. In this thesis an attempt is made to unravel the overall process of foam formation, resulting in an overview of sub processes and properties determining or affecting foam formation and stability.

The process of instant foam formation out of an aerosol can will be described in chapter 2. The process is divided into three different stages: the situation in the aerosol can, the (two-phase) flow through the nozzle and the situation directly after the formed foam leaves the nozzle. The latter stage corresponds to the initial foam

properties. Theory of physics related to the instant foam process will be applied to the production of aerosol whipped cream. Because the solubility of the propellant seems to play a major role in the whole process, study on the solubility properties of nitrous oxide in cream is included.

During the spraying process the pressure inside an aerosol can drops, thereby affecting the foam formation process and the resulting foam properties. In order to be able to produce aerosol whipped cream under standardised conditions, an apparatus, called the Aerosol Can Simulator (ACS), was developed to extend the knowledge of the instant foam production. Chapter 3 describes the working principle of this apparatus. Moreover, the foam formation and foam properties of aerosol whipped cream produced with the ACS will be presented. The studied processes will be related to and compared with analogous processes occurring when using an aerosol can.

More information about the foam properties of aerosol whipped cream is given in chapter 4. In this chapter, the foam stability and several processes affecting this stability will be described. Since surface rheological properties of a liquid play an important role in the stability of the foam produced from that liquid, the surface rheological properties of unwhipped cream will be discussed in relation to the stability of aerosol whipped cream. Special attention is paid to the susceptibility of the foam to the process of disproportionation.

In the last chapter of this thesis the main conclusions of the study will be outlined to review the overall picture of the instant foam production of aerosol whipped cream. Finally, some perspectives of the research will be given.

1.6   References

- Anderson, M. and Brooker, B.E.,1988. Dairy Foams. In: Advances in Food Emulsions and Foams. Dickinson, E. and Stainsby, G.(eds.), Elsevier Applied Science, London, 221-255.
- Anderson, M., Brooker, B.E. and Needs, E.C., 1987. The Role of Proteins in the Stabilisation/Destabilisation of Dairy Foams. In: Food Emulsions and Foams, Dickinson, E. (ed.), Royal Society of Chemistry, 100-109.
- Anon, 1970. Southern Dairy Packs Dozen Brands Of Whipped Cream, Toppings in Aerosols. American Dairy Review, 52 (3), 50-51.
- Barford, N.M. and Krog, N., 1987. Destabilisation and Fat Crystallisation of Whippable Emulsions (Toppings) Studied by Pulsed NMR. JAOCS, 64 (1), 112-119.

- Boode, K., 1992. Partial Coalescence in Oil-in-Water Emulsions. Ph.D. Thesis, Wageningen Agricultural University.
- Boode, K., Bisperink, C. and Walstra, P., 1991. Destabilisation of O/W Emulsions Containing Fat Crystals by Temperature Cycling. Colloids and Surfaces, 61, 55-74.
- Brooker, B.E., 1993. The Stabilisation of Air in Foods Containing Fat - a Review. Food Structure, 12, 115-122.
- Brooker, B.E., Anderson, M. and Andrews, A.T., 1986. The Development of Structure in Whipped Cream. Food Microstructure, 5, 277-285.
- Buchheim, W. Mikrostruktur von Geschlagenem Rahm. Gordian, 1978 (6), pp. 184-188.
- Buchheim, W., Barford, N.M. and Krog, N., 1985. Relation Between Microstructure, Destabilisation Phenomena and Rheological Properties of Whippable Emulsions. Food Microstructure 4, 1985, 221-232.
- Darling, D.F., 1982, Recent Advances in the Destabilisation of Dairy Emulsions. Journal of Dairy Research, 49, 695-712.
- Dickinson, E., 1992. An Introduction to Food Colloids, Springer Verlag, New York, Oxford University Press.
- Getz, C.A., Smith, G.F. and Tracy, P.H., 1936. Instant Whipping of Cream by Aeration. Journal of Dairy Science 19, 1936, 490-491.
- Graf, E. and Bauer, H., 1976. Milk and Milk Products. In: Food Emulsions. Friberg, S. (ed). Marcel Dekker Inc., New York, 295-384.
- Graf, E. and Müller, H.R., 1965. Fine Structure and Whippability of Sterilised Cream. Milchwissenschaft, 20 (6), 302-308.
- Kieseker, F.G. and Zadow, J.G., 1973a. The Whipping Properties of Homogenised and Sterilised Cream. The Australian Journal of Dairy Technology, 28(3), 108-113.
- Kieseker, F.G. and Zadow, J.G., 1973b. Factors Influencing the Preparation of U.H.T. Whipping Cream. The Australian Journal of Dairy Technology, 28(4), 165-169.
- Kieseker, F.G., Zadow, J.G. and Aitken, B., 1979. The Manufacture of Powdered Whipping Creams. The Austalian Journal of Dairy Technology, March, 21-24.
- Kikuchi, M., Endo, M., Yoshioka, T., Watanabe, R. and Matsumoto, S., 1995. Modelling and Dynamic Analysis of a Continuous Whipping System. Milchwissenschaft 50 (3), 129-134.
- Knightly, W.H., 1968. The Role of Ingredients in the Formulation of Whipped Toppings. Food Technology 22 (1), 731-744.
- Krog, N., Barford, N.M. and Buchheim, W., 1987. Protein-Fat-Surfactant Interactions in Whippable Emulsions. In: Food Emulsions and Foams. Dickinson, E. (ed.). Royal Society of Chemistry, London, 144-157.
- Lang, F. and Lang., A., 1975 More European Ideas for the Manufacture of New Milk Products. The Milk Industry, 77(5), 9-11.
- Mansvelt, J.W., 1976. The Use of Foams in Foods and Food Production. In: Foams, Aker, R.J. (ed.), Academic Press, London, 283-296.
- Mulder, H. and Walstra, P., 1974. The Milk Fat Globule; Emulsion Science as Applied to Milk Products and Comparable Foods. Centre for Agricultural Publishing and Documentation, Wageningen, the Netherlands.
- Needs, E.C. and Huitson, A., 1991. The Contribution of Milk Serum Proteins to the Development of Whipped Cream Structure. Food Structure, 10, 353-360.
- Noda, M. and Shiinoki, Y., 1986. Microstructure and Rheological Behaviour of Whipping Cream. Journal of Texture Studies, 17(2), 189-204.

- Pader, M. and Gershon, S.D., 1965 Aerosol Topping, United States Patent Office, 3224883.
- Peter, P., 1971. Neue Entwicklungen auf dem Gebiet der Lebensmittelaerosole. Riechstoffe, Aromen, Körperpflegemittel 21(12), 454-457.
- Precht, D., Peters, K.H. and Petersen, J., 1988. Improvement of Storage Stability and Foaming Properties of Cream by addition of Carrageenan and Milk Constituents. Food Hydrocolloids, 2(6), 491-506.
- Prins, A., 1988. Principles of Foam Stability. In: Advances in Food Emulsions and Foams, Dickinson E. and Stainsby, G. (eds.), Elsevier Applied Science, England, 91-122.
- Schmidt, D.G. and van Hooydonk, A.C.M., 1980. A Scanning Electron Microscopical Investigation of the Whipping of Cream. Scanning Electron Microscopy, III, 653-658.
- Sone, T., Noda, M., Shiinoki, Y. and Kako, M. 1986. Structure and Rheological Behaviour of Whipped Cream. In: Developments in Food Science 12: The Shelf Life of Foods and Beverages, Charalambous, G. (ed.), Elsevier, Amsterdam.
- Stanley, D.W., Goff, H.D. and Smith, A.K., 1996. Texture-Structure Relationships in Foamed Dairy Emulsions. Food Research International 29 (1), 1-13.
- Streuper, A. and van Hooydonk, A.C.M., 1986. Heat Treatment of Whipping Cream. II. Effect on Cream Plug Formation. Milchwissenschaft 41(9), 547-552.
- Takada, M. and Kanda, H., 1984. Aerosol Whipped cream. In: Emulsions and Emulsifier Applications, Recent Developments, Torrey, S. (ed). Chemical Technology Review no. 229, Noyes Data Corporation, New Jersey.
- Tanaka, M., Deman, J.M. and Voisey, P.W., 1973. Some Rheological Properties of Whipped Toppings. Chemie Microbiologie Technologie der Lebensmittel, 2, 1-6.
- Vanrusselt, R. , 1992. Room in Spuitbussen. Melk en Wij, 1, 13-17.
- Varnam, A.H. and Sutherland, J.P., 1994. Milk and Milk Products; Technology, Chemistry and Microbiology. Chapman & Hall, London.
- Walstra, P., 1989. Principles of Foam Formation and Stability. In: Foams: Physics, Chemistry and Structure, Wilson, A.J. (ed.), Springer Verlag, London, 1-15.
- Walstra, P. and Jennes, R., 1984. Dairy Chemistry and Physics. John Wiley & Sons, Inc., USA.
- Werner, K., 1970. The Present State of Food Aerosol Technology. International Bottler & Packer, october 1970, 52-55.
- Wijnen, M.E. and Prins, A., 1995. Disproportionation in Aerosol Whipped Cream. In: Food Macromolecules and Colloids, Dickinson, E. and Lorient, D. (eds.), Royal Society of Chemistry, 309-311.

Chapter 2

Aspects of foam formation out of an aerosol can

2.1   Introduction

This chapter describes different aspects of foam formation out of an aerosol can, taking aerosol whipped cream as an example. Three different stages in the foam formation process are considered successively. Firstly, the situation in the aerosol can is studied. The aerosol can contains cream and gas, in practice mostly nitrous oxide, which is partly dissolved in the cream. The amount of gas dissolved in the cream is linked to the amount of gas present in the headspace of the can and, therefore, to the pressure in the can. In practice, the pressure in the aerosol can varies between 5 and 10 bar, depending on the amount of product inside the can.
By opening the valve of an aerosol can a direct contact is created between the inner and the outside of the can via a standardised small opening, resulting in a local pressure drop. This causes the cream to flow from the higher pressure to the lower pressure. The cream becomes supersaturated with gas, resulting in foam formation and bubble growth. The amount of gas dissolved in the cream influences the bubble growth velocity, the bubble size and the resulting overrun of the foam. Furthermore, the foam is exposed to mechanical forces while passing through the nozzle. These forces, which can affect the foam properties, depend on the magnitude of the pressure drop. The pressure drop is determined by the conditions in the can and the small opening.
It is assumed that the actual foam formation takes place in the nozzle. Therefore, the second stage considered in the process of foam formation is the flow of the (aerated) cream through the nozzle. To describe the processes occurring in the nozzle, theory on two-phase flow is applied which relates the situation in the can to the flow properties in the nozzle. Furthermore, the influence of the geometry of the nozzle on the flow phenomena is studied.
The third stage considered in the foam formation out of an aerosol can is the situation directly after the foam leaves the nozzle. The initial foam properties of the aerosol whipped cream supply information about the process of foam formation.
Since the process of foam formation out of an aerosol can seems to be strongly related to the solubility properties of the propellant, some theoretical aspects of the solubility of gas in liquid will be described first. Additionally, the solubility properties of nitrous oxide in aerosol whipping cream are determined experimentally.

2.2   Initial condition in the aerosol can

2.2.1   Theory of gas solubility

Solubility properties of gas in liquid

The solubility of a gas in a liquid is determined by the equations of phase equilibrium. The ideal gas solubility of component i is given by Raoult's law:

$$x_i = \frac{p_i}{P_i^s} \tag{2.1}$$

where x_i is the mole fraction of the (dissolved) gas in the liquid, p_i the partial pressure of component i in the gas phase and P_i^s the (saturation) vapor pressure of pure liquid i at the temperature of the solution (Hildebrand et al., 1970; Prausnitz, 1969). In practice, most of the systems do not show ideal behaviour; measured gas solubilities are usually lower than the ideal solubility. When dilute solutions are considered ($x_i \ll 1$) Henry's law is often used:

$$x_i = \frac{p_i}{H_{i,j}} \tag{2.2}$$

where Henry's constant $H_{i,j}$ depends on the temperature as well as on the properties of the gas and the liquid. When there is a positive interaction between gas and liquid, the gas solubility tends to be larger, resulting in a smaller value of $H_{i,j}$ (Barton, 1991).

Henry's law is only valid when the solubility and partial pressure of the gas are small. It is roughly estimated that for many systems equation (2.2) applies when the solubility remains below about 3 mol % and the partial pressure does not exceed 5 or 10 atm (Prausnitz, 1969). At higher pressures the gas molecules will approach each other and thereby influence each other; a correction on Henry's law is then necessary. Instead of using the partial pressure p_i in the gas phase, the fugacity f_i of component i has to be considered now. The fugacity can be seen as an effective gas pressure corrected for deviations from the perfect gas law (Hildebrand et al., 1970). An equation used to fit high-pressure gas solubilities is the Krichevsky-Kasarnovsky equation (Prausnitz, 1969; Battino and Clever, 1966):

$$\ln \frac{f_i}{x_i} = \ln H_{i,j}^{(P_j^s)} + \frac{v_j^\infty (P - P_i^s)}{RT} \tag{2.3}$$

where $H_{i,j}$ at pressure P_j^s is the Henry constant at the saturation pressure P_j^s of the

solvent, P the total pressure, v_i^∞ the partial molar volume of i in the liquid phase at infinite dilution, R the gas constant and T the temperature.

An other parameter that has to be considered while studying solubility properties is the temperature. The effect of temperature depends on the intermolecular forces of the gas-liquid system. For the majority of systems the gas solubility in a liquid decreases with increasing temperature. However, if the gas is only sparingly soluble the temperature effect is the opposite; the gas solubility increases with increasing temperature (Shinoda and Becher, 1978; Prausnitz, 1969).

The gas solubility in a mixture of liquids can be estimated using the solubility in the separate solvents (Hildebrand et al., 1970; Prausnitz, 1969):

$$\ln H_{i,m} = x_j \ln H_{i,j} + x_k \ln H_{i,k} - a_{j,k} x_j x_k \qquad (2.4)$$

where $H_{i,m}$,$H_{i,j}$ and $H_{i,k}$ are the Henry constants for gas i in respectively the mixture of the solvents, the pure solvent j and the pure solvent k. x_j and x_k are the mole fractions of respectively solvent j and solvent k in the mixture, $a_{j,k}$ is a constant characteristic of the jk binary pair. For ideal mixtures, $a_{j,k} = 0$ resulting in a linear relation between the logarithm of Henry's constant in the mixture and the mole fraction of the liquids.

Equation (2.4) holds when the solvents considered have (effectively) spherical molecules, all of roughly the same size. When the molar volumes of the components are very different, it is preferable to rewrite the equation into:

$$\ln H_{i,m} = \phi_j \ln H_{i,j} + \phi_k \ln H_{i,k} - v_i b_{j,k} \phi_j \phi_k \qquad (2.5)$$

where ϕ_j and ϕ_k are the volume fractions of respectively solvent j and k, v_i is the molar volume of pure 'liquid' i (fictitious) and $b_{j,k}$ an empirical coefficient analogous to $a_{j,k}$ (Hildebrand et al., 1970)

Solubility of nitrous oxide in cream

Nitrous oxide (N_2O), or laughing gas, is in practice used as propellant in the production of aerosol whipped cream. Because of the relevance of the solubility properties of the gas in the process of foam formation of the cream it is important to study these properties. Since cream is an oil in water emulsion the gas solubility in both components has to be considered. In literature there are a number of data available on the solubility of N_2O in water. There is, however, little information about the solubility of N_2O in an oil or fat phase. An overview on the solubility parameters of nitrous oxide in water and several oils is given in appendix I.

The solubility of nitrous oxide in water is about 50 times larger than the solubility of nitrogen. Furthermore, it seems to have a higher affinity for liquid oils. This can be explained considering the bond character of the interacting molecules. The bond

between hydrogen and oxygen (as in water) is covalent polar. On the other hand, a covalent non-polar bond exists between carbon and hydrogen (the main elements in a fat phase). The bond between nitrogen and oxygen (as in nitrous oxide) is also covalent non-polar (Luhman, 1994). This indicates that nitrous oxide molecules will interact better with molecules of a fat phase than with water molecules.

The milk fat phase of whipping cream is, depending on the temperature, partly crystallised. It is expected that the amount of solid fat in the oil phase will have a negative effect on the gas solubility properties. Studying a practical system like cream makes it difficult to correctly estimate the solubility properties. However, experimental observations can be used to determine the solubility of nitrous oxide in cream.

The fixed volume of an aerosol can is occupied by a volume of cream and a headspace with gas. The pressure in the can is a measure for the number of moles gas, and thus the mass of gas, present in the headspace. When the total mass of gas present in the can is known, the mass of gas dissolved in the cream can be calculated.

The volume of cream V_l in the can follows from the mass of the cream $w_l = \rho_l . V_l$, in which the cream density ρ_l can be derived from:

$$\frac{1}{\rho_l} = \frac{x}{\rho_o} + \frac{(1-x)}{\rho_w} \tag{2.6}$$

In this equation x is the mass fraction of fat in the cream; ρ_o and ρ_w are the densities of respectively the milk fat and the skim milk. ρ_o and ρ_w depend on the temperature as can be seen in appendix II (Walstra and Jennes, 1984).

When the volume of the can is known, the volume of the headspace in the can V_h follows from the volume of the cream. The headspace contains mainly nitrous oxide, but also a known amount of air which is enclosed before the sealing of the can. The total pressure in the can P_t equals $p_a + p_g$, where p_a and p_g are respectively the partial pressure of the air and the nitrous oxide in the can. According to the ideal gas law the number of moles gas n follows from:

$$PV = nRT \tag{2.7}$$

where P is the pressure, V the volume, R the gas constant and T the temperature. Since air is approximately 50 times less soluble than nitrous oxide, it seems justified to neglect the solubility of air in the cream. The mass of dissolved N_2O in the cream, G_s, can now be calculated using the measured pressure P_t inside the can:

$$G_s = w_g - n_g * M_g = w_g - \left(\frac{(P_t - p_a)V_h}{RT}\right) * M_g \qquad (2.8)$$

with w_g being the mass of nitrous oxide added to the can, n_g the number of moles nitrous oxide present in the headspace of the can and M_g the molar weight of N_2O (44.013 g/mol).

When G_s is determined at different values of the partial pressure p_g of nitrous oxide in the can, the mass of gas dissolved per mass of cream, G_s/w_l, can be plotted versus p_g. Assuming that Henry's law applies, the slope of the plot can be used to find the gas solubility (equation (2.2)). This is only valid in the presence of phase equilibrium between the gas present in the headspace and the gas dissolved in the cream. The slope of the plot will be referred to as the solubility S of the gas in the cream. Note that S is proportional to the reciprocal of the Henry constant.

2.2.2 Experimental

In order to study the solubility properties of nitrous oxide in cream, the solubility S of N_2O in cream was determined as a function of the fat content of the cream and the temperature.

Method
Aerosol cans with a volume of 405 ml were filled with 250 g aerosol whipping cream. To study the effect of the fat content on the gas solubility, varying fat contents were used: 0 % (skim milk), 10 %, 20 %, 30 % and 38 % w/w. After closing the cans with a nozzle, different amounts of (food grade) nitrous oxide were added: 3.0 g, 4.5 g, 6.0 g and 6.7 g. These amounts of gas were chosen because they induce a pressure range from approximately 5 to 10 bar in the cans. The variation in the added mass of gas and cream was less than 0.1 g. The cans were stored during 8 days at different temperatures: 3 °C, 8 °C, 12 °C, 20 °C and 30 °C. For each combination of storage temperature and fat content of the cream, three cans were studied. The pressure in the cans after storage was measured. For this purpose a manometer was equipped with a small extension piece that fitted on top of the nozzle of an aerosol can. Some random measurements were performed to check whether the pressure in the cans had reached an equilibrium value after 8 days of storage. Within the measuring precision of the manometer (± 0.1 bar) no differences were found in the pressures after 6 and 8 days of storage. It was therefore assumed that equilibrium between the gas dissolved in the cream and the gas present in the headspace of the can was established.

Calculation

The amount of nitrous oxide dissolved in the cream (G_s) was calculated with equation (2.8), using the mass of N_2O added to the can (w_g) and the measured pressure P_t in the can. The volume of the headspace V_h easily follows from the total volume of the aerosol can and the cream volume V_l. Since the mass of cream present in the aerosol can is known, V_l can be found using equation (2.6). The partial gas pressure p_a of the air results from the ideal gas law out of the number of moles air n_a present in the can. n_a is determined by the pressure (1 atm) and temperature (20 °C) during the filling of the can and by the volume of the headspace directly after the filling process. This volume depends on the density and thus on the temperature of the cream. The filling temperature of the cream is estimated to be 10 °C (= 283.15 K).

The calculated values of G_s/w_l were plotted against the partial pressure of the nitrous oxide in the can. The solubility S was found after linear regression of the data, where the intercept was forced to be zero.

2.2.3 Results and Discussion

For each combination of storage temperature and fat content of the cream, the mass of nitrous oxide dissolved in the cream can be plotted versus the partial gas pressure in the aerosol can.
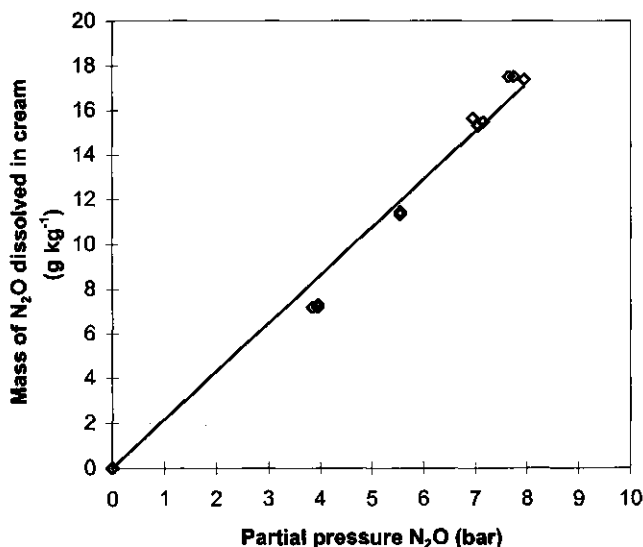

Figure 2.1   Mass of nitrous oxide dissolved in the cream (◇) versus partial gas pressure in the can and calculated Henry's law (———); fat content 30 % w/w, T = 3 °C.

The results of cream with a fat content of 30 % w/w stored at 3 °C are shown in figure 2.1 as a typical example of these plots. The symbols mark the (calculated) data; the trend line, indicating Henry's law, is obtained after linear regression of the data where the intercept is forced to be zero. Comparison of the data with the trend line shows that the solubility of N_2O in cream deviates from Henry's law. This is not surprising for a practical system like cream. Since the slope of the plot does not exactly agree with the solubility S (which is proportional to the reciprocal of Henry's constant), it is preferable to refer to it as the *apparent* solubility S'.

Although the values of the apparent solubilities differ from the actual gas solubilities, they are a good tool for comparing the different sets of data. Figure 2.2 shows the apparent solubilities for the different fat contents as a function of temperature.
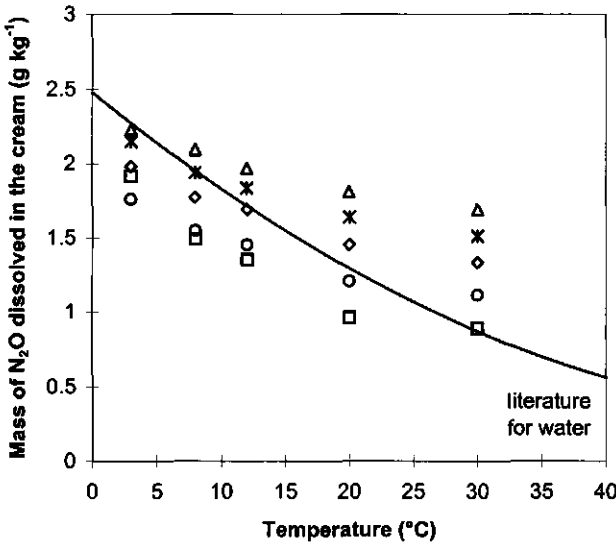
Figure 2.2   Apparent solubility of nitrous oxide in cream as a function of temperature for a fat content 0 % w/w (□), 10 % w/w (○); 20 % w/w (◇), 30 % w/w (✱) and 38 % w/w (△); line is an average for the actual solubility of nitrous oxide in water, taken from literature (Perry, 1963; Marshall, 1976; Braker and Mossman, 1980; Ahlberg, 1985).

The symbols indicate the various fat contents; the line gives an average for the actual gas solubility of nitrous oxide in water obtained from literature (appendix I). According to Marshall (1976), the solubility of nitrous oxide in different oils at a temperature of 20 °C is at least twice as large as in water (appendix I).

The plot shows that the apparent solubility of N_2O in the cream decreases with increasing temperature, similar to the gas solubility in water. It can be noted that

the slope of the line indicating the literature data for water is comparable to the slope of the skim milk data, up to 20 °C inclusive. Apparently, the different components present in the skim milk do not affect the temperature dependency of the gas solubility in the liquid.

In the presence of a fat phase, two effects of temperature on the gas solubility have to be considered. Firstly, an increasing temperature in general negatively affects the gas solubility, as was described for water and skim milk. Figure 2.2 shows that this effect also occurs in the presence of a fat phase. Secondly, the temperature determines the amount of solid and liquid fat in the fat phase and thus the solubility properties. It is expected that the solubility of N_2O in the solid fat phase will be much lower, if not negligible, compared to the amount of gas dissolved in the skim milk and the liquid fat phase. An increasing temperature, accompanied by an increasing amount of liquid fat, will therefore positively affect the gas solubility. The second temperature effect thus counteracts the first one. This is reflected in a tendency to a less steep slope of the apparent solubility versus the temperature with increasing fat content in figure 2.2.

Finally, it can be noted that the apparent solubility of nitrous oxide in cream increases with increasing fat content; the gas is more soluble in the fat phase than in the 'skim milk phase'. Apparently, the higher solubility in the liquid fat phase than in the 'skim milk phase', due to the bond character of the interacting molecules (§ 2.2.1), dominates the assumed lower solubility in the solid fat phase.

2.3   Condition in the can during the spraying process

It is obvious that the process of foam formation out of an aerosol can is strongly related to the conditions in the can. A major parameter in this process is the amount of gas dissolved in the cream, which is of course strongly related to the pressure in the can. During the spraying process the pressure inside the can drops, thereby affecting the mass of gas G_s dissolved in the cream. The state of the equilibrium between the gas present in the headspace of the can and the gas dissolved in the cream determines the relation between the decrease in pressure and G_s. The importance of the state of the phase equilibrium is apparent.

Before the spraying process phase equilibrium is assumed, since the pressure in the cans remained stable during the last two days of storage (§ 2.2.2). During the spraying process the time scales are, however, in the order of seconds instead of days. The effect of these shorter time scales on the state of the equilibrium between the gas present in the headspace of the can and the gas dissolved in the cream is studied.

2.3.1 Theoretical considerations on the gas equilibrium

The state of the phase equilibrium affects the course of the pressure inside the aerosol can during the spraying process as a function of time. The pressure in the can at time t, $P_{t,t}$ equals:

$$P_{t,t} = \frac{n_{h,t}RT}{V_{h,t}}$$

with (2.9)

$$n_{h,t} = n_{t,t} - n_{s,t} = n_{t,t} - \frac{\rho_{s,t}V_{l,t}}{M_g}$$

where $n_{h,t}$, $n_{t,t}$ and $n_{s,t}$ are respectively the number of moles gas in the headspace, the total number of moles in the can and the moles dissolved in the cream, $V_{h,t}$ and $V_{l,t}$ respectively the volume of the headspace and of the cream and $\rho_{s,t}$ the amount of gas dissolved in the cream, all at time t. M_g is the molar weight of the gas.

The value of $\rho_{s,t}$ depends on the state of the phase equilibrium which knows two ultimate situations. On the one hand, it is conceivable that, within the short time scales considered, there is no time for the gas equilibrium to adjust to the change in pressure during the spraying process; in the extreme situation the amount of gas dissolved per amount of cream remains constant in time:

$$\rho_{s,t} = \rho_l S p_{g,0}$$ (2.10)

where ρ_l is the density of the cream, S the gas solubility in the cream and $p_{g,0}$ the partial pressure in the can before the spraying process ($t = 0$). On the other hand, it is possible that the equilibrium between the gas present in the headspace of the can and the gas dissolved in the cream remains established during the spraying process, or:

$$\rho_{s,t} = \rho_l S p_{g,t}$$ (2.11)

where $p_{g,t}$ is the partial gas pressure in the can at time t.

Measurement of the pressure inside the can during the spraying process gives information about the state of the phase equilibrium.

2.3.2 Experimental

Method

Considering the foam formation process out of an aerosol can, it is important to

know the proportion of the gas and cream flow. The gas flow consists of two parts. There will always be an amount of gas dissolved in the cream. Additionally, part of the gas can be present as bubbles in the flow.

It is assumed that ratio k of the mass of the gas flow m_g to the mass of the cream flow m_l that leaves the can, remains constant during the spraying process:

$$k = \frac{m_g}{m_l} \qquad (2.12)$$

It is expected that shaking of the can will affect k. Moreover, shaking causes bubble formation in the cream which may affect the state of the phase equilibrium. Two extreme situations were studied and compared:

Not shaken can: there will be no, or only a very small amount of bubbles present in the cream. It is assumed that in this situation only the gas dissolved in the cream leaves the can during the spraying process. The ratio k will thus equal the mass of dissolved gas per mass of cream in the can. In the absence of bubbles, there is no large exchanging interface between gas and cream, which makes it difficult to achieve phase equilibrium within the short time scales of the spraying process.

Shaken aerosol can: shaking of the can causes bubble formation in the cream. It is speculated that the total amount of gas flows with the cream through the nozzle, both dissolved and in the form of bubbles. k therefore equals the total mass of gas divided by the total mass of cream in the can. The presence of bubbles is accompanied with a large exchanging interface between gas and cream. This will stimulate the establishment of the phase equilibrium.

The aerosol cans used for the experiments had a volume of 405 ml and contained 243 ± 1 g aerosol whipping cream (fat content 35 % w/w, ρ_l = 1008 kg/m^3), 7.0 ± 0.1 g nitrous oxide (food grade) and 0.2 g air. Before use they were stored during several weeks at a temperature of approximately 5 °C. For both situations, shaken and not shaken, the pressure inside the can $P_{t,t}$ was measured as a function of the total mass $m_{t,t}$ of the flow that has left the can. The time scale of the whole experiments was a few minutes. The pressure was measured by means of a manometer (§ 2.2.2); the mass of the flow was measured using a balance. Experiments were performed in duplicate.

Calculation

The calculations of the pressure in the can $P_{t,t}$ as a function of the total mass of the flow $m_{t,t}$ out of the can were performed numerically. The mass of the cream flow $m_{l,t}$ at time t was increased to its maximum value in 25 steps. After each step the volume of the headspace in the can $V_{h,t}$ follows from:

$$V_{h,t} = V_c - V_{l,t} = V_c - \left(V_{l,0} - \frac{m_{l,t}}{\rho_l} \right) \qquad (2.13)$$

where V_c is the volume of the aerosol can and $V_{l,0}$ the cream volume at time $t = 0$. Since the mass of the gas flow at time t, $m_{g,t}$ equals $k \cdot m_{l,t}$ (equation (2.12)), the mass of gas that has left the can, and thus the number of moles gas present in the can at time t ($n_{l,t}$), is known. The pressure as a function of the total mass flow ($m_{l,t} + m_{g,t}$) can now be found by combining equation (2.9) with equation (2.10) (no phase equilibrium) or equation (2.11) (phase equilibrium).

It has to be noted that the initial pressure in the can is affected by shaking as can be seen later (figures 2.3 and 2.4). This leads to the suspicion that the assumed phase equilibrium before the spraying process in the can has not yet been established. Since the observed difference in initial pressure correlates to a different amount of dissolved gas in the cream, different values for S were used for shaken and not shaken aerosol cans. The solubilities were calculated by correlating the initial pressure measured in the can $P_{t,0}$ to the amount of dissolved gas ρ_s (equation (2.9)); the values for S additionally followed from equation (2.10).

2.3.3 Results and discussion

The pressure versus the mass of the cream flow was measured for an unshaken can. Figure 2.3 gives the results (symbols) and the calculations (lines) corresponding to the measured $P_{t,0}$. The dotted line indicates the absence of phase equilibrium (ρ_s is constant); the solid line assumes equilibrium between the gas dissolved in the cream and the gas present in the headspace of the aerosol can. In the calculations k is taken to be $1.82 \cdot 10^{-2}$.

The results indicate that the pressure inside the unshaken aerosol can initially decreases with the mass flow according to the non equilibrium situation (dashed line). Furthermore, the shape of the measured curve seems most similar to the shape of the non equilibrium calculation. The absence of bubbles in the can apparently hinders the establishment of a phase equilibrium at this point. During the spraying process the measured data, however, deviate from the non equilibrium situation. It seems that the amount of dissolved gas does not remain constant; part of the gas moves from the liquid phase to the gas phase in the can during the spraying process. It can be speculated that, due to the pressure decrease, bubbles are formed in the cream. Because of the increase in exchanging interface between gas and cream this will stimulate the establishment of the phase equilibrium.

Figure 2.3   Pressure in the can versus mass of the flow out of an unshaken can, measured (▲)
                   and calculated assuming absence of phase equilibrium (- - -) or phase equilibrium
                   (——); only the gas dissolved in the cream before the spraying process leaves the
                   can. S = 2.2 g/kg/bar; k = 1.82·10^{-2}.

Figure 2.4 shows the results (symbols) and the calculations (lines) corresponding to
the measured $P_{t,0}$ in a shaken aerosol can. The dashed line indicates the situation
assuming that the amount of gas dissolved in the cream remains constant during
the spraying process (no phase equilibrium); the solid line assumes equilibrium
between the gas dissolved in the cream and the gas present in the headspace of
the aerosol can. The value of k is 2.96·10^{-2}.

The results mark that the pressure inside a shaken aerosol can decreases linear
with the mass flow of the cream, indicating that the phase equilibrium seems to be
approached. The shaking of the can causes bubble formation in the cream. This
results in a large exchanging interface between the gas and cream, which
promotes the establishment of the phase equilibrium. Nevertheless, the pressure
measured in the can does not decrease as fast as is calculated (solid line). This
can be explained by the value of k. In the calculation it is assumed that due to the
shaking of the can the gas and cream are homogeneously mixed. The total mass
of gas present in the can would thus contribute to k. It is however likely that a
certain amount of gas will remain in the headspace of the can, therefore not
contributing to the value k. A smaller value of k, meaning a smaller mass of gas
leaving the can with the cream, is expected to result in a smaller decrease in
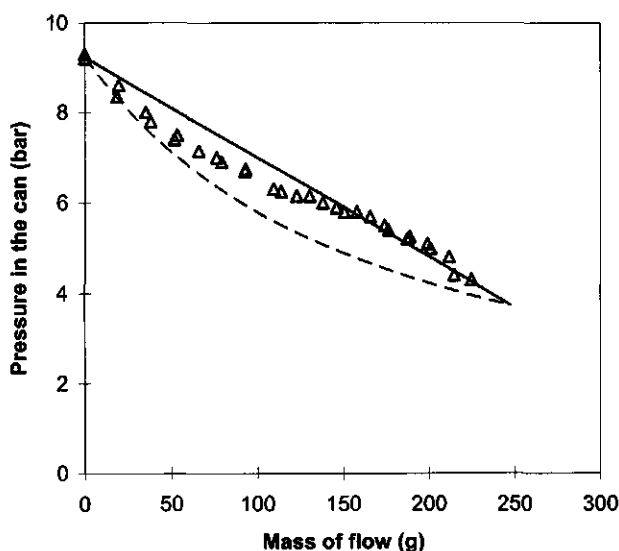pressure with the mass of the flow.

Figure 2.4   Pressure in the can versus mass of the flow out of a shaken can, measured (□) and calculated assuming absence of phase equilibrium (– – –) or phase equilibrium (——); total amount of gas leaves the can with the cream. $S = 2.44$ g/kg/bar; $k = 2.96 \cdot 10^{-2}$.

The amount of gas that remains in the headspace of the aerosol can after shaking is estimated by mixing some gas (air) and cream in a measuring cylinder. The volume ratio gas to cream was comparable to the contents of an aerosol can. After shaking of the cylinder approximately 20 vol % of the gas was entrapped in bubbles. Adjusting k results in a value for k of $2.10 \cdot 10^{-2}$. Figure 2.5 shows the results of figure 2.4 (symbols) and the adjusted calculations (lines).

After adjusting the parameter k as mentioned, the calculated pressure decrease with the mass of flow is indeed smaller than followed from the corresponding calculations performed with the larger k (figure 2.4). However, figure 2.5 shows that the measured data are now positioned below the solid line which is calculated assuming phase equilibrium. Apparently, it is impossible to achieve complete phase equilibrium within the relatively short time scales of the experiment.
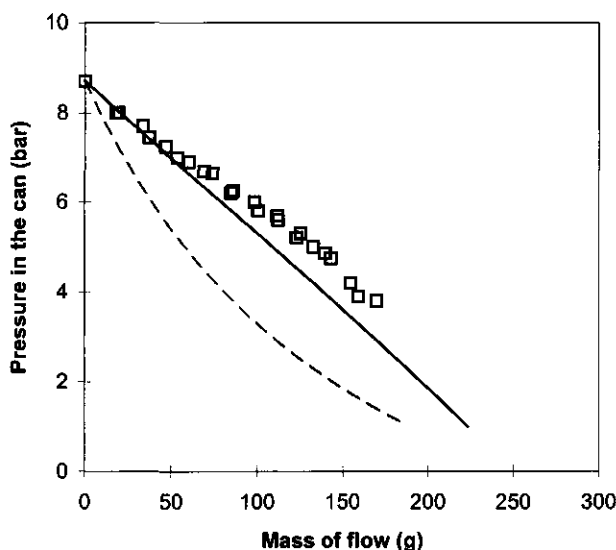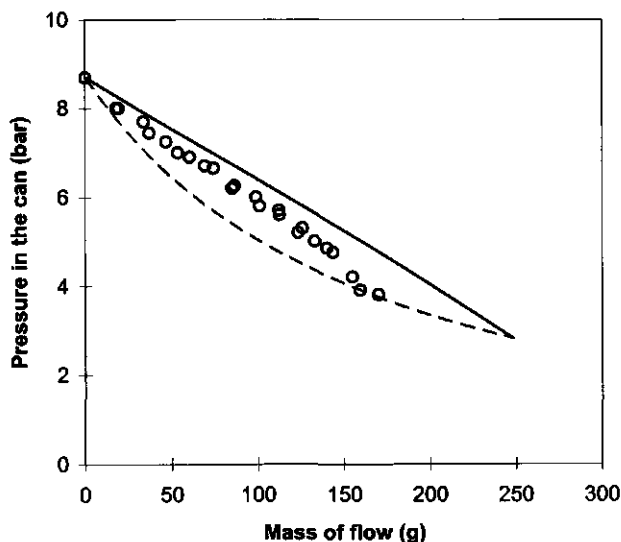
Figure 2.5   Pressure in the can versus mass of the flow out of a shaken can, measured (o) and calculated assuming absence of phase equilibrium (- - -) or phase equilibrium (——); dissolved gas and 20 vol % of not dissolved gas leaves the can with the cream. S = 2.44 g/kg/bar; k = $2.10 \cdot 10^{-2}$.

As mentioned before (§ 2.3.2) the shaking of the can has an effect on the initial pressure; the pressure decreases due to the shaking. In the absence of bubbles in the cream, there is only a relatively small interacting interface between gas and cream and a relatively long diffusion length for the gas molecules. Therefore, it is not unlikely that the assumed phase equilibrium in the cans is not achieved after storage during several weeks.

2.4   Flow properties of aerated cream through a nozzle

2.4.1 Theory on two-phase flow

In a restricted system, such as a pipe, the flow of a homogeneous medium cannot exceed the propagation velocity of a longitudinal pressure wave. The flow is limited to the so called 'choking' conditions where the velocity equals the speed of sound.

Speed of sound
The speed of sound c is the velocity with which a longitudinal pressure wave propagates through a continuous medium. The general equation for the speed of

sound in solids, liquids and gases at constant entropy is (de Nevers, 1991):

$$c = \left(\frac{\partial P}{\partial \rho}\right)_s^{1/2} \tag{2.14}$$

where P is the pressure, ρ the density of the medium and subscript s indicates the isentropic condition.

For solids and liquids it is justified and easier to use the speed of sound at constant temperature T. In practice the compression modulus K of the bulk, which is the reciprocal of the isothermal compressibility κ, is used to calculate c. The speed of sound in a liquid c_l is then given by:

$$c_l \approx \left(\frac{\partial P}{\partial \rho}\right)_T^{1/2} = \left(\frac{K}{\rho}\right)^{1/2} \tag{2.15}$$

For real gases it is not justified to use c at constant temperature instead of constant entropy. The speed of sound now depends on the constant γ, which is the ratio of the specific heat capacity of the gas at constant pressure $C_{g,P}$ and at constant volume $C_{g,V}$. The speed of sound c_g for a perfect gas is:

$$c_g = \left(\frac{\partial P}{\partial \rho}\right)_S^{1/2} = \left(\frac{\gamma P}{\rho}\right)^{1/2} = \left(\frac{\gamma RT}{M_g}\right)^{1/2} \tag{2.16}$$

For the derivation of the speed of sound in two-component gas-liquid flow an homogeneous bubbly mixture is considered (van Wijngaarden, 1972; Wallis, 1969). The gas is assumed to be insoluble in the liquid. The density of the mixture equals:

$$\rho_f = \alpha \rho_g + (1 - \alpha)\rho_l \tag{2.17}$$

where ρ_f, ρ_g and ρ_l are the densities of respectively the foam, gas and liquid; α is the volume fraction of gas in the foam. This equation can be used to derive the speed of sound in the foam c_f:

$$\frac{1}{c_f^2} = \left(\frac{d\rho_f}{dP}\right)_S = \alpha \frac{d\rho_g}{dP} + (\rho_g - \rho_l)\frac{d\alpha}{dP} + (1 - \alpha)\frac{d\rho_l}{dP} \tag{2.18}$$

In a homogeneous mixture, the gas and liquid move with the same velocity. Therefore, the ratio of the mass of gas to the mass of liquid is constant:

$$\frac{\alpha \rho_g}{(1 - \alpha)\rho_l} = \text{constant} = k \tag{2.19}$$

Differentiating equation (2.19), combining it with equation (2.18) and writing c_g^2 for $dP/d\rho_g$ and c_l^2 for $dP/d\rho_l$ results in an equation for c_f :

$$\frac{1}{c_f^2} = \rho_f \left(\frac{\alpha}{\rho_g c_g^2} + \frac{(1-\alpha)}{\rho_l c_l^2} \right) \tag{2.20}$$

It can be assumed that frictionless flow through a hole is adiabatic (isentropic). The expansion of the mixture will depend upon the heat transfer between the gas and the liquid phase (Wallis, 1969). In the absence of mutual heat transfer, the gas phase will expand isentropically according to:

$$P_t \rho_g^{-\gamma} = \text{constant} \tag{2.21}$$

where γ equals $C_{g,P}/C_{g,V}$. On the other hand, if the gas and liquid are in thermal equilibrium, meaning equal temperature in both phases due to rapid heat transfer, it can be derived from the equation for energy conservation that (Tangren et al., 1949; Wallis, 1969):

$$P_t \rho_g^{-\Gamma} = \text{constant} \tag{2.22}$$

Here, Γ is the two-phase isentropic exponent for a thermal equilibrium process:

$$\Gamma = \frac{k C_{g,P} + C_{l,P}}{k C_{g,V} + C_{l,P}} \tag{2.23}$$

with k being the constant as defined by equation (2.19) and $C_{l,P}$ the specific heat capacity of the liquid at constant pressure. Note that in the absence of liquid ($k = \infty$) the value of Γ equals γ. Thus, for pure gas equation (2.22) reduces to equation (2.21). For relatively small values of k (in aerosol cans $k \approx 0.02$) the gas expansion approaches the isothermic relation ($\Gamma = 1$).

Because a homogeneous mixture is considered it seems justified to assume thermal equilibrium. The velocity of sound in aerosol whipped cream can now be plotted as a function of the volume fraction of gas using equation (2.20) in combination with equation (2.22). In pure nitrous oxide ($\alpha = 1$) c_g equals 262 m/s; in cream with a fat content of 35 % w/w ($\rho_l = 1008$ kg/m^3) at a temperature of 5 °C ($\alpha = 0$) c_l is estimated to be 1500 m/s (appendix III). Unless α is very close either to zero or to unity, the latter term in equation (2.20) can be neglected and the value of c_l does not significantly affect the speed of sound in the mixture.

Figure 2.6   The velocity of sound in aerosol whipped cream versus the volume fraction of gas at atmospheric pressure (———) and at 9 bar (- - -) calculated using equation (2.20), gas solubility neglected; c_g = 262 m/s, c_l = 1500 m/s.

It is interesting to note that, except close to the single phase situations, the speed of sound in the two-phase mixture is considerably lower than the speed of sound in pure gas. When the volume fraction of gas is very close to zero, the strong decrease in c_f with increasing α follows from a noticeable decrease of the compression modulus with only a small decrease of the density of the mixture (equation (2.15)). For a volume fraction of gas very close to unity, the compression modulus does not change very much with increasing α but the difference in density in the presence or absence of liquid is considerable. This results in the strong increase of the velocity of sound. The minimum velocity of sound in the bubbly cream is reached at a volume fraction α of 0.5.

At a higher pressure the velocity of sound for a similar value of α becomes larger as can be seen in figure 2.6. Since ρ_l does not change significantly with pressure and c_g is independent of the pressure (equation (2.16)), the higher gas density is responsible for this larger value of c_f (equation (2.20)).

In the derivation of equation (2.20) the solubility of nitrous oxide in cream is neglected. In practice it is not justified to do so since a considerable amount of the gas can be dissolved in the cream. This has to be accounted for in the calculation of the velocity of sound. Assuming that phase equilibrium is established, the mass of gas dissolved in the liquid phase ρ_s is related to the total pressure P, according

to:

$$p_s = \rho_1 S_c P_t \qquad (2.24)$$

where S_c is the solubility of the gas in the liquid, corrected for the presence of other gases; S_c equals $S.p_g/P_t$ with p_g being the partial gas pressure and P_t the total pressure.

The density of the aerosol whipped cream ρ_f can now be written as:

$$\rho_f = \alpha \rho_g + (1-\alpha)(\rho_s + \rho_1) \qquad (2.25)$$

The ratio k of the gas mass flow to the cream mass flow in the presence of dissolved gas follows from:

$$\frac{\alpha \rho_g + (1-\alpha)\rho_s}{(1-\alpha)\rho_1} = k \qquad (2.26)$$

As described before, a relation for the velocity of sound can be derived using these equations for the foam density and the constant k. Including the effect of the dissolved gas, the relation for c_f becomes:

$$\frac{1}{c_f^2} = \rho_f \left(\frac{\alpha}{\rho_g c_g^2} + \frac{(1-\alpha)}{\rho_1 c_1^2} + \frac{(1-\alpha)\rho_1 S_c}{\rho_g} \right) \qquad (2.27)$$

Plotting the velocity of sound as a function of the volume fraction of gas (again assuming thermal equilibrium) now gives a complete different picture compared to figure 2.6.

Again, the speed of sound in the two-phase mixture is lower than the speed of sound in pure gas. It is even lower compared to the speed of sound in a two-phase mixture when the gas solubility is neglected (figure 2.6). Moreover, the shape of the curve changes when the gas solubility is taken into account; the velocity of sound increases with increasing volume fraction of gas. c_f is minimal when the volume fraction of gas is zero. Here, there is a striking difference with figure 2.6 where the speed of sound in pure liquid ($\alpha = 0$) is maximal.
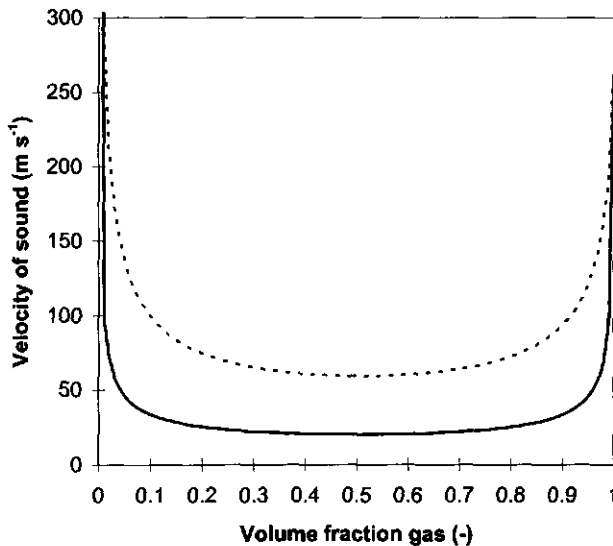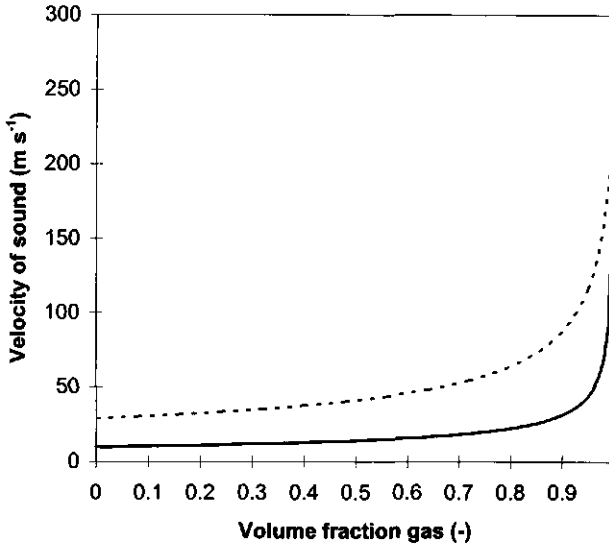
Figure 2.7   The velocity of sound in aerosol whipped cream versus the volume fraction of gas at atmospheric pressure (———) and at 9 bar (- - -) calculated with equation (2.27); the effect of the gas solubility is included assuming phase equilibrium. S_c = 2 g/kg/bar.

In the absence of a gas phase it seems out of place to consider phase equilibrium. The relation between the pressure and the mass of gas dissolved in the cream in this situation is ambiguous. It is therefore important to mark that the value of c_f at α = 0 in figure 2.7 is, analogous to the other values, calculated with equation (2.27), assuming fictitious phase equilibrium; the mass of gas dissolved in the cream is determined by equation (2.24). Thus, despite of the absence of a gas phase, the mass of gas present is not zero but completely dissolved in the cream. Since in this situation the cream is saturated with gas, a small decrease in pressure will result in the formation of the gas phase. This causes a large change in density and a small value of c_f.

Equation (2.27) assumes equilibrium between the gas dissolved in the cream and the gas present in the gas phase. In the ultimate absence of phase equilibrium ρ_s does not change with pressure. In this situation, the latter term of equation (2.27) is cancelled, turning the relation for the speed of sound into equation (2.20). Thus, depending on the state of the phase equilibrium, the speed of sound in a homogeneous mixture will vary between equation (2.20), plotted in figure 2.6, and equation (2.27), shown in figure 2.7. Note that in particular the speed of sound at α = 0 greatly depends on the mass of gas dissolved ρ_s. At atmospheric pressure, c_f can vary between and 10 and 1500 m/s. If the cream is not saturated with gas, a

small pressure fluctuation will hardly affect the density and consequently the speed of sound will be high. As soon as saturation is achieved, a gas phase can be formed due to a small pressure decrease, resulting in a low c_f.

Choked flow

Two-phase flow through a nozzle is a well described phenomenon in literature. When a compressible medium flows through a nozzle during pressure release, choking can occur; the flow is limited to a maximum value, dictated by the velocity of sound. There are numerous models describing choked flow varying from simple models to more elaborate theories. An overview of several theories is given by Wallis (1980), Isbin (1980) and Giot (1981).

Relatively simple models describing choking assume homogeneous flow (complete momentum exchange between the phases); both phases move with the same velocity, so inertia effects are neglected. For a homogeneous medium the critical flow is at sonic velocity. Two extreme cases of homogeneous flow are the equilibrium flow and the frozen flow model. Homogeneous equilibrium flow assumes thermodynamic equilibrium between the phases. Although it may be a simplification, it has been found adequate in application (Leung and Epstein, 1990; Leung, 1990; Leung and Grolms, 1987; Leung, 1986). The frozen flow model assumes no heat or mass transfer between the two phases (Henry and Fauske, 1971).

Henry and Fauske (1971) developed a non-equilibrium critical flow model that assumes neither completely frozen nor complete equilibrium heat and mass transfer processes. Instead, the model uses data to approximate the interphase heat, mass and momentum transfer. In the article, the model was compared with experimental data as were approximate models of homogeneous equilibrium and frozen flow. Although the homogeneous frozen model gave a good estimate for the critical flow rate, it predicted a lower pressure in the nozzle. The homogeneous equilibrium model, on the other hand, resulted in a good estimate of the critical pressure but underestimated the flow rate.

Alad'yev et al. (1976) described a model for two-phase nozzle flow, considering thermal equilibrium, mass transfer between the phases and allowing for phase slip. In the presence of slip the two phases move with a different velocity, the gas velocity being higher than the liquid velocity. Asbjornsen (1989) studied the effect of interfacial slip between the two phases in choked flow. Assuming equilibrium in temperature (heat) and composition (mass), the increase of the choked mass flow due to the effect of slip was calculated to be less than 5 %. Furthermore, the pressure found in the presence of slip was approximately 15 % lower.

Several authors describe more complex models on two-phase critical flow. A general mathematical model describing single and two-phase flow in relation to

choked flow is given by Bouré et al. (1976). Ishii et al. (1993) investigated bubbly flows through a converging-diverging nozzle. Assuming that the temperatures of the two phases are equal, they focused on the momentum equations; velocity slip was accounted for. The model included the particle diffusion and the repulsive force for the bubbles. Dobran (1987) and Schwellnus and Shoukri (1991) modelled two-phase critical flow allowing for hydrodynamic and thermal non-equilibrium, the former arising from differences in velocity (and sometimes pressure) and the latter from differences in temperature between the two phases. They considered different flow regimes. Shwellnus and Shoukri also accounted for bubble growth in the bubbly flow regime.

To describe the flow of aerated cream through a nozzle in the present work, a relatively simple model is applied; the flow is considered to be homogeneous. Since the amount of dissolved gas changes with pressure (equation (2.24)), mass transport is allowed for. Furthermore, thermal equilibrium between the phases is assumed.

Homogeneous flow through a nozzle

The properties of homogeneous flow of foam through a tube can be studied using the equation of continuity:

$$\dot{m}_f = \rho_f v A = \text{constant} \tag{2.28}$$

and the equation of motion:

$$\rho_f A v \, dv + A dP + f \rho_f \frac{v^2}{2} \pi D \, dL = 0 \tag{2.29}$$

where $\dot{m}_f$ is the mass flow rate of the foam, v the velocity, A the area of the tube, f the friction factor relating to the shear stress at the tube wall, D the diameter of the tube and dL part of the length of the tube over which dv and dP take place.

During the spraying process the aerosol cream passes through the cone of the valve. There are different valves used in practice with a varying amount of holes in the cone. Figure 2.8 shows a schematic drawing of the cone of a valve containing four holes; also nozzles with two holes in the cone are studied. For the description of the flow properties of the aerated cream through the nozzle, the flow is divided into three parts:

-       flow out of the can into the holes (position $0 \rightarrow 1$)
-       flow out of the holes into the tube (position $1 \rightarrow 2$)
-       flow through the tube (position $2 \rightarrow 3$)
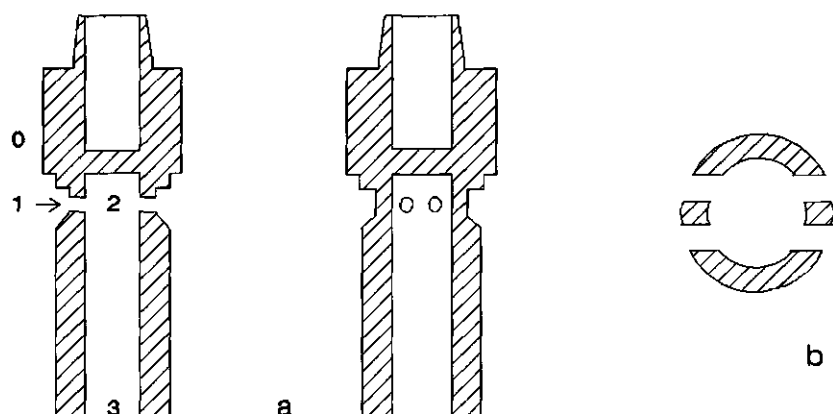
Figure 2.8   Schematic picture of the cone of an aerosol valve containing four holes; a: cross section of the cone and b: top view of the cross section (on scale); 0: inside the can, 1: in the holes, 2: directly after the holes in the tube and 3: at the end of the tube, indicating the different positions used in calculating the flow properties.

Flow out of the can into the holes (0 → 1)

Describing the flow properties through the holes in the nozzle, the equation of motion (equation (2.29)) has to be satisfied. If choking occurs, the flow properties are furthermore determined by the speed of sound (equation (2.27)). Combining these two relations gives the flow conditions in the holes.

When flow through the holes is considered, the assumption of frictionless behaviour appears to be acceptable. The equation of motion (equation (2.29)) becomes ($f = 0$):

$$v dv = -\frac{dP}{\rho_f} = -\frac{dP}{\alpha \rho_g + (1-\alpha)(\rho_s + \rho_l)} \tag{2.30}$$

or,

$$\frac{1}{2}v_1^2 = -\int_0^1 \frac{dP}{\alpha \rho_g + (1-\alpha)(\rho_s + \rho_l)} \tag{2.30'}$$

The cream is assumed to be incompressible (ρ_l = constant). Combining equation (2.30') with the relation for gas expansion ($P_t . \rho_g^{-r}$ = constant), the amount of gas dissolved ($\rho_s = \rho_l \, S_c \, P_t$) and the constant k (equation (2.26)) results in an equation for the velocity in the holes, v_1 :

$$v_1 = \sqrt{2\left[\frac{P_0 - P_1}{\rho_1(k+1)} + \frac{\Gamma k}{(\Gamma-1)(k+1)}\frac{P_0}{\rho_{g,0}}\left(1 - \left(\frac{P_1}{P_0}\right)^{\frac{\Gamma-1}{\Gamma}}\right) - \frac{\Gamma S_c}{(2\Gamma-1)(k+1)}\frac{P_0^2}{\rho_{g,0}}\left(1 - \left(\frac{P_1}{P_0}\right)^{\frac{2\Gamma-1}{\Gamma}}\right)\right]}$$

(2.31)

where P_0 is the pressure in the can, P_1 the pressure in the holes and $\rho_{g,0}$ the gas density inside the can. The derivation of the equation for v_1 is given in more detail in appendix IV.

Assuming that choking occurs, there is a physical barrier to the foam discharge through the nozzle. The mass flow rate is limited to a maximum value which prevents the pressure in the holes P_1 to decrease to the outlet conditions. At choking conditions, P_1 will therefore be higher than atmospheric pressure. The critical mass flow rate can be obtained after setting the derivative of the mass flow rate (equation (2.28)) equal to zero. Combining the result with the momentum balance (equation (2.30')) gives:

$$v_1^2 = \frac{dP}{d\rho}$$

(2.32)

Since the aerated cream is considered to be an homogeneous mixture equation (2.32) corresponds to the velocity of sound (equation (2.27)). This gives a second relation for the mean flow velocity of the aerated product in the holes:

$$\frac{1}{v_1^2} = \frac{1}{c_f^2} = \rho_f \left(\frac{\alpha}{\rho_g c_g^2} + \frac{(1-\alpha)}{\rho_1 c_1^2} + \frac{(1-\alpha)\rho_1 S_c}{\rho_g} \right)$$

(2.32a)

In the occurrence of choking, the flow conditions in the holes therefore follow from the combination of equation (2.31) and equation (2.32a).

Flow out of the holes into the tube (1 → 2)
The different flows of foam out of the separate holes collide with one another when entering the tube. Additionally, they have to make a bend and the flow area is enlarged. These events are accompanied by a pressure drop resulting in a change of the flow properties. It is difficult to calculate this pressure drop, since it is composed of different parts. Literature on transport phenomena (Beek and Muttzall, 1975; Bird et al.,1960) describes that in general the pressure drop induced by the presence of a fitting in a tube follows from:

$$\Delta P_{e_v} = \frac{1}{2}\rho_f v_e^2 e_v \tag{2.33}$$

with v_e being the velocity downstream of the fitting (in the nozzle this is velocity v_2, at the entrance of the tube) and e_v the friction loss factor. In the presence of several fittings, the total pressure drop is simply given by the sum of the pressure drops induced per single fitting. A bend induces a friction loss factor of 0.02-2.43, depending on the angle and the shape (rounded or square) of the bend (Beek and Muttzall, 1975). For a sudden enlargement of the area the friction loss factor is given by:

$$e_v = \left(\frac{A_2}{A_1} - 1\right)^2 \tag{2.34}$$

where A_1 is the total area of the holes and A_2 is the area of the tube.

When the pressure P_2 is known, the gas density $\rho_{g,2}$ at the position directly after the holes (position 2 in figure 2.8) can be calculated; isothermic expansion of the gas is assumed:

$$\frac{P_t}{\rho_g} = \text{constant} \tag{2.35}$$

The mass flow rate follows from the choking conditions in the holes. Using the areas of the holes and the tube, the velocity v_2 results from the continuity equation (2.28).

Flow through the tube (2 → 3)

Describing the flow through the tube, the friction cannot be neglected. It is difficult to accurately describe the frictional flow of foam. Depending on the dimensions of the bubbles and the tube, it is not always justified to neglect the fact that foam is a heterogeneous dispersion. Furthermore, the compressibility and instability of a foam affects the flow properties (Heller and Kuntamukkula, 1987).

Müller-Steinhagen and Heck (1986) used the frictional pressure drop of the respective single-phase flow to describe a relatively simple correlation for the two-phase gas-liquid flow. Other authors used experimental data to derive a correlation between the friction factor and the Reynolds number (Dziubinski, 1995; Davis and Wang, 1994). The friction factor depends on the viscosity of the foam. Usually the apparent foam viscosity η^* can be described by means of a power law relation (Kroezen, 1988; Wenzel et al., 1970):

$$\eta^* = \frac{\tau}{\dot{\gamma}} = p\dot{\gamma}^{q-1} \tag{2.36}$$

where τ is the shear stress, $\dot{\gamma}$ the shear rate, p a rheological constant and q a plasticity factor. The viscosity of a foam depends on the other foam properties and increases with decreasing bubble diameter and decreasing foam density. Additionally, it strongly depends on the viscosity of the liquid phase. Aerosol whipping cream is a shear thinning fluid; the viscosity decreases with increasing shear rate. At large shear rates (> 1000 s^{-1}) the viscosity seems to reach a plateau value of approximately 0.04 Pa s (appendix II).

Kroezen (1988) measured the apparent viscosity of foams of varying density, produced from liquids with varying viscosity (at $\alpha = 0$) using a coaxial Brabender viscometer. From his results a plasticity factor q of 0.5 and a rheological constant p of 5.65 Pa $s^{0.5}$ were derived for a foam with properties similar to aerosol whipped cream (liquid viscosity of 0.05 Pa s, $\rho_f = 300$ g/l, bubble diameter 75 μm). These values were used to estimate a friction factor for the flow of aerosol whipped cream through a tube. Since $q < 1$ the foam behaves pseudoplastic (shear-thinning).

When the foam is considered to be a continuous, non-Newtonian (power law) fluid the friction factor f for laminar flow through a tube, in the absence of slip at the wall, follows from (de Nevers, 1991; Astarita and Marrucci, 1974; Bird et al., 1960; Metzner and Reed, 1955):

$$f = \frac{16}{Re}$$

with $\hspace{9cm}$ (2.37)

$$Re = \frac{\rho_f v^{2-q} D^q}{p \, 2^{q-3}\left(\frac{3q+1}{q}\right)^q}$$

where Re is the Reynolds number, ρ_f the foam density, v the velocity and D the tube diameter.

With use of the friction factor for flow through the tube, the flow conditions (v, P, ρ_f) of aerosol whipped cream can be derived from the momentum equation (2.29) and the continuity equation (2.28). The friction factor is taken to be constant during the flow. Since in practice the tube of a nozzle is usually straight, the tube area A is also constant. Furthermore, the gas expansion is considered to be isothermic (equation (2.35)) and phase equilibrium is assumed (equation (2.24)). During the flow through the tube the pressure drops, which is accompanied by a change in the

foam density and velocity. Therefore, it is more accurate to combine the equations
(2.28) and (2.29) with the pressure gradient, the velocity and the length in a
differential form. The resulting relations between dL, dv and dP are:

$$dP = \frac{2}{D} \frac{f\rho_g \rho_f P v^2}{\rho_f v^2 (\alpha \rho_g + (1-\alpha)\rho_s) - \rho_g P} dL \qquad (2.38)$$

and

$$dv = -\left(\frac{\alpha \rho_g + (1-\alpha)\rho_s}{\rho_g P}\right) v \, dP \qquad (2.39)$$

The derivation of these equations is given in more detail in appendix V.

2.4.2 Experimental

Choked flow
To check whether the theory of choked flow is valid for the flow of aerosol whipped
cream out of an aerosol can, the theory was used to calculate the mass flow rate
through the nozzle during the spraying process. Since the pressure decreases as a
function of the mass of flow out of the can (§ 2.3), the mass flow rate will also
decrease in time. This has to be accounted for. Additionally, the mass flow was
experimentally determined as a function of time. The calculations and experiments
were compared with each other.
The calculations were performed numerically by increasing the mass of the flow to
its maximum value in 25 steps. After each step the pressure P_0 was calculated
using the relation between P_0 and the mass of the flow m. This relation was
obtained by fitting the measured data of P_0 versus m of figure 2.3 (not shaken can)
or figure 2.5 (shaken can). For the unshaken can this resulted in a third grade
polynomial function; in the shaken can the pressure decreased linear with the mass
of flow.
When the pressure in the can is known, the choking conditions in the holes can be
found by equating the equations (2.27) and (2.31). With the resulting velocity in the
holes the mass flow rate $\dot{m}_{1,t}$ at time t was calculated:

$$\dot{m}_{1,t} = \rho_{f,t} v_{1,t} A_1 \qquad (2.40)$$

where $\rho_{f,t}$ is the foam density at time t, $v_{1,t}$ the velocity in the holes at time t and A_1
the area of the holes. The mass flow rate relates the mass of the flow out of the
can to time:

$$m_{t,i} = m_{t,i-1} + (t_i - t_{i-1})\dot{m}_{t,i} \qquad (2.41)$$

with $m_{t,i}$ indicating the total mass of the flow at time t_i. Thus, the calculated curve of mass of flow versus time follows.

The experimental measurements of the mass flow in the time were performed using aerosol cans with a volume of 405 ml, equipped with nozzles having the following dimensions:

4 holes: diameter = 0.6 mm; length = 0.6 mm

1 tube: diameter = 2.0 mm; length = 7.5 mm

The cans were filled with 243 ± 1 g of cream with a fat content of 35 % w/w; 7.0 ± 0.1 g of nitrous oxide was added and the cans were stored at approximately 5 °C during several weeks. Besides the nitrous oxide there was approximately 0.2 g of air present in the cans.

The mass flow out of the can was determined in time by emptying the can at one stretch in a bowl on a balance. Simultaneously, time was monitored by means of a computer connected to the balance. The experiments were performed in duplicate. To study the effect of shaking, both shaken and not shaken aerosol cans were used.

Nozzle geometry

When the nozzle geometry is known, the complete flow properties through the nozzle can be calculated: out of the can into the holes ($0 \rightarrow 1$), out of the holes into the tube ($1 \rightarrow 2$) and through the tube ($2 \rightarrow 3$) (figure 2.8). These calculations were performed for a nozzle as described in the previous section.

The properties of the flow out of the can into the holes follow from the theory on choked flow. Since it is difficult to estimate the pressure drop caused by the flow out of the holes into the tube (§ 2.4.1), P_2 and the resulting flow properties directly after the holes, cannot be calculated directly. However, the situation at the end of the nozzle is known; it is either choking condition or the pressure is atmospheric. Hence, the flow properties in the second and third part of the nozzle were calculated in combination with each other.

In order to be able to calculate the flow properties through the tube, the conditions at the entrance of the tube have to be known. Therefore, the pressure at the entrance of the tube P_2 was estimated. P_2 determines the value of $\rho_{g,2}$ (equation (2.35)) and $\rho_{s,2}$ (equation (2.24)) and thus α_2 can be calculated using the constant k (equation (2.26)). $\rho_{f,2}$ now easily follows from equation (2.25). Finally, the velocity v_2 can be calculated with the continuity equation (2.28).

Knowing the conditions at the entrance of the tube, the flow conditions through the

tube can be calculated with equations (2.38) and (2.39); the friction factor f was estimated to be 0.025, agreeing with the flow conditions in the tube. The calculations were performed numerically by means of a computer program. In this program the length of the tube L was increased in steps of ΔL = 0.1 mm. This change in length ΔL was used to calculate the change in pressure ΔP and the change in velocity Δv, resulting in a 'new' P and v (equations (2.38) and (2.39)). The calculations were repeated until $\Sigma \Delta L$ equalled the total length of the tube and values for P_3 and v_3 were obtained. Additionally, $\rho_{g,3}$, $\rho_{s,3}$ and α_3 at pressure P_3 were calculated using respectively equations (2.35), (2.24) and (2.26).

During this procedure, the velocity in the tube was limited to the speed of sound. If, however, choking conditions were not reached the pressure P_3 at the end of the tube had to be atmospheric. If these requirements were not fulfilled an other P_2 was estimated and the procedure was repeated. With the final results of the calculations the complete flow through the nozzle could be described.

Changing the geometry of the nozzle can supply more information about the flow phenomena through the nozzle. The effect of the nozzle geometry on the spraying process was studied by measuring and comparing the mass flow curves for the different nozzle geometries. Experiments were performed with both shaken and not shaken aerosol cans.

The aerosol cans used for the experiments were analogous to the cans described in the previous section (on choked flow), having the same contents. The nozzle geometry was varied at two positions. Firstly, two types of nozzles with different holes in the nozzle cone were compared:

> nozzle 2: 2 holes with a diameter and length of 1.0 mm

> nozzle 4: 4 holes with a diameter and length of 0.6 mm

Secondly, the length of the nozzle tube was extended with a plastic tube. This tube was positioned on an extension piece which fits on the tube of the nozzle. The nozzle could be opened by pressing the extension piece. The length of the nozzle tube was varied from 0.8 cm (no extension) to 20 cm.

2.4.3 Results and Discussion

Choked flow

The mass flow versus time was measured for an aerosol can that was not shaken before spraying. The measured data (symbols) and the calculations, assuming either phase equilibrium (solid line) or no phase equilibrium (dashed line) in the nozzle, are plotted in figure 2.9.

Figure 2.9   Mass of the flow versus time out of aerosol can equipped with nozzle 4, measured
(▲) and calculated assuming absence of phase equilibrium (– – –) or phase
equilibrium (——); can not shaken before use. S = 2.2 g/kg/bar.

In the ultimate absence of phase equilibrium, indicated by the dashed line in the
graph, the gas will remain dissolved in the cream while passing through the nozzle.
The speed of sound in liquid is high and will not form a restriction to the mass flow;
the velocity is simply determined by liquid transport phenomena. In the presence of
bubbles, the flow properties will be restricted to the choking conditions. Figure 2.9
shows that the flow of aerosol whipped cream through the nozzle indeed can be
described by theory of choked flow; the experimental data excellently follow the
calculation for the two-phase flow equilibrium situation. Apparently, it only takes a
very short time for the newly formed bubbles to approach an equilibrium situation
with the surrounding liquid.
Processes that effect establishment of the equilibrium are gas diffusion and
convection. The penetration theory states that the diffusion length can be estimated
by $\sqrt{(\pi \, D \, t)}$, where D is the diffusion coefficient of the gas in the liquid. The cream
passes through the holes of the nozzle within a very short time ($\approx 2 \cdot 10^{-5}$ s). Using a
D of $2.11 \cdot 10^{-9}$ m^2/s (D for N_2O in water at 20 °C; Jansen and Warmoeskerken,
1987), the diffusion length in $2 \cdot 10^{-5}$ s is estimated to be 0.36 μm. Since it is not
very likely that the distance between the bubbles in the nozzle holes is on average
this small, it seems impossible that the equilibrium between the gas bubbles and
the cream is established only by gas diffusion. Therefore, convection will probably

contribute to the transport of gas.

Shaking of the can has a noticeable effect on the mass flow as can be seen in figure 2.10. Again the measured data (symbols) are compared with the calculations corresponding to the absence (dashed line) and presence (solid line) of phase equilibrium.
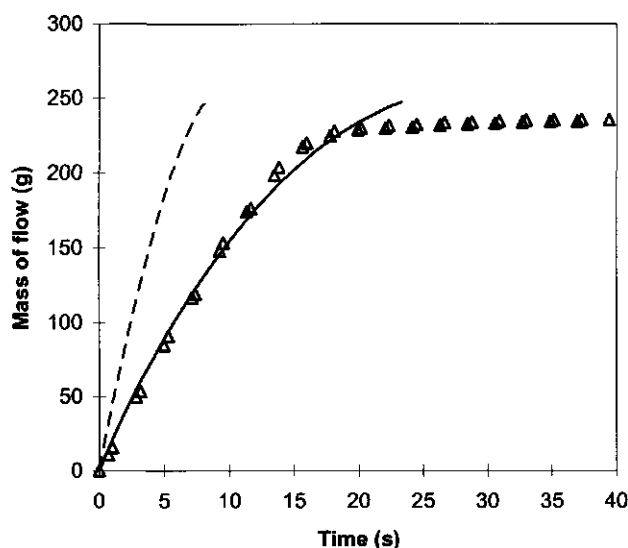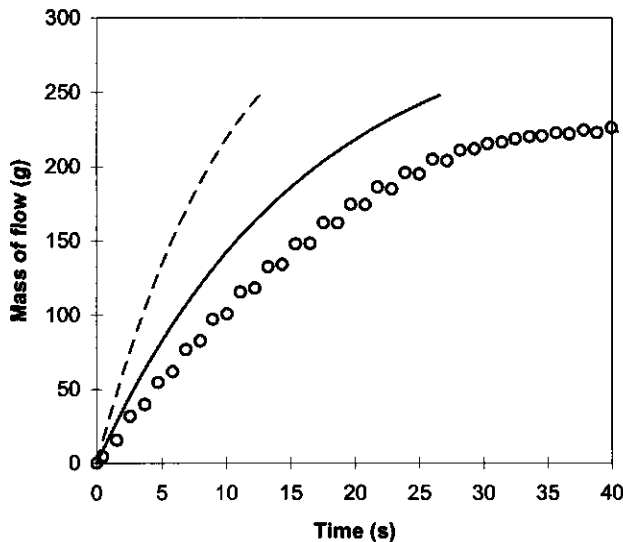

Figure 2.10   Mass of the flow versus time out of aerosol can equipped with nozzle 4, measured (o) and calculated assuming absence of phase equilibrium (– – –) or phase equilibrium (——); can shaken before use. S = 2.44 g/kg/bar.

Since the results for the unshaken aerosol can indicated phase equilibrium in the nozzle, it is likely that also in the nozzle of a shaken can the phase equilibrium is approached. The measured data indeed show most resemblance with the equilibrium situation. There is, however, a considerable deviation between calculation and experiment; the measured mass flow curve is positioned below the curve calculated for the equilibrium situation. The presence of relatively large bubbles, flowing out of the can through the nozzle, probably hinders the flow phenomena. When the size of the bubbles is in the order of the size of the holes it is imaginable that, after the pressure drop, the bubbles will completely fill the holes. The flow will locally be dominated by gas flow phenomena, thereby disturbing the homogeneous two-phase flow. An indication for this disturbance is the amount of sputtering of the whipped cream while it leaves the nozzle. Emptying an unshaken aerosol can gives a smooth, silent flow. Shaking of the can clearly induces

sputtering; this can be heard and seen.

Nozzle geometry

The complete flow properties through the nozzle follow from the calculations described in § 2.4.2. Since the flow out of an unshaken can through the nozzle smoothly followed the theory of choked flow, the calculations were performed for an unshaken can; constant $k = 1.82 \cdot 10^{-2}$, $P_{1,0} = 9.24$ bar. Figure 2.11 shows the pressure (a), the velocity (b) and the volume fraction of gas (c) as a function of the distance in the nozzle. A distance of zero corresponds to the position directly after the holes.

The solid triangle and circle in the plots represent respectively position 0 in the can (directly before the holes) and position 1 in the holes, the solid squares indicate the entrance (position 2) and the end (position 3) of the tube. Since it is not exactly known how the flow properties develop in and directly after the holes of the nozzle, the course of the parameters is given by a dotted line. The solid line represents the calculations for the different parameters during flow through the tube; the dashed line in figure 2.11.b corresponds to the calculated speed of sound.

Figure 2.11.a shows that the pressure between the can and the holes drops with approximately a factor 1.5. The pressure is larger than atmospheric, indicating choked flow. This is confirmed by the velocity in the holes, which indeed equals the speed of sound (figure 2.11.b). Also at the end of the nozzle tube choking occurs. Figure 2.11.c shows that the volume fraction of gas strongly increases when flowing through the holes. This indicates that foam formation occurs in the holes. At the end of the tube it reaches a value of 0.8 which is close to the volume fraction of gas in the resulting foam (0.86).

The effect of the geometry of the nozzle cone on the mass flow curves is plotted in figure 2.12. The dashed lines correspond to nozzle 2 (cone with two holes); the dotted lines indicate nozzle 4 (cone with four holes). The effect of shaking of the aerosol can is included.

The major difference between the two nozzles is the total area of the holes in the cone, being 1.57 mm^2 for nozzle 2 and 1.13 mm^2 for nozzle 4. From the theory used on choked flow it is expected that the flow area will not influence the choking conditions. Therefore, the difference in area of the holes should have a proportional effect on the mass flow rate through the nozzle.
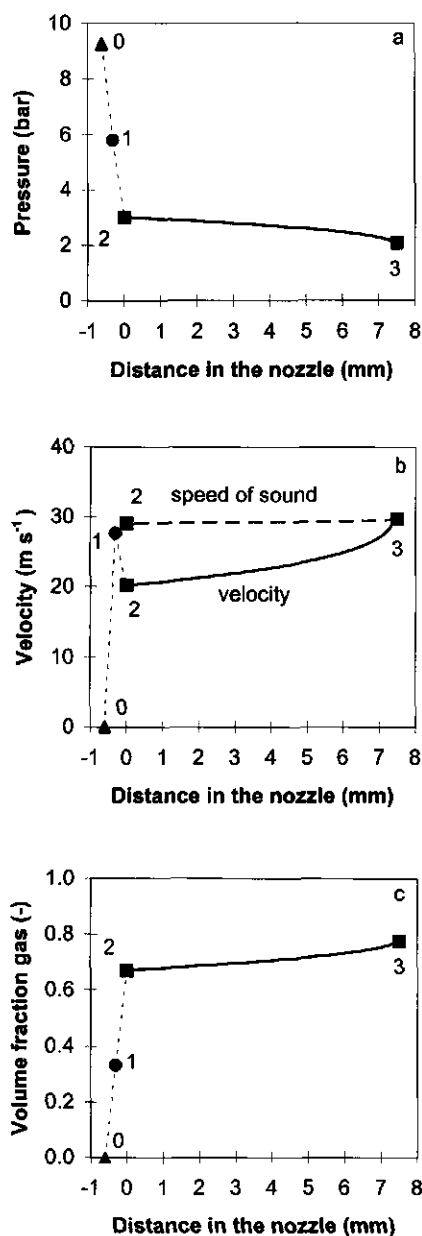
Figure 2.11   Pressure (a), velocity (b) and volume fraction of gas (c) as a function of the distance
in nozzle 4, calculated for a not shaken aerosol can; S = 2.2 g/kg/bar. 0 (▲)
corresponds to the position in the can, 1 (●) to the holes, 2 (■) and 3(■)
correspond to the entrance and end of the nozzle tube (figure 2.8).
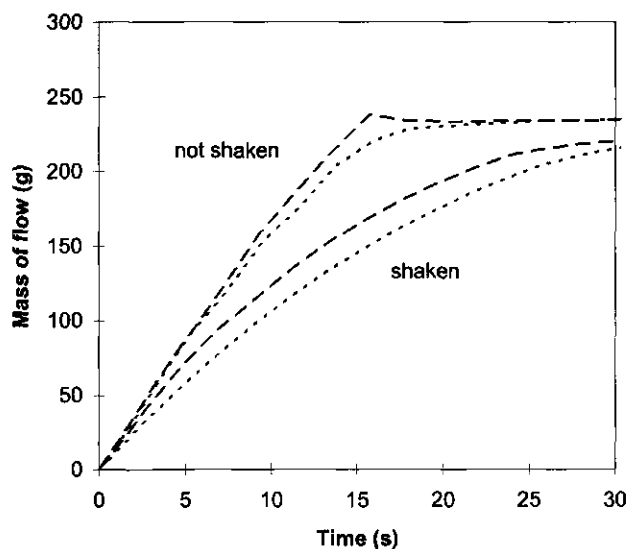
Figure 2.12   Mass of flow versus time for nozzle 2 (– –) and nozzle 4 (- - -) having different geometry of the cone and demonstrating the effect of shaking.

Figure 2.12 indeed shows an effect of the flow area on the mass flow curve. Compared to nozzle 4, the mass flow rate through nozzle 2 is approximately 10 % larger, independent of the shaking of the can. From the difference in flow area between the nozzles, however, a difference of 40 % was expected.

Two effects might partly account for the fact that the observed mass flow rate through nozzle 2 was lower than expected. The first effect follows from the geometry of the nozzle. Woschitz et al. (1986) studied air-water flow (water particles in air) through multiple-hole radial nozzles with a varying amount of holes. Comparing two types of nozzles with different amount of holes (2 or 4) but equal hole area showed that the mass flow rate through a nozzle with four holes is somewhat larger than twice the mass flow rate through a nozzle with two holes. They attributed this difference to more favourable flow properties in the four-hole nozzle. A similar effect could be found from their data considering the size of the holes; tripling of the diameter resulted in a proportional slightly lower mass flow rate. Depending on the liquid flow and the volume faction of gas, differences up to 10 % were found in both cases. Although the radial nozzles studied clearly differ from the nozzles used for aerosol cans, it is possible that similar effects occur there also.

A second reason for the lower mass flow rate through nozzle 2 might be found in the material properties of the nozzle. It has been observed that pressing the nozzle

can result in deformation of the plastic cone. This affects the flow area of the holes in the cone in a negative way. The cone of nozzle 4 showed to be less susceptible to deformation.

The effect of the length of the nozzle tube on the mass flow curves is plotted in figure 2.13 for not shaken cans.
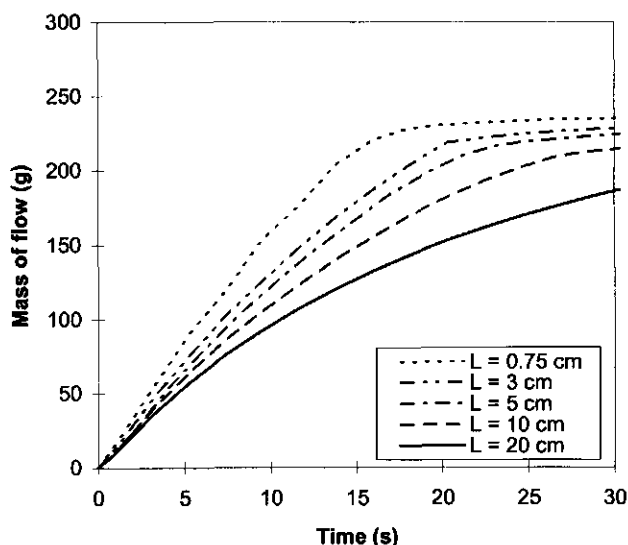
Figure 2.13   Mass of flow versus time for varying length of the nozzle tube for not shaken aerosol cans; nozzle 4.

The length of a not extended nozzle tube is 0.75 cm. Doubling of this length to 1.5 cm showed no effect on the mass flow curve; the mass flow rate is still determined by choking conditions. For longer tubes, starting at a length of 3 cm, the mass flow rate lowers with increasing length. This indicates that choking no longer occurs in the nozzle. For shaken cans similar effects were found.

The calculations described in § 2.4.2 can be used to estimate the tube length at which the choking conditions can no longer be reached. As was pointed out before, it is difficult to calculate the pressure drop resulting from the flow of foam out of the holes into the tube. For the area enlargement a friction loss factor of 3.16 can be calculated (equation (2.34); A_1 = 1.13 mm, A_2 = 3.14 mm). The friction caused by the collision of the flows out of the different holes and by the presence of the bend is more difficult to estimate.

Assuming choked flow, a pressure P_0 of 9.24 bar induces a pressure of 5.80 bar in the holes. The resulting flow properties through the nozzle were calculated for

tubes with a length L of 0.75, 1.5 and 3 cm. The calculated conditions directly after the holes are given in table 2.1.

Table 2.1   Flow conditions directly after the holes for tubes with a length of 0.75, 1.5 and 3 cm; P_1 = 5.80 bar.

L (cm)	P_2 (bar)	ρ_2 (kg m^{-3})	v_2 (m s^{-1})	ΔP_{area} (bar)
0.75	3.01	338	20.2	2.18
1.5	3.28	370	18.4	1.98
3.0	4.00	458	14.9	1.61

The last column of the table gives the calculated pressure drop ΔP_{area} induced by the area enlargement (equation (2.34)); $e_{v,area}$ = 3.16.
Since the pressure drop caused by the presence of the fittings has to equal P_1-P_2, the remaining friction loss factor $e_{v,rem}$ can be calculated using equation (2.33). From the data for the nozzle with L = 0.75 cm, the resulting friction loss factor for the collision of the flows and the presence of the bend equals 0.88. Note that this value is in the range of the friction loss factor for a bend (0.02-2.43; § 2.4.1).
The total pressure drop ΔP_{ev} caused by the several fittings can be calculated using the total fiction loss factor $e_{v,area}$+ $e_{v,rem}$= 4.04 (equation (2.33)). Addition of ΔP_{ev} to P_2 gives a value for the pressure in the holes. This value, P_1', can be used to check whether the pressure drop necessary for the choking conditions can be achieved. For L = 1.5 cm the calculated P_1' is 5.81 bar, which equals the choking condition. For L = 3 cm the calculated P_1' = 6.05 bar, exceeding 5.80 bar; choking will therefore not occur. This is in agreement with the mass flow measurements (figure 2.13).

2.5   Initial foam properties of aerosol whipped cream

2.5.1 Theoretical considerations

There are several parameters that can be used to describe the initial foam properties, the properties of the foam directly after production. Characteristic initial properties of a foam are the overrun, the firmness and the bubble size distribution. The overrun O (%) is a measure for the amount of gas that is retained in the foam:

$$O = \frac{100\,\alpha}{1-\alpha} \qquad (2.42)$$

where α is the volume fraction of gas in the foam. Aerosol whipped cream is known

to be a light product, having a relatively high overrun (chapter 1).

The firmness of a product is a vaguely defined term for a property that relates to the viscosity and elasticity of that product. Considering foams, as a compressible medium, it is even more difficult to specify this property. The firmness greatly depends on the measuring method and since there are numerous methods to measure it, there is an equal amount of ways to define it. In this study the firmness is defined to be the maximum resistance of the aerosol whipped cream against a standardised deformation (compression), applied by a cylindrical plunger.

Since aerosol whipped cream destabilises very fast (chapter 1), it is necessary to characterise the foam within a short time (within a minute). The overrun and firmness of aerosol whipped cream can be determined within this short time. The determination of the bubble size distribution is however a more complex procedure (see chapter 4), which takes more time. Therefore, the latter property was not considered.

Mass of dissolved gas

As described before aerosol whipped cream originates from with nitrous oxide supersaturated cream. It is speculated that the initial foam properties, in particular the overrun of the foam, are directly determined by the amount of gas dissolved in the cream. A larger mass of dissolved gas is expected to give a higher overrun. In theory, the overrun is limited to a maximum value, the feasible overrun O_f:

$$O_f = \frac{(\rho_{s,0} - \rho_{s,atm})}{\rho_{g,atm}} * 100 = \frac{(p_{g,0} - P_{atm})\rho_l S}{\rho_{g,atm}} * 100 \qquad (2.43)$$

where $\rho_{s,0}$ and $\rho_{s,atm}$ are respectively the mass of gas dissolved in the cream in the can (determined by the partial gas pressure $p_{g,0}$) and at atmospheric pressure P_{atm}. $\rho_{g,atm}$ is the gas density at atmospheric pressure. Note that immediately after the spraying process the gas in the whipped product is mainly nitrous oxide; the partial pressure is approximately 1 bar.

The firmness of a foam depends on the foam structure, which is a difficult to measure parameter in all its details. The foam structure obviously relates to the density and hence to the overrun of the foam. A correlation between the firmness and the overrun of aerosol whipped cream is therefore expected.

Geometry of the nozzle

In § 2.4 it was shown that the geometry of the nozzle influences the flow properties of aerated cream through that nozzle. In particular extension of the nozzle tube induced a significant change in the mass flow curve. At a tube length longer than 3 cm choking conditions were no longer achieved (figure 2.13). Different flow

properties through the nozzle might affect the foam formation process. It is therefore interesting to study the effect of the nozzle geometry on the initial foam properties of aerosol whipped cream.

2.5.2 Experimental

Mass of dissolved gas

The effect of the mass of gas dissolved in the cream on the initial overrun of the foam is studied in two ways. From the conditions in the can during the spraying process (§ 2.3) it followed that shaking of the can affects the state of equilibrium between the gas dissolved in the cream and the gas present in the headspace of the can. Therefore, the effect of shaking on the initial overrun of the foam is studied first. For this purpose the aerosol cans described in § 2.4.2 were used. The overrun is calculated using the mass of a fixed volume of foam:

$$O = \frac{W_i - W_f}{W_f} * 100 \qquad (2.44)$$

where W_i is the mass of a fixed volume of unaerated cream and W_f the mass of the same volume of aerated cream. Equation (2.44) is slightly different from equation (2.42). They become similar when W_f in equation (2.44) is replaced by $(1-\alpha) W_i$, which means that the mass of gas in W_f has to be corrected for. Because the mass of gas is small compared to the mass of cream in the foam, the difference between the two equations is small; the calculated overrun is (relatively) approximately 1 % smaller than the actual overrun. This difference can be neglected compared to the differences measured between triplicates of the overrun (§ 2.5.3).

For the measurement of W_f an excessive amount of foam was sprayed into a bowl with a volume of 169 ml and a height of 3.5 cm. In order to get rid of large 'holes' in the foam, formed during the filling of the bowl, the top of the foam was slightly pushed three times with a wide spatula, after each time turning the bowl 120 °. Additionally, the foam surface in the bowl was smoothed, using the spatula to remove the excess of foam.

The overrun was measured as a function of the total mass of the flow out of the can, which was derived from the (change in) mass of the can with contents. The time scale of the measurements, which were performed in triplicate, was a few minutes. The data were compared with the calculated feasible overrun.

Secondly, the mass of dissolved gas is influenced by the temperature and fat content of the cream as described in § 2.2. The series of aerosol cans used for those experiments were also used to study the effect of the gas solubility on the initial overrun. The cans were shaken before use and the overrun was determined

for the first sample (blob) of cream. Again, the experiments were performed in triplicate and compared with the calculated feasible overrun.

Geometry of the nozzle

The effect of the nozzle geometry on the initial foam properties was studied by varying the holes (number and size) and the tube length as described in § 2.4.2, using the same aerosol cans. Measurements of the overrun as a function of the mass of flow out of the shaken can were carried out using the different nozzles.

Additional measurements of the firmness of the produced foams were performed using a Stevens Texture Analyser. The apparatus was equipped with a cylindrical plunger having a diameter of 35 mm. During the measurements, the plunger moved with a velocity of 1 mm/s to a depth of 15 mm in the foam. The maximum resistance against the deformation, referred to as the firmness of the foam (unit of gramforce), was recorded. Measurements were carried out directly after the determination of the overrun, at the same samples of foam.

2.5.3 Results and Discussion

Mass of dissolved gas

The overrun as a function of the produced mass of flow out of the can is plotted in figure 2.14 for shaken and not shaken cans. It can be seen that the triplicates relatively differ approximately 10 %; this is especially visible at the relatively high overruns.

The effect of the mass of dissolved gas on the overrun clearly follows from the plot. The overrun for not shaken cans initially remains more or less constant as a function of the mass flow. This can be directly related to the absence of phase equilibrium in the aerosol can where, in the ultimate situation, the mass of dissolved gas remains constant in time (§ 2.3). Assuming that the mass of dissolved gas is directly responsible for the overrun this indeed would result in a constant overrun as a function of the mass flow. Near the end of the spraying process, at a total mass of flow of about 150 g, the overrun decreases. This correlates to a deviation from the non equilibrium situation, where less gas will remain dissolved in the cream.

When the can is shaken, a different picture results; the overrun decreases with the mass flow. Again, this can be related to the phase equilibrium in the can. As was shown in figure 2.5 the pressure in the can, and therefore the mass of dissolved gas, decreases linearly with the mass of flow if phase equilibrium is assumed. The result is a linear decrease of the overrun with the mass of flow as can be seen in figure 2.14. The relation between the amount of dissolved gas and the overrun is apparent.
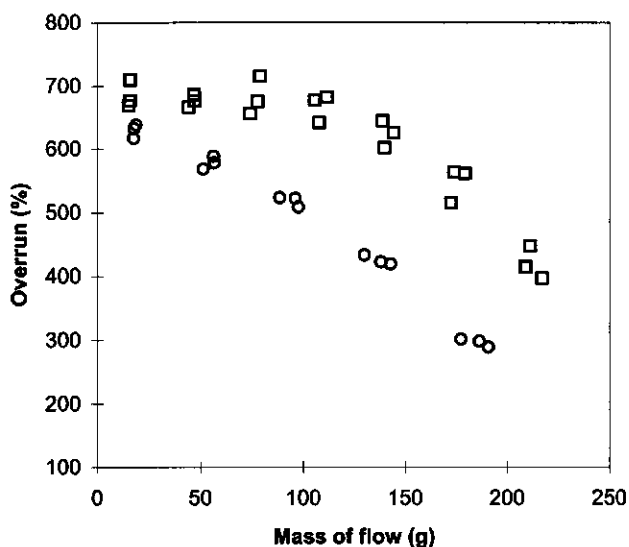
Figure 2.14   Overrun versus mass of flow for shaken (o) and not shaken (□) cans; nozzle 4.

The feasible overrun can be calculated using equation (2.43). For the initial sample of cream the feasible overrun is, depending on the pressure and the gas solubility, on average 850 %. The measured overruns are lower (figure 2.14). The foam formation of aerosol whipped cream is apparently accompanied with the loss of an amount of gas, referred to as 'blow by'. The 'blow by' is approximately 20 % (relatively) of the feasible overrun, being somewhat lower for an unshaken can than for a shaken can. It is speculated that this 'blow by' is induced by the presence of mechanical forces in the nozzle, acting upon the foam. The magnitude of these forces, which depends on the pressure drop over the nozzle, will be smaller in the nozzle of a shaken can than of an unshaken can since the pressure in the former is lower (§ 2.3). Ergo, contrary to the findings, the 'blow by' induced by mechanical forces is expected to be lower if the can is shaken. Probably, the presence of relatively large bubbles in the cream flow through the nozzle of a shaken can also negatively affects the overrun.

Besides the state of the phase equilibrium, the temperature and fat content of the cream also affect the mass of gas dissolved in the cream (§ 2.2). The initial overrun was measured as a function of the mass of gas dissolved in the cream for different temperature - fat content combinations. The fat content of the cream does have no significant effect on the relation between the overrun of the foam and the mass of gas dissolved in the cream. On the other hand, the effect of temperature on the overrun is much more pronounced. Therefore, it seems justified to group the

data per temperature. For reasons of clarity not all the data are plotted, but trend lines are shown in figure 2.15.
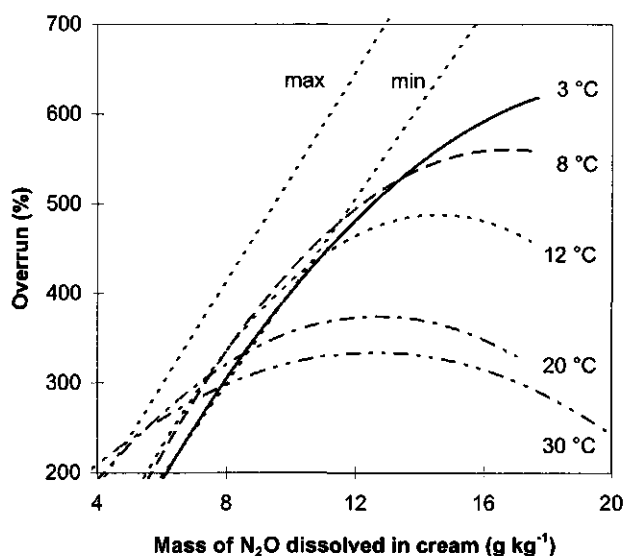
Figure 2.15   Overrun of aerosol whipped cream with different fat contents versus mass of gas dissolved in the cream at different temperatures (3 °C, 8 °C, 12 °C, 20 °C and 30 °C).

The feasible overrun depends on the solubility of the gas in the cream (equation (2.43)) and therefore on the fat content and the temperature (figure 2.2). Figure 2.15 shows two lines for the feasible overrun versus the mass of gas dissolved in the cream, indicated by 'max' and 'min'. 'Max' indicates the maximum feasible overrun caused by a low solubility of the gas (low fat content, high temperature); 'min' indicates the minimum feasible overrun caused by a high solubility of the gas (high fat content, low temperature). It can be noted that, at small masses of dissolved gas, the overrun is in reasonable agreement with the feasible overrun and, thus, indeed seems to be determined by the amount of dissolved gas. At higher masses of dissolved gas the measured overrun deviates more from the feasible overrun and in the end the overrun even shows a decrease. These observations indicate more 'blow by'. This could be caused by the increase of the pressure drop over the nozzle accompanying the increase of the mass of dissolved gas. A larger pressure drop will result in larger mechanical forces acting upon the bubbles.

Geometry of the nozzle

Figure 2.16 shows the initial overrun of the first sample of aerosol whipped cream versus the length of the nozzle tube for nozzle 4. Some data measured with nozzle 2, are included. Again it can be noted that especially at relatively high overruns (short lengths), scattering of the data becomes apparent.
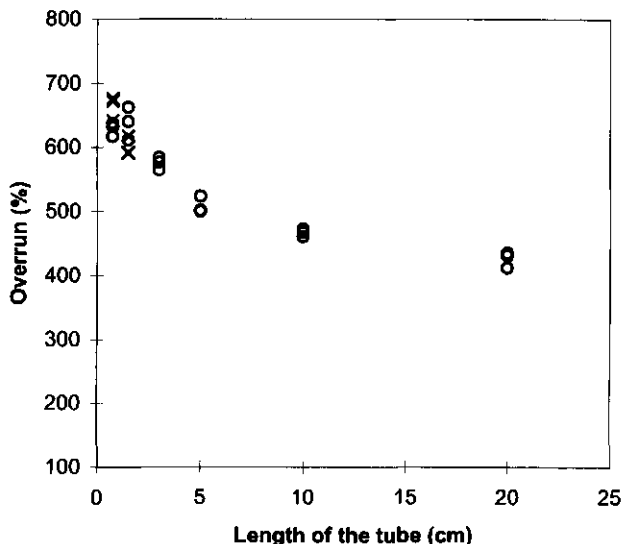
Figure 2.16   Overrun of aerosol whipped cream versus length of the nozzle tube for nozzle 2 (x) and nozzle 4 (o); aerosol cans shaken before use.

Measurements of the overrun of aerosol whipped cream, using nozzles with a different amount and size of holes in the cone (nozzle 2 and nozzle 4), showed no significant difference between the compared nozzles. The length of the nozzle tube, however, did have a considerable effect on the initial foam properties; an increasing length resulted in a decrease of the measured overrun. As described before, the overrun is determined by the mass of gas dissolved in the cream. The conditions in the aerosol can, therefore the mass of dissolved gas and thus the feasible overrun, are independent of the nozzle. These parameters can not explain the influence of the tube length on the overrun.

The foam is subjected to mechanical forces while flowing through the nozzle tube. It is speculated that these forces cause coalescence of the bubbles in the foam. The size of the bubbles will increase as coalescence proceeds. The longer the nozzle tube, the more time for coalescence to occur. Assuming that the relatively large bubbles will not remain stable during the flow out of the nozzle, this results in

an increase of the 'blow by' and, therefore, a decrease of the measured overrun of the foam.

It is not known at which position in the tube the bubbles will coalesce. Shearing forces, being maximal at the wall of the tube, might cause break up instead of coalescence of the bubbles near the wall. In the center of the tube the bubbles are subjected to smaller forces and thus it seems likely that coalescence occurs there. On the other hand, the system is so closely packed with bubbles ($\alpha \approx 0.7$) that it is questionable whether the bubbles will have enough space to break up. Besides, at such a high volume fraction of gas, the shearing forces will act upon the foam as a whole instead of acting upon individual bubbles, meaning that the forces will have less grip on the bubbles. Considering the local forces acting upon the bubbles, it is furthermore a simplification to assume that they act in only one direction (parallel to the wall). The bubbles will locally be subjected to numerous forces, the characteristics of which are for the moment impossible to describe. As a result of these irregular forces, the bubble stability will be put to the test. Especially in a closely packed system, bubble coalescence might be induced, in particular near the tube wall where the forces are maximal. With the lack of detailed knowledge about the processes occurring in the tube, it is unfortunately not possible to go beyond these speculations.

Figure 2.17 shows the effect of the overrun on the firmness of the foams. The data were obtained using different lengths of the nozzle tube. Because of the overlapping relation between firmness and overrun for the different tube lengths, the data are combined.

The scattering in the data is apparent; differences up to 25 % in the firmness measurements were found. It has to be noted that the method is sensitive to the presence of large gas 'holes' in the foam. Gas holes disturb a continuous structure of the product and will thereby affect the measurement. Unfortunately, it is difficult to prevent the formation of the holes and impossible to check on their presence before the measurement.

Initially, the firmness of the foam increases with increasing overrun. In this region a higher volume fraction of gas will give the bubbles less space to move. This results in an increase of the resistance of the foam against deformation. When the overrun exceeds 400 %, the firmness seems to remain more or less constant. It can be marked that maximal packing between bubbles of equal size is reached at a volume fraction gas of 0.74 ($O \approx 300$ %) (Princen, 1979). For a heterogeneous bubble size distribution, as in aerosol whipped cream, this value will even be higher. When the volume fraction of gas increases further, the bubbles will deform each other resulting in a polyhedral foam. Since the bubbles no longer have space to move, the firmness is maximal.
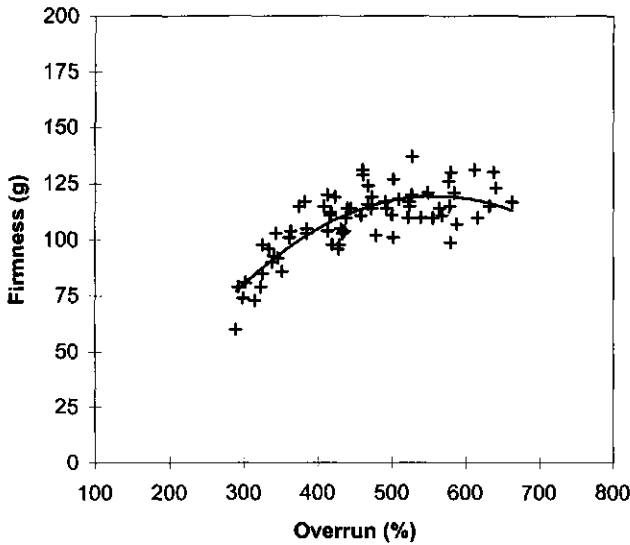
Figure 2.17   Firmness of aerosol whipped cream as a function of the overrun; aerosol can shaken.

Figure 2.17 shows that the maximum measured firmness is 100-130 g, which (multiplied by 9.81 m/s^2) corresponds to a force of 1-1.3 N. The contact area between the cylindrical plunger of the texture analyser and the foam equals πR_c^2, where R_c is the radius of the plunger (= 17.5 mm). Thus, the deformation stress, the force divided by the contact area, equals $1 \cdot 10^3$-$1.3 \cdot 10^3$ Pa. Considering individual bubbles, the resistance against deformation is given by the Laplace pressure difference ΔP_L over the bubble surface, $\Delta P_L = 2\gamma/R_b$, where γ is the surface tension of the liquid and R_b the bubble radius. For bubbles in aerosol whipped cream ($\gamma \approx 40$ mN/m, $R_b \approx 50$ μm), $\Delta P_L = 1.6 \cdot 10^3$ Pa. Note that the Laplace pressure difference corresponds very well with the measured deformation stress. Apparently, the measurement of the maximum firmness relates to the resistance of individual bubbles against deformation.

Besides the overrun of the foam, the bubble size distribution will also affect the firmness of the product. Aerosol whipped cream has a wide bubble size distribution (chapter 4). Since the bubble size distribution was not determined during the described experiments, it is difficult to discuss the relation with the firmness. It is however expected that the smaller the bubbles, the larger the measured firmness due to the larger Laplace pressure difference inside the bubbles.

2.6   Conclusions

An important conclusion from the presented results is that the flow of aerosol whipped cream is controlled by choking conditions in the nozzle; the velocity in the smallest opening of the nozzle (the holes) is limited to the speed of sound. The speed of sound is affected by the solubility of the gas in the cream. Theory on homogeneous equilibrium two-phase flow, including the effect of gas solubility, was adequately applied to describe the flow properties through the nozzle. Calculations on the volume fraction of gas indicated that foam formation occurs in the holes of the nozzle.

An other significant finding is that the process of foam formation is influenced by shaking of the can. Shaking, which results in the formation of bubbles in the cream, disturbs the flow phenomena. This was concluded from a decrease in the mass flow rate, accompanied by sputtering of the whipped cream while leaving the nozzle. Moreover, the initial overrun of the foam also seemed to be negatively affected by the presence of relatively large bubbles in the flow.

It was shown that the initial overrun is determined by the mass of gas dissolved in the cream, varied by temperature-fat content combinations of the cream and by shaking of the can. The presence of bubbles in the cream in the can promotes the phase equilibrium between the gas dissolved in the cream and the gas present in the headspace of the can and thus affects the mass of gas dissolved. In the absence of bubbles the establishment of the phase equilibrium is impeded and more gas will remain dissolved in the cream. This is expressed by a higher overrun of the foam.

The overrun seems to be negatively affected by mechanical forces in the nozzle. This is especially visible at higher pressures in the can (before the nozzle), and thus larger forces in the nozzle. Here, the deviation of the measured overrun from the feasible overrun, calculated out of the mass of dissolved gas, becomes apparent.

In the process of foam formation out of an aerosol can, the solubility properties of the nitrous oxide in the cream showed to play a central role. Experiments indicated that, even at a temperature of 3 °C where approximately half of the fat is crystallised, the gas is more soluble in the fat phase than in the skim milk phase of the cream. This is caused by the bond character of the interacting molecules of the gas and the liquid phases.

It was demonstrated that the nozzle geometry affects the flow conditions. By increasing the flow area, a proportional effect on the mass flow rate through the nozzle was expected. However, the effect turned out to be less than proportional. It might be possible that the flow properties are less favourable in the presence of more or larger holes, thereby affecting the mass flow rate. Additionally, the nozzle

with the larger flow area was far more susceptible to deformation. This might (negatively) affect the flow area during pressing the nozzle. Extension of the nozzle tube results in an increase in flow resistance due to friction with the tube wall. Experimental data indicated that, at longer tube lengths (> 3 cm), the mass flow rate lowered with increasing length; the choking conditions could no longer be reached. This transition to non-choked flow was confirmed theoretically.

The nozzle geometry also showed to affect the initial foam properties. Although the foam properties of the whipped cream did not vary significantly with the geometry of the nozzle cone, the initial overrun of the foam decreased with extension of the nozzle tube. It is speculated that this is caused by mechanical forces in the nozzle, inducing coalescence of bubbles in the foam. As the tube length increases, the process of coalescence will proceed further. The resulting relatively large bubbles might not remain stable during the flow out of the nozzle and thus induce 'blow by'. Finally it can be noted that, at overruns < 400 %, there appears to be a link between the overrun and firmness of aerosol whipped cream. At higher volume fractions of gas, the foam is assumed to be polyhedral; the maximal firmness is achieved. The deformation stress corresponding to this firmness seems to relate to the resistance of individual bubbles against deformation (Laplace pressure difference over the bubble surface).

2.7   References

- Ahlberg, K., 1985. AGA Gas Handbook.
- Alad'yev, I.T., Pchelkin, I.M., Klakutskaya, N.A. and Parfent'yeva, I.F., 1976. An Estimate of the Specific Impulse of Two-Phase Mixtures of Various Compositions Discharged from Nozzles. Fluid Mechanics-Soviet Research 5 (1), 86-100.
- Asbjornsen, O.A., Majeed, A., Hartmann, C. and Bringedal, B., 1989. Physical Phenomena Affecting Choked Two-Phase Flow. An Investigation by Modelling and Simulation. Proc. Summer Comput. Simul. Conf. 21 st., 277-282.
- Astarita, G. and Marrucci, G., 1974. Principles of Non-Newtonian Fluid Mechanics. McGraw-Hill Book Company (UK) Limited. Great Britain.
- Barton, A.F.M., 1991. Handbook of Solubility Parameters and other Cohesion Parameters, CRC Press.

- Battino, R. and Lawrence, H.L., 1966. The Solubility of Gases in Liquids. Chemical Reviews, 66, 395-463.
- Beek, W.J. and Muttzall, K.M.K., 1975. Transport Phenomena. John Wiley & Sons, LTD, London.
- Bird, R.B., Steward, W.E. and Lightfoot, E.N., 1960. Transport Phenomena. John Wiley & Sons, Inc., Singapore.
- Bouré, J.A., Fritte, A.A., Giot, M.M. and Réocreux, M.L., 1976. Highlights of Two-Phase Critical Flow: on the Links between Maximum Flow Rates, Sonic Velocities, Propagation and Transfer Phenomena in Single and Two-Phase Flows. International Journal of Multiphase Flow, 3, 1-22.
- Braker, W. and Mossman, A.L., 1980. Matheson Gas Data Book, Matheson, USA.
- Creemers, M.R., Leijendeckerss, P.H.H., van Maarschalkerwaart, M.C.M., Rijnsdorp, J.E. and Tysma., S., 1990. Poly-Technisch Zakboekje. 44e Druk. Koninklijke PBNA, Arnhem.
- Davis, M.R. and Wang, D., 1994. Dual Pressure Drop Metering of Gas-Liquid Mixture Flows. International Journal of Multiphase Flow, 20 (5), 865-884.
- Dobran, F., 1987. Nonequilibrium Modelling of Two-Phase Critical Flow in Tubes. Journal of Heat Transfer, 109, 713-738.
- Dziubinski, M., 1995. A General Correlation for Two-Phase Pressure Drop in Intermittent Flow of Gas and Non-Newtonian Liquid Mixtures in a Pipe. Trans IChemE, 73 (A), 528-534.
- Giot, M. Critical Flows. In: Delhaye, J.M., Giot, M. and Riethmuller, M.L., 1981. Thermodynamics of Two-Phase Systems for Industrial Design and Nuclear Engineering. Hemisphere Publishing Corporation, Washington, New York, 405-452.
- Hildebrand, J.H., Prausnitz, J.M. and Scott, R.L., 1970. Regular and Related Solutions. Van Nostrand Reinhold Company, New York.
- Heller, J.P. and Kuntamukkula, M.S., 1987. Critical Review of the Foam Rheology Literature. Ind. Eng. Chem. Res., 26, 318-325.
- Henry, R.E. and Fauske, H.F., 1971. The Two-Phase Critical Flow of One-Component Mixtures in Nozzles, Orifices, and Short Tubes. Journal of Heat Transfer, 93, 179-187.
- Isbin, H.S., 1980. Some Observations on the Status of Two-Phase Critical Flow Models. International Journal of Multiphase Flow, 6, 131-137.
- Ishii, R., Umeda, Y., Murata, S. and Shishido, N., 1994. Bubbly flows through a converging-diverging nozzle. Phys. Fluids 5 (7), 1630-1643.
- Jansen, L.P.B.M. and Warmoeskerken, N.M.C.G., 1987. Transport Phenomena Data Companion. Edward Arnold (Publishers) Ltd., London, Delftse Uitgevers Maatschappij bv, Delft.
- Kroezen, A.B.J., 1988. Flow Properties of foam in rotor-stator mixers and distribution equipment. Ph.D. Thesis, University of Twente, The Netherlands.
- Leung, J.C., 1986. A Generalised Correlation for One-Component Homogeneous Equilibrium Flashing Choked Flow. AIChE Journal, 32 (10), 1743-1746.
- Leung, J.C. and Grolmes, M.A., 1987. The Discharge of Two-Phase Flashing Flow in a horizontal Duct. AIChE Journal, 33 (3), 524-527.
- Leung, J.C., 1990. Two-Phase Flow Discharge in Nozzles and Pipes- a Unified Approach. J. Loss Prev. Process. Ind., 3, 27-32.
- Leung, J.C. and Epstein, M., 1990. A Generalised Correlation for Two-Phase Nonflashing Homogeneous Choked Flow. Journal of Heat Transfer, 112, 528-530.

- Luhman, R.S., 1994. Periodic Table of Elements, version 2.02g for windows. SMI Corporation.
- Marshall, N., 1976. Encyclopedie des Gaz, Division Scientifique, Elsevier, Amsterdam.
- Metzner, A.B. and Reed, J.C., 1955 Flow of Non-Newtonian Fluids - Correlation of the Laminar, Transition, and Turbulent-flow Regions. AIChE Journal, 1(4), 434-440.
- Müller-Steinhagen, H. and Heck, K., 1986. A Simple Friction Pressure Drop Correlation for Two-Phase Flow in Pipes. Chem. Eng. Process., 20 (6), 297-308.
- Nevers, N. de, 1991. Fluid Mechanics for Chemical Engineers. Second Edition. McGraw-Hill, Inc., New York.
- Perry, J.H., 1963. Chemical Engineers' Handbook, Mc Graw-Hill, Inc., New York.
- Prausnitz, J.M., 1969. Molecular Thermodynamics of Fluid-Phase Equilibria. Prentice-Hall, Inc., Englewood Cliffs, New Jersey.
- Princen, H.M., 1979. Highly Concentrated Emulsions. I. Cylindrical Systems. Journal of Colloid and Interface Science, 71(1), 55-66.
- Schwellnus, C.F. and Shoukri, M., 1991. A Two-Fluid Model for Non-Equilibrium Two-Phase Critical Discharge. The Canadian Journal of Chemical Engineering, 69, 188-197.
- Shinoda, K. and Becher, P., 1978. Principles of Solution and Solubility, Marcel Dekker, Inc., New York.
- Tangren, R.F., Dodge, C.H. and Seifert, H.S., 1949. Compressibility Effects in Two-Phase Flow. Journal of Applied Physics, 20 (7), 637-645.
- Wallis, B.W., 1969. One-Dimensional Two-Phase Flow. McGraw-Hill, Inc. New York.
- Wallis, G.B., 1980. Critical Two-Phase Flow. International Journal of Multiphase Flow, 6, 97-112.
- Walstra, P. and R. Jennes, 1984. Dairy Chemistry and Physics. John Wiley & Sons, Inc. USA.
- Wenzel, H.G., Brungraber, R.J. and Stelson, T.E., 1970. The Viscosity of High Expansion Foam. Journal of Materials, 5 (2), 396-412.
- Wijngaarden, L. van, 1972. One-Dimensional Flow of Liquids Containing Small Gas Bubbles, in: Dyke, M. van, Vincent, W.G. and J.V. Wehausen. Annual Review of Fluid Mechanics Volume 4, Annual Reviews, Inc., California, 369-396.
- Woschitz, D., Widmer, F., Covelli, B. and Wyss, E., 1986. Modellrechnung des Druckabfalls von -Mehrloch-Radialdüsen bei Zweiphasenströmung. Swiss Chem., 8 (4), 49-57.

Chapter 3

The aerosol can simulator

3.1   Introduction

In chapter 2 different principles of the foam formation process out of an aerosol can have been described. By applying theory of two-phase flow and considering the amount of gas dissolved in the cream in relation to phase equilibrium, more insight was obtained about the aspects that determine and affect the process. It turned out, however, that the aerosol can is a complex apparatus to study. During the spraying process the pressure inside the can drops (§ 2.3), resulting in a change in flow properties through the nozzle (§ 2.4) and affecting the initial foam properties of the aerosol whipped cream (§ 2.5). These factors complicate a detailed description and therefore understanding of the overall process of foam formation.

In order to extend the physical knowledge of the process of instant foam formation, search has been made for an apparatus that works according to the same principles as an aerosol can, but produces instant foam under standardised and controllable conditions. This search resulted in the development of an apparatus, called the Aerosol Can Simulator (ACS). In the ACS a gas and liquid phase with constant flow are mixed in order to dissolve the gas in the liquid. The magnitude of the flows can be varied. At the exit of the apparatus the mixed fluid is forced through a nozzle. This is accompanied by a pressure drop over the nozzle and results in the formation of the instant product. The working of the ACS has been extensively studied as will be described in this chapter. The effects of varying physical conditions in the apparatus, within the practical limits existing in an aerosol can, are used to unravel the process of instant foam formation.

The system used to study instant foam formation with the ACS is mostly aerosol whipping cream in combination with nitrous oxide as the gas phase. Corresponding to chapter 2, different stages in the process of foam formation are explored. Since the amount of gas dissolved in the cream showed to have a strong influence on the process of foam formation out of an aerosol can (§ 2.5), special attention is paid to the amount of dissolved gas while passing through the ACS. Theory on the dissolution of gas bubbles in liquid is being applied to estimate the state of the phase equilibrium in the ACS. In fact the dissolution of the gas is speeded up by the presence of a static mixer in the ACS. Flow through a static mixer causes a pressure drop which influences the dissolution process and the flow properties.

These effects will be studied using theory of flow through a packed bed.

The presence of a nozzle at the exit of the ACS introduces the possibility to create choking conditions. Theory on two-phase flow through a nozzle, as described in chapter 2, is being applied to check for the presence of these conditions in the nozzle. Furthermore, the effect of the nozzle geometry on the flow phenomena is studied.

There are several parameters that affect the process of foam formation in the ACS and thus the initial foam properties. Since the flow determines the pressure in the apparatus and thereby the foam formation, the effect of the gas and liquid flow on the characteristics of the initial foam is studied. Additionally, the composition of the gas is varied to investigate whether this results in different foam properties. The effect of the nozzle geometry is also included in this study.

To extend the insight into the process of instant foam formation, the results obtained using the ACS will be compared and combined in the whole chapter with the findings that resulted from the aerosol can (chapter 2).

3.2   Method

The ACS is constructed to simulate the working of an aerosol can. Besides the fact that the ACS operates under steady state conditions and the aerosol can does not, an important difference between the methods is in the cause and effect of the different parameters. In an aerosol can the pressure determines the flow properties whereas in the ACS the flow of foam through the nozzle determines the pressure. A schematic representation of the ACS is shown in figure 3.1.

In the experiments, the liquid (cream) is pumped out of a thermostated container (1) (V = 12 l) into a pipe using a reciprocating, positively displacement dosing pump (2) (Prominent® Meta) of continuous variable dose length. This packed-plunger pump consists of a main pump (Meta HK101-50S) in combination with an add-on pump (Meta AK-50S) which both operate with the same stroking rate (144 strokes/minute). The strokes of the two pumps superimpose each other, thereby smoothing out the sinusoidally varying discharge flow. This pulsating flow is damped significantly when gas is added to the cream flow. By changing the stroke length settings of the pumps, ranging from 0 to 100 %, the corresponding dosing rate can be varied from 0 to 98.6 l/h, with a dosing accuracy of 1 %. In the experiments the settings of the two pumps were always equal.
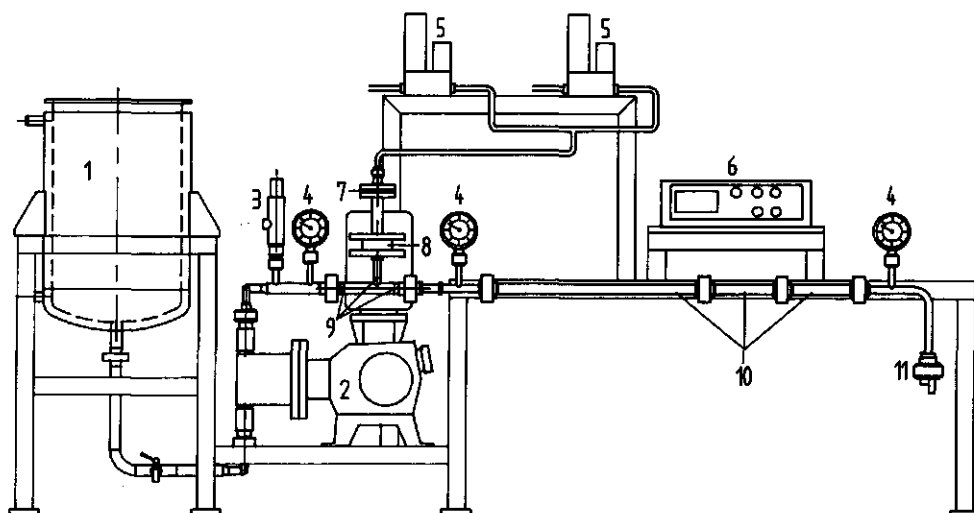
Figure 3.1   Schematic representation of the aerosol can simulator. (1) container for liquid, (2)
                    pump, (3) safety valve, (4) pressure gauge, (5) mass flow controller for gas, (6)
                    power supply, read-out and control unit, (7) gas mixing chamber, (8) one-way valve,
                    (9) perforated plate, (10) static mixer, (11) nozzle.

The gas enters the ACS via a mass flow controller (5) (Brooks, model 5850E). In
this study two different gases are used, nitrous oxide and nitrogen. The mass flow
controller used for the nitrous oxide has a range of 0-1000 l/h, the flow of nitrogen
can be varied from 0-250 l/h. The instruments have an accuracy of 1 % full scale.
For the control and measuring of the gas flow, a power supply, read out and control
unit (6) (Brooks, model 5878) is used. After flowing through a mixing chamber (7)
where, in the presence of both gases, the gases are mixed, the gas passes
through a one-way valve (8).

Analogous to the process in an aerosol can (chapter 2), it is aimed at dissolving the
gas for the larger part in the cream. For this purpose, as will be elaborated in the
next section, the gas phase enters the cream via a perforated plate (9) and
additionally flows with the liquid through a static mixer (10) (D = 15 mm,
L = 60 cm). The mixer is packed with glass beads having a diameter of ± 3 mm.
The void fraction or porosity ε in the packed mixer is 0.4.

The (over)pressure at different positions in the ACS is monitored by manometers
(4) (read-off accuracy of 0.1 bar). The presence of a safety valve (3) (Gresswell

valves) in the ACS limits the local pressure to a maximum of approximately 15 bar. All the elements of the ACS are able to perform correctly at this pressure.

At the end of the ACS a nozzle (11), similar to the nozzles used on aerosol cans (chapter 2), is positioned. The nozzle is clasped between the end of a pipe and an accessory which fits on the tube of the nozzle. Because this accessory is pressed against the nozzle, the ACS opens. The gas-cream mixture is forced to flow through the nozzle, finally resulting in the foamed product.

3.3   Processes occurring in the ACS

In an aerosol can the gas is for the larger part dissolved in the cream. Therefore, it is necessary to ensure optimal dissolution of the gas in the cream when imitating the process of instant foam formation with the ACS. The process of dissolution is enhanced by a large exchanging interface between the gas phase and the cream over which gas diffusion can take place.

The exchanging interface between the gas phase and the cream is enlarged when the gas flow breaks up into bubbles. For this purpose the gas flow enters the cream via a perforated plate. Moreover, the ACS contains a static mixer packed with glass beads. It is assumed that the gas bubbles will split up further while flowing through the mixer.

Since experiments (§ 3.3.3) indicated that the presence of the static mixer is crucial in the process of instant foam formation using the ACS, special attention is paid to the different processes occurring in the mixer. The first process studied is the flow through the mixer, resulting in a pressure drop. This process intensifies the break up of the gas bubbles, which is the next mechanism described. Finally, the dissolution of the gas bubbles is studied. This process is determined by the bubble size and by the pressure. The pressure affects both the bubble size and the gas solubility and, thus, the rate of gas dissolution.

3.3.1 Theoretical and practical considerations

Pressure drop over the static mixer

It is a known phenomenon that flow through a packed bed of spheres results in a pressure drop over the static mixer. This pressure drop ΔP_m is given by the equation of Ergun (Ergun, 1952; Bird et al., 1960):

$$\frac{\Delta P_m}{L} = \frac{150\,\eta\,v_0}{D_p^2}\frac{(1-\epsilon)^2}{\epsilon^3} + \frac{1.75\rho v_0^2}{D_p}\frac{(1-\epsilon)}{\epsilon^3} \tag{3.1}$$

where L is the length of the static mixer, η the fluid viscosity, D_p the mean diameter of the glass beads, ϵ the void fraction and ρ the density of the fluid. v_0 is the superficial velocity, which is the average velocity the fluid would have in the absence of the glass beads. The actual velocity v in the mixer is of course higher, $v = v_0/\epsilon$.

The first term on the right-hand side of equation (3.1) accounts for viscous energy losses per unit length and is significant at laminar flow. The second term expresses kinetic energy losses and dominates under turbulent flow conditions (Ergun, 1952). For the flow of water ($\eta = 0.001$ Pa s) through the mixer of the ACS it can be calculated that at a flow of 50 l/h, the pressure drop per unit length becomes 0.4 bar/m. Of this pressure drop 82 % is caused by kinetic energy losses. The same calculation for flow of cream through the mixer (taking $\eta = 0.04$ Pa s (appendix II)), results in a $\Delta P_m/L$ of 3.3 bar/m. It is interesting to note that in this situation 90 % of the pressure drop is caused by viscous energy losses.

For a compressible fluid (gas/cream mixture) the density and velocity change while flowing through the mixer. In this situation equation (3.1) can be used with the pressure gradient and the length in a differential form. Nevertheless, it is complicated to accurately calculate the pressure drop over the static mixer in the ACS because the different parameters are difficult to estimate. At a constant mass flow rate, the velocity in the mixer is inversely proportional to the density of the gas/cream mixture. This density decreases during flow through the mixer due to the pressure drop. However, at the same time the density increases because the gas bubbles dissolve in the cream.

The viscosity of the fluid is also difficult to estimate. A homogeneous foam in general behaves as a power law fluid (§ 2.4.1) with a viscosity being higher than the viscosity of the liquid from which it is produced (Kroezen, 1988). Savins (1969) reviewed the flow phenomena of power law fluids through porous media. Several relations to describe this type of flow have been published, an overview of which is given by Kemblowski and Michniewics (1979) and Srinivas and Chhabra (1992). However, it is questionable whether foam may considered to be a continuous medium while flowing through a static mixer. This is only allowed when the bubbles are small compared to the size of the channels in the mixer.

Hirasaki and Lawson (1985) showed that the apparent viscosity of foam in capillary tubes is strongly geometry dependent. This was expressed by a decrease of the viscosity with increasing ratio of bubble diameter to tube diameter. Kroezen (1988)

and Lemmen (1991) found similar effects while studying the flow of foam through narrow slits and perforated and woven screens. The latter concluded that in order to describe this type of foam flow some sort of bulk foam viscosity has to be combined with a contribution of bubble distortion.

An other aspect that has to be taken into account in studying flow through a static mixer is the wall effect. Mehta and Hawley (1969) showed that a correction for the friction due to the wall surface area is necessary, especially when the ratio of the mixer diameter to the particle diameter is less than 50 to 1. Srinivas and Chhabra (1992) also described extra frictional loss during flow of power law fluids through a packed bed due to this wall effect. They studied mixer to particle diameter ratios smaller than 40. In the mixer of the ACS this ratio is 5. A correction for extra frictional loss therefore seems necessary. This correction is difficult to approximate. Since it seems almost impossible to accurately calculate the pressure drop over the static mixer, the values measured in experiment are used for further calculations. The value of the pressure drop is of course affected by the flow of gas and cream. In the experiments the cream flow is varied between 30 and 70 l/h with a gas flow being 2 to 20 times larger (at atmospheric pressure). These conditions induce pressure drops ranging from 2.1-5.2 bar over a static mixer with a length of 0.6 m.

Break up of the bubbles

During flow through the static mixer the gas bubbles are subjected to a shear stress τ which determines the bubble size in the mixer. The average shear stress is expressed by (Ergun, 1952):

$$\tau = \frac{\epsilon A \Delta P_m}{S_t} = R_h \frac{\Delta P_m}{L} \tag{3.2}$$

where A is the cross-sectional area of the empty mixer, S_t the total geometric surface area of the solid particles and ΔP_m corresponds to the pressure drop over the static mixer (equation (3.1)). The hydraulic radius R_h is defined as the ratio of volume occupied by the fluid in the mixer (ϵAL), divided by the surface area it sweeps (S_t) (Ergun, 1952). For a packed bed R_h is given by (de Nevers, 1991):

$$R_h = \frac{\epsilon AL}{S_t} = \frac{\epsilon D_p}{6(1-\epsilon)} \tag{3.3}$$

Substituting equations (3.1) and (3.3) in equation (3.2) gives for the average shear stress:

$$\tau = R_h \frac{\Delta P_m}{L} = \frac{150 \eta v_0 (1 - \epsilon)}{6 D_p \epsilon^2} + \frac{1.75 \rho v_0^2}{6 \epsilon^2} \tag{3.4}$$

In the ACS $\Delta P_m/L$ over the mixer was measured to vary from 3.5-8.7 bar/m. For the static mixer, using a void fraction of 0.4 and glass beads with a diameter of 3 mm, R_h is $3.33 \cdot 10^{-4}$ m (equation (3.3)). With the measured values of $\Delta P_m/L$ and R_h the resulting average shear stress is roughly calculated to be 100-300 Pa (equation (3.4)). It is important to note that the shear stress exerted on the gas bubbles can locally be much higher than the average shear stress, although it is difficult to estimate how much higher this will be.

When the shear stress in the mixer exceeds the Laplace pressure difference ΔP_L inside the bubbles, the bubbles can break up into smaller ones. The Laplace pressure difference over the surface of a gas bubble with radius R_b equals:

$$\Delta P_L = \frac{2\gamma}{R_b} \tag{3.5}$$

with γ being the surface tension of the liquid. Combining the average shear stress in the mixer (equation (3.4)) with equation (3.5) gives an indication for the resulting bubble size in the static mixer:

$$R_b = \frac{2\gamma}{\tau} = \frac{12\gamma D_p \epsilon^2}{150 \eta v_0 (1 - \epsilon) + 1.75 D_p \rho v_0^2} \tag{3.6}$$

Using a surface tension of 40 mN/m (chapter 4) and the calculated average shear stress (100-300 Pa), the bubble radius in the static mixer varies between 300 and 800 µm. It has to be marked that due to the locally higher shear stresses the actual bubble size may become much smaller.

Dissolution of the bubbles
It is the aim to dissolve the gas bubbles while flowing through the mixer. The growth and dissolution of bubbles is investigated in many studies. Reviews of literature on this topic are given by Yung et al. (1989) and Ronteltap (1989). Most of the studies consider stationary, isothermal growth or dissolution of a single spherical bubble in an infinite liquid. Tao (1978) obtained an exact solution to describe bubble growth or dissolution, neglecting convection. Approximate solutions were described by Hsieh (1965) and Rosner and Epstein (1972), amongst others. The effect of different parameters on the dissolution and growth of bubbles is

included in several studies. Adsorption of surface active agents (e.g. proteins) is found to slow down the dissolution process. The surface tension is also known to affect the dissolution for small bubbles when the system is close to saturation (Yung et al., 1989; Berge 1990). Furthermore, surface rheological properties might be responsible for a retardation of the dissolution process as described by Ronteltap (1990a,b). Other parameters that have to be considered are the gas expansion effect and, very importantly, the gas composition in the bubble (Yung et al, 1989; Ronteltap, 1990a,b).

The process of dissolution is much more complicated when numerous bubbles are involved. In this case it is no longer justified to consider the liquid around the bubble to be infinite. The dissolution process of an individual bubble is bound to be affected by the dissolution of surrounding bubbles. De Vries (1958a,b) described the gas diffusion between bubbles in a foam in relation to the foam stability. He calculated the dissolution rate of a bubble, caused by gas diffusion to an other bubble with an infinite radius. More references of literature on the gas transport in foams in relation to foam stability are given by Ronteltap (1989).

When gas bubbles are being mixed with the liquid while flowing through the mixer, the dissolution process of the bubbles differs from the process of gas transport in a foam 'at rest'. Ruckenstein and Davis (1970) showed that the rate of mass transfer between a moving bubble and the surrounding liquid can be substantially enhanced by translational effects. Therefore, convection caused by the mixing has to be accounted for.

As a first approach for the dissolution of gas bubbles in the static mixer, the dissolution time of a single bubble is calculated using an adapted form of the model of Bisperink and Prins (1994). They studied the bubble growth at a model cavity in carbonated liquids. Their theory, in which convection is not involved, showed to describe the bubble growth rate rather well and can easily be applied to calculate the dissolution time of a spherical bubble.

In the model used, the driving force for the dissolution of bubbles is the concentration difference between the bubble surface and the liquid bulk. From this the mass flux over the bubble surface can be derived with Fick's first law. The model accounts for two geometrical changes of the boundary layer, which is the layer around the bubble over which the gas diffusion takes place. Firstly, there will be an increase in the thickness of the boundary layer in time caused by penetration of the concentration gradient into the liquid. Secondly, for a shrinking bubble, there is an increase of the boundary layer due to the contraction of the layer caused by the surface compression of the bubble. The thickness of the boundary layer is calculated assuming a linear concentration profile in the layer between the bubble and the bulk. By means of a computer program the times needed for very small

consecutive decreases in bubble radius are calculated, thereby describing the shrinking of the bubble. More details about the applied model are given in appendix VI.

Accounting for the Laplace pressure difference over the bubble surface (equation (3.5)), the gas concentration at the bubble surface follows from Henry's law (§ 2.2.1). Henry's constant in the ACS is taken to be 0.5 kg/g/bar (derived from figure 2.2 for cream with a fat content of 35 % w/w at 10 °C). Additionally, zero bulk concentration is assumed. For the diffusion constant D of nitrous oxide a value of $2.11 \cdot 10^{-9}$ m^2/s is used (D for N$_2$O in water at 20 °C; Jansen and Warmoeskerken, 1987). The dissolution time for bubbles with a radius of 300-800 μm is calculated to be 30-200 s.

The mean residence time of the bubbles in the mixer follows from the flow velocity. For the experimentally varied flow conditions the residence time is in the order of a few seconds. Although this time is much shorter than the calculated time needed for the bubbles to dissolve completely, experiments indicated that optimal dissolution of the gas in the cream is achieved within the residence time. This will be discussed in more detail in § 3.3.3.

3.3.2 Experimental

It is assumed that only the gas dissolved in the cream contributes to the foam properties of aerosol whipped cream (chapter 2). The efficiency of the gas dissolution process in the ACS will therefore be reflected in the overrun of the produced foam. To study the role of the static mixer in the dissolution process the overrun is measured as a function of the static mixer length. This length is varied from 0.12 to 0.6 m. Measurements were performed at two different cream flow rates, 40 and 60 l/h. The gas flow rate (at atmospheric conditions) was varied relative to the cream flow rate, being 6 to 14 times larger. It is known from experience that within these combinations of gas and liquid flow the resulting foam properties are comparable to those of aerosol whipped cream produced with an aerosol can.

3.3.3 Results and Discussion

The effect of static mixer length on the overrun of the foam produced with the ACS, and therefore on the dissolution process of the gas in the cream, follows from figure 3.2. The results plotted in the graph correspond to a gas:liquid ratio of 12. For the other gas:liquid ratios similar trends were obtained.

It can be noted that the presence of a static mixer in the ACS is essential for the

process of foam formation. Without it, no foamed product was formed. Figure 3.2 shows that the static mixer indeed affects the dissolution of the gas. Initially, the overrun of the whipped cream increases with increasing mixer length. The dissolution process is improved by extension of the static mixer up to a length of 0.36 m. At larger lengths the overrun remains more or less the same. Apparently, hardly any extra gas is dissolved in the cream by further extension of the mixer. The maximum amount of gas that can be dissolved under the experimental conditions is reached. The reason that the overrun of foams produced at a cream flow of 60 l/h is higher than that of foams produced at a cream flow of 40 l/h will be discussed in § 3.5.
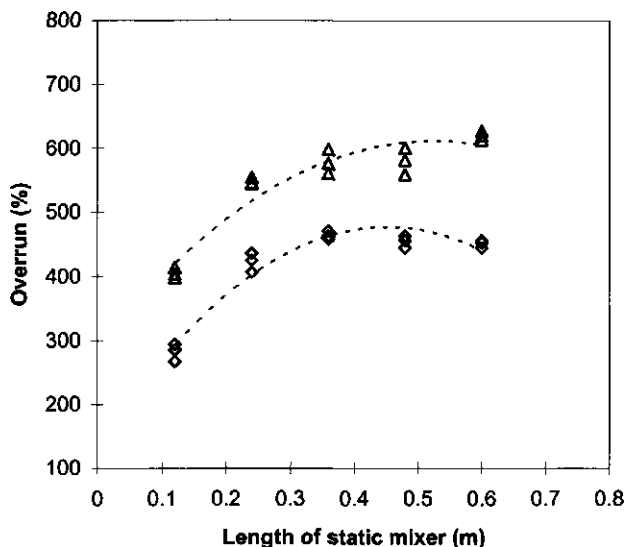
Figure 3.2   The overrun versus the length of the static mixer for cream flow rates of 40 l/h (◇) and 60 l/h (△). The gas:liquid ratio is 12 at atmospheric conditions.

From the theoretical considerations concerning the dissolution of the gas bubbles (§ 3.3.1) it followed that the bubbles are not expected to completely dissolve in the cream within the residence time in the mixer. The fact that in practice the maximum amount of gas is dissolved within this time can be explained by one of the following reasons. Firstly, the applied model does not account for the presence of numerous bubbles (which would slow down the dissolution rate) or for convection caused by the surrounding liquid (speeding up the process). The effect of these factors is difficult to estimate but is not expected to explain the difference between the

calculated dissolution time and the experimental residence time. It is more likely that the actual dissolution time of the bubbles is much shorter because the bubbles are initially smaller than estimated. This results when the shear stress in the mixer is locally higher than the average value used for the calculation of the bubble size. Finally, it is possible that the dissolution process involves a different mechanism than the diffusion controlled model that was used to estimate the dissolution time. The shear forces acting on a bubble might be able to sweep the boundary layer from the surface. A 'clean' surface would result in an instantaneous dissolution of the gas and consequently very short dissolution times.

The shear stress acting on a bubble expands the bubble surface at one side and results in a compressed surface at the opposite side. This causes the existence of a counteracting surface tension gradient along the surface which equals, in the ultimate situation, the maximum surface tension difference (72 mN/m). The gradient is able to withstand a shear stress with a magnitude of the surface tension gradient divided by the distance along the bubble surface (πR_b m). For the bubbles in the static mixer (300-800 µm) this corresponds to a maximum stress of resistance between 30 and 80 Pa. It can be noted that these values are somewhat lower than the shear stress in the mixer (100-300 Pa). Therefore, it is not unlikely that the bubble surfaces are stripped by the shear stress resulting from the fluid flow through the mixer.

3.4 Flow properties of aerated cream through a nozzle

An important conclusion following from the results in chapter 2 was that the flow properties of aerated cream out of an aerosol can are controlled by choking conditions in the nozzle. Studying the flow properties out of the ACS, which is equipped with the same type of nozzle, it is first of all interesting to know whether choking conditions in this case also have a determining role. Furthermore, the effect of the nozzle geometry is considered.

3.4.1 Theoretical considerations

Choked flow

The principles of choked flow in the nozzle of an aerosol can have extensively been described in chapter 2. As mentioned before, the pressure in an aerosol can determines the flow properties through the nozzle, whereas in the ACS the conditions are regulated by the flow rate of the gas and the cream. The relation between the pressure and the flow properties is however defined by fluid

mechanics and is presumed to be similar for the two techniques.

The mass flow rate $\dot{m}_f$ of foam out of the ACS is linked to the flow velocity v_1 in the holes of the nozzle (analogous to equation (2.40)):

$$\dot{m}_f = \rho_f v_1 A_1 \tag{3.7}$$

where ρ_f is the foam density and A_1 the total of the cross-sectional area of the holes.

As described in chapter 2 (appendix IV), the pressure P_0 before the nozzle and the velocity v_1 in the nozzle are related via equation (2.31). This equation is derived assuming that the velocity before the nozzle is zero. Considering an aerosol can this is approximately the case. Since the flow area in the ACS before the nozzle is roughly 50 times larger than the total hole area, the velocity before the nozzle is small compared to the velocity in the holes and may therefore be neglected. It seems justified to use equation (2.31).

For the calculation of velocity v_1 the constant k, the ratio of gas mass flow to cream mass flow, has to be known. In the ACS the value of k can easily be found from the gas and cream flow rates:

$$k = \frac{\rho_g Q_g}{\rho_l Q_l} \tag{3.8}$$

where ρ_g is the density and Q_g the volumetric flow rate of the gas, both at atmospheric conditions, Q_l the volumetric cream flow rate and ρ_l the cream density. Choking conditions in the nozzle of the ACS are fulfilled when the velocity in the nozzle equals the speed of sound in the foam c_f. Assuming phase equilibrium between the gas dissolved in the cream and the gas in the bubbles, c_f follows from equation (2.27) (chapter 2).

Nozzle geometry

The geometry of the nozzle is expected to affect the flow properties of foam (§ 2.4.1). A change in number and total area of the holes in the nozzle did not result in a major difference in flow conditions out of an aerosol can (§ 2.4.3). Extension of the nozzle tube however showed a more pronounced effect, caused by the increase of frictional resistance against flow (figure 2.13). At longer tube lengths ($L > 1.5$ cm) the flow was no longer determined by choking conditions. Instead it appeared that the frictional resistance, caused by the flow through the tube, limited the flow. Therefore, special attention is paid to the flow through the tube.

The flow of foam through a tube can be described by a combination of the

continuity and the momentum equation. This results in relations between the pressure P, the flow velocity v and the length L of the tube (appendix V), given by equations (2.38) and (2.39). The ACS is a good tool for studying the effect of the tube length on the flow properties in more detail, since both the mass flow rate and the pressure are easy to measure parameters.

3.4.2 Experimental

Choked flow
In order to check for the presence of choking conditions in the nozzle of the ACS the theoretical and experimental conditions have to be compared. The flow conditions in the ACS determine the pressure P_0 before the nozzle. With the measured pressure the choked velocity v_1 in the holes was calculated by combining equations (2.27) and (2.31). Some of the pressures were obtained using a shorter static mixer (0.36 m) in the ACS. Experiments however showed that extension of the mixer did not significantly affect the values of the pressures.

Using the flow area and the calculated v_1, the theoretical expected mass flow rate followed from equation (3.7). The majority of the measurements was performed with nozzle 2 (A_1 = 1.57 mm^2) and some occasional measurements were carried out using nozzle 4 (A_1 = 1.13 mm^2). More information about the dimensions of these nozzles is given in § 2.4.2.

The experimental mass flow rate of the gas/cream mixture simply followed from the two separate flows. For cream four flow rates were used: 30, 40, 50 and 60 l/h. The volumetric gas flow rate (at atmospheric conditions) was varied relative to the cream flow rate, being 2 - 20 times larger, in steps of 2.

Since the aim was to simulate the foam formation process out of an aerosol can as accurate as possible, it was assured that the cream could be saturated with gas. This means that at least the maximum amount of gas that can dissolve in the cream at the prevailing pressure was present in the ACS. Conditions where less gas was present were not considered.

Nozzle geometry
To study the effect of the nozzle tube length on the flow properties in more detail, the tube length was varied at different mass flow rates. A change in frictional resistance against flow will be reflected in a change in pressure at the beginning of the tube and thereby in a change in pressure before the nozzle in the ACS.

Calculations of the pressure at the beginning of the tube in the nozzle were compared with measurements of the pressure before the nozzle. Both were performed using nozzle 2. For the description of the flow properties of foam through

the tube, equations (2.38) and (2.39) were used. It was assumed that the pressure at the end of the tube is either atmospheric or caused by choking conditions ($v = c$). Accordingly, the pressure drop over the tube and thus the pressure at the beginning of the tube was calculated. The friction factor was taken to be 0.025, as was done for flow out of an aerosol can (§ 2.4.2).

The pressure before the nozzle in the ACS was measured for the varying experimental conditions. To change the length of the nozzle tube an extension piece was used which fits on the tube of the nozzle. This tool extends the tube length to 1.5 cm. After attaching a plastic tube to the extension piece, the tube length was varied from 20 cm to 1.5 cm by successively cutting of a piece of the tube. For the measurements with an unextended nozzle (L = 0.8 cm) a different accessory had to be used.

The volumetric flow rates of the cream through the nozzle was 30, 40, 50 or 60 l/h. The volumetric gas flow rate, measured at atmospheric conditions, was taken to be 10 times larger than the accompanying cream flow rate. At this ratio optimal foam properties are obtained (§ 3.5.3).

3.4.3 Results and Discussion

Choked flow

Choking conditions in the nozzle were verified by comparing the experimental mass flow rate with the mass flow rate calculated from the measured pressure P_0 in the ACS. For this calculation the total hole area of the nozzle has to be known (equation (3.7)). In practice, this gives rise to a problem. The majority of the measurements were performed with nozzle 2. The hole area of this nozzle turned out to depend greatly on the positioning of the nozzle. In the ACS the nozzle is clasped between the end of a pipe and an accessory which is placed in a ring. By tightening the ring, deformation of the nozzle cone can occur. The resulting decrease of the total hole area becomes visible in a higher pressure. For similar flow conditions, using the same type of nozzle, pressures differing up to 20 % were measured. It is therefore difficult to quantify the total hole area of the nozzle during the spraying process. Unfortunately, less experiments were performed with nozzle 4. For this type of nozzle the data showed no sign of material deformation. In the calculations the value of the undeformed nozzles were used.

Figure 3.3 shows the experimental mass flow rate versus the calculated one for nozzle 4 (indicated by the circles) and nozzle 2 (squares and crosses). The squares indicate the data for a minimal deformation of the nozzle cone, the crosses correspond to a relatively strong deformed nozzle cone. The effect of deformation is apparent.
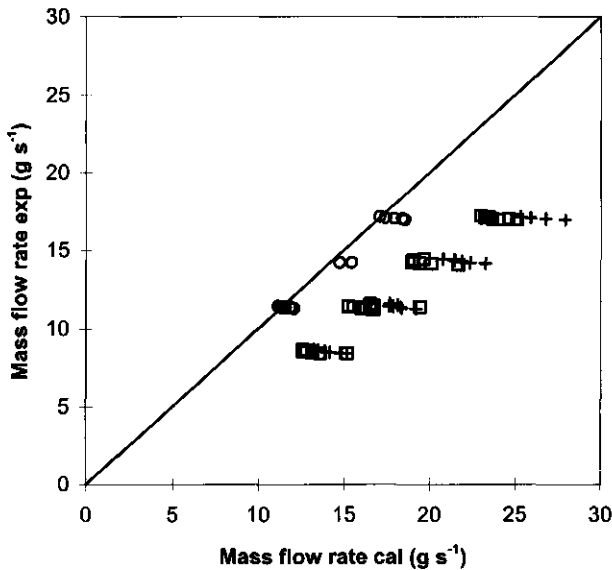
Figure 3.3   Experimental mass flow rates versus mass flow rates calculated out of measured
pressure before the nozzle; nozzle 4 (o) and nozzle 2 with minimal cone
deformation (□) and relatively strong deformation (+).

From the results in this graph it can be seen that the measured mass flow rates
through nozzle 4 are only slightly lower than the calculated ones. This indicates that
choking conditions in the nozzle are fulfilled. In chapter 2 it was shown that shaking
of the aerosol can negatively affected the (choked) mass flow rate out of the can,
which resulted in a deviation from the theoretical values. Therefore, the results from
figure 3.3 lead to the conclusion that the flow conditions out of the ACS agree most
with the flow conditions out of a not shaken aerosol can. This might seem strange
because on average there is an excess of gas, and thus bubbles, present in the
ACS. Maybe, the bubbles are too small to give a similar amount of disturbance in
the flow.

It can be marked that the pressure in the ACS equipped with nozzle 4 hardly
differed from the pressure in the ACS using nozzle 2 with minimal deformation of
the nozzle cone. A more or less similar pressure in the ACS results in a larger
calculated mass flow rate through nozzle 2 than through nozzle 4 because of the
difference in total hole area. However, the experimental mass flow rate is the same.
From this it follows that the mass flow rate through nozzle 2 is smaller in
experiment than would be expected from theory (figure 3.3). These findings agree
with the results from the aerosol cans where the mass flow rate through nozzle 2
was lower than expected from theory. The measured difference in the mass flow

rate through the two different nozzles was small (figure 2.12). The flow properties are probably less favourable in the presence of more or larger holes in the nozzle (§ 2.4.3).

Nozzle geometry

In the previous section it was demonstrated that the cone of nozzle 2 is susceptible to deformation when it is clamped at the end of the ACS. Repositioning of the nozzle can change the degree of deformation and consequently the nozzle geometry. This can not be done in a reproducible way and will affect the results. Since the tube length was varied by successively cutting of a piece of the tube, the nozzle did not need to be repositioned during the experiments. The effect of deformation of the nozzle cone is therefore constant in all the measurements. For the measurements with the unextended tube a different accessory was used, meaning repositioning of the nozzle. These measurements were not included. Figure 3.4 shows the results of the calculated pressures at the beginning of the nozzle tube and the measured pressures before the nozzle in the ACS as a function of the tube length for different mass flow rates.
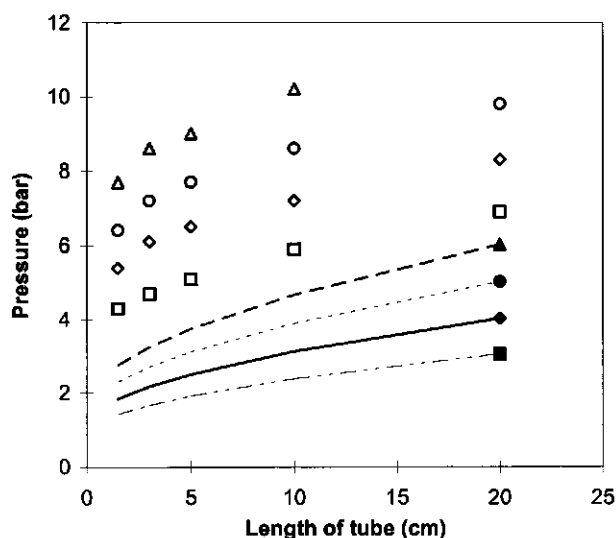

Figure 3.4   The calculated pressure at the beginning of the tube (lines with closed symbols) and the measured pressure before the nozzle (open symbols) as a function of the tube length for a cream flow rates of 30 l/h ($\square$), 40 l/h ($\diamond$), 50 l/h (o) and 60 l/h ($\triangle$) at a gas:liquid ratio of 10 (at atmospheric conditions).

The lines with the closed symbols correspond to the calculated pressures at the beginning of the tube. The open symbols in this graph mark the measured pressures before the nozzle. At a cream flow rate of 60 l/h and a tube length of 20 cm the pressure inside the ACS (before the static mixer) exceeded the 15 bar, resulting in an exit of the cream via the safety element. Therefore, this data point could not be measured.

Figure 3.4 shows that the shape of the curve of the calculated pressures at the beginning of the tube corresponds very well with that of the measured pressures before the nozzle. It was demonstrated that the flow through an unextended tube is determined by choking conditions (figure 3.3). When the tube is extended, the frictional resistance against flow increases. As a result, the pressure at the beginning of the tube increases and eventually choking conditions in the holes can no longer be achieved. This is expressed by an increase of the pressure in and before the nozzle. Furthermore, a higher flow rate induces a larger frictional resistance, which is reflected by a higher pressure.

The difference in magnitude of the calculated and measured pressures accounts for the pressure drops caused by the flow of foam through the holes and into the tube of the nozzle. Theory to describe these processes was given in § 2.4. For the calculation of the pressure drops the geometry of the nozzle has to be known. Because of the deformation of the nozzle cone it is however difficult to estimate the geometry of the holes. Consequently, the pressure drop resulting from the flow through the holes and into the tube could not be calculated.

It has to be noted that the friction factor used to calculate the pressures at the beginning of the tube ($f = 0.025$) was derived for a relatively large flow rate ($\pm$ 80 l/h). At lower flow rates, the Reynolds number will be lower and therefore the friction factor will be higher. This will result in a steeper curve of the calculated data, especially at the lower flow rates. Furthermore, at a similar flow rate, the friction factor will differ per tube length. In a longer tube the pressure is on average higher. Consequently, the fluid density is higher and the flow velocity lower. This will affect the foam viscosity and thereby the friction factor. Because the influences of a higher density and a lower velocity on the friction factor counteract each other, it is difficult to estimate the ultimate effect.

3.5   Initial foam properties of aerosol whipped cream

An important conclusion from chapter 2 was that the initial foam properties of aerosol whipped cream were directly determined by the amount of gas dissolved in the cream. The initial overrun, however, showed to be affected by large mechanical

forces at higher pressure drops over the nozzle, the presence of bubbles caused by shaking of the can and the nozzle geometry (§ 2.5.3).

This section describes whether the same effects can be observed in the instant foam production using the ACS. In the ACS the amount of gas dissolved in the cream, which is related to the amount of bubbles present, is determined by the pressure before the nozzle. The magnitude of the mechanical forces in the nozzle also results from this pressure. Since the pressure is regulated by the gas and liquid flow, the influence of these parameters on the initial foam properties was studied. Furthermore, the consequence of a different nozzle geometry was included.

As mentioned in the first chapter, the stability of aerosol whipped cream against the process of disproportionation (chapter 4) can be improved by using a less soluble gas in the production of aerosol whipped cream. Because the gas solubility proved to be very important in the process of foam formation, it was studied how addition of a less soluble gas affects the initial foam properties.

3.5.1 Theoretical considerations

Gas and liquid flow

The initial overrun of aerosol whipped cream is linked to the amount of gas dissolved in the cream. This amount is determined by the local pressure in the ACS. At a higher flow rate of the gas and cream the pressure in the ACS is on average higher, resulting in a larger amount of dissolved gas. This is expected to be expressed in a larger overrun of the produced foam.

It is assumed that only the gas dissolved in the cream contributes to the foam formation and thereby determines the initial overrun. When the total amount of gas present in the ACS can be dissolved at the local pressure, the feasible overrun O_f of the produced foam is limited to:

$$O_f = \frac{(k - SP_{atm})\rho_l}{\rho_{g,atm}} * 100 \qquad (3.9)$$

where k is given by equation (3.8), S is the gas solubility and P_{atm} and $\rho_{g,atm}$ are respectively the pressure and gas density at atmospheric conditions.

In the presence of an excess of gas, the feasible overrun follows from:

$$O_f = \frac{(p_{g,0} - P_{atm})\rho_l S}{\rho_{g,atm}} * 100 \qquad (2.43)$$

where $p_{g,0}$ is the partial pressure of nitrous oxide in the ACS before the nozzle.

Since N_2O is the only gas added to the cream, $p_{g,0}$ equals P_0.

The measurements with the aerosol cans showed a relation between the firmness of the whipped cream and the overrun of the foam (figure 2.17). It is expected that the same dependency will be found in the initial foam properties of whipped cream produced with the ACS. This expectation also holds for the results of the experiments performed with different nozzle geometries and with addition of a less soluble gas.

Nozzle geometry

In chapter 2 it was shown that extension of the nozzle tube positioned on an aerosol can affects the initial properties of the whipped cream. An increase in the tube length of the nozzle results in a decrease in the overrun of the foam. This was probably caused by shearing forces at the tube wall. These forces may cause coalescence of bubbles, thereby making them more susceptible to break up after leaving the nozzle.

The experiments performed with the ACS have one main difference with the corresponding experiments performed with the aerosol can. When foam flows out of an aerosol can, the pressure drop over the nozzle has almost the same value for the different tube lengths. The flow rate depends on the frictional resistance against flow. Consequently, the flow rate was lower at a longer tube length (figure 2.13). In the ACS the experiments were performed at a constant flow rate. Here, the pressure drop over the nozzle increases with increasing tube length.

It is assumed that, analogous to the aerosol can, extension of the nozzle tube on the ACS will result in a decreasing overrun of the whipped cream. This decrease is expected to be more pronounced at a higher mass flow rate because of larger shearing forces.

Gas composition

Aerosol whipped cream is susceptible to disproportionation (chapter 4) because of the good solubility of laughing gas in cream. The process will be slowed down when a less soluble gas is present in the gas phase (Ronteltap, 1989). However, this can also affect the amount of gas dissolved and thereby the initial foam properties.

Since the solubility of nitrogen in water is approximately 50 times less than the solubility of nitrous oxide, it is assumed that the amount of nitrogen dissolved in the cream can be neglected. The nitrogen will be present in the form of bubbles which might disturb the initial foam properties. Furthermore, the addition of nitrogen gives a higher total pressure before the nozzle. The resulting increase of the mechanical forces can also negatively affect the initial overrun.

3.5.2 Experimental

Gas and liquid flow

To study the relation with the initial foam properties, the amount of gas dissolved in the cream was varied by changing the pressure in the ACS. This change in pressure was induced by using different combinations of the gas and cream flow. The feasible overrun O_f was calculated with the pressure measured before the nozzle. When this pressure was high enough for the total amount of gas to be dissolved, equation (3.9) was used. Otherwise, the feasible overrun was calculated with equation (2.43).

The initial overrun was measured as a function of the gas:liquid ratio, using nozzle 2. The flow rate of the cream was taken to be 30, 40, 50 or 60 l/h. The gas flow rate was varied relative to the cream flow rate in a ratio of 2 to 20 (at atmospheric conditions), in steps of 2. For each combination of gas and cream flow, three samples of the whipped product were obtained. Their overrun was determined as described in § 2.5.2.

The firmness of the produced foams was measured using the Stevens texture analyser (§ 2.5.2). Again the cylindrical plunger moved with a velocity of 1 mm/s to a depth of 15 mm in the whipped cream. Because the foams collapse very fast, the measurements were performed as soon as possible after the production. While the last sample of foam was coming out of the ACS, the firmness of the first sample was already being measured. As duplicate, the firmness of the third (freshest) sample was determined. The foam deterioration was however so fast that the firmness of this sample was in general significantly lower than that of the first one. It is difficult to relate the firmness of a collapsed foam to the initial measured overrun. Therefore, the results of the last measured samples were not included. If the firmness of the first sample was not larger than that of the third one, the measurement was assumed to be false. These data were also not considered in the overall results.

Nozzle geometry

The tube of nozzle 2 was extended from a length of 0.8 cm up to a length of 20 cm. The overrun of the whipped cream produced with the ACS was determined in triplicate. Measurements were performed at a cream flow rate of 30, 40, 50 and 60 l/h and a gas:liquid ratio varying from 6 to 14 (at atmospheric conditions). Furthermore, firmness measurements were included. To check on the effect of the geometry of the holes in the nozzle, some additional experiments were performed with (an unextended) nozzle 4.

Gas composition

Nitrogen, as a less soluble gas, was added to the nitrous oxide flow in the ACS. The effect on the initial overrun of the produced foams was studied. In order to keep the feasible overrun constant, the amount of nitrous oxide present in the ACS (equation (3.9)) or the partial pressure of the N_2O (equation (2.43)) has to be similar in the comparative experiments. For this purpose, the nitrous oxide:cream ratio is kept constant and nitrogen is added to that.

The cream flow rate was varied from 30 to 60 l/h. The nitrous oxide:liquid ratio ranged from 4 to 14 (at atmospheric conditions) and the nitrogen flow rate was taken to be 0, 12.5 or 25 vol % of the nitrous oxide flow rate. The ACS was equipped with nozzle 2. Overruns were determined in triplicate. Additionally, firmness measurements were performed.

3.5.3 Results and discussion

Gas and liquid flow

The overrun of aerosol whipped cream produced with the ACS was determined at different combinations of the gas and liquid flow. Figure 3.5 shows the mean data of the measurements in triplicate (open symbols) as a function of the gas:liquid ratio. Analogous to the overruns of foams produced with an aerosol can, the triplicates relatively differed up to 10 %. At the higher cream flow rates and gas:liquid ratios the pressure inside the ACS became larger than 15 bar. Therefore, these data could not be measured. The calculated feasible overruns are expressed by the lines in the graph. The closed symbols indicate the cream flow rate belonging to the calculated line.

This graph shows that, initially, an increase in the gas:liquid ratio, which is accompanied by a higher pressure before the nozzle, results in a higher overrun of the foam. At gas:liquid ratios larger than 10, the overrun seems to reach a plateau value; further addition of gas does not significantly affect the overrun.

An important observation was an optimum in optical and rheological quality of the foams as the gas:liquid ratio changed. For all the cream flow rates, this optimum was obtained at a ratio of 8-10. At this ratio the foams were optimal springy and had a nice dry appearance. Furthermore, the blob had a beautiful shape, characterised by sharp edges. At lower gas:liquid ratios (< 8) the foams felt less springy. They appeared shiny and showed flowing edges. At higher ratios (> 10) the foams also felt less springy. Here, the edges of the blob were no longer sharp but showed some sign of destruction. The foam quality was obviously over the top. Mark that the initial overrun of the foam now has reached its plateau value (figure 3.5).
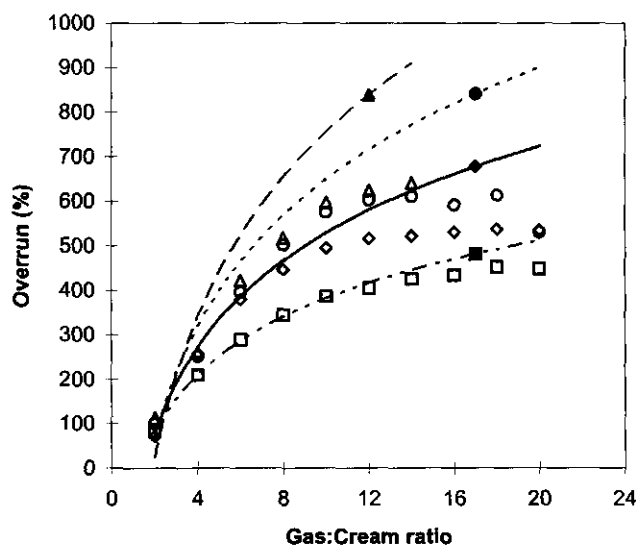
Figure 3.5   The measured (open symbols) and feasible (lines with closed symbol) overrun of
whipped cream produced with the ACS versus the gas:liquid ratio for a cream flow
rate of 30 l/h (□), 40 l/h (◇), 50 l/h (○) and 60 l/h (▵).

At a gas:liquid ratio of 8 the foams have an overrun of at least 300 %. In theory this
is high enough to give a polyhedral foam where gas bubbles deform each other.
The surfaces of the Plateau borders between the bubbles (§ 4.2.1) are curved into
a cylindrical shape. As a result, the foam is able to retain liquid by means of
capillary suction (Prins, 1988). The initially flat menisci at the exterior of the foam
will be drawn into the foam and turn concave. This gives a dry appearance to the
product, which agrees with the experimental findings.
A significant conclusion that follows from the results in figure 3.5 is, that in order to
produce a foam with an overrun comparable to that of whipped cream produced
with an aerosol can (about 600 %), it is not enough to simply add the required
amount of gas (gas:liquid ratio of 6). Several things have to be accounted for.
Firstly, there is always an amount of gas that remains dissolved in the cream after
it leaves the nozzle (approximately 1 litre gas per litre cream). More importantly, in
order to dissolve the necessary amount of gas in the ACS, the pressure before the
nozzle has to be sufficiently high. This pressure depends on the mass flow rate
through the nozzle. It follows from figure 3.5 that, at a gas:liquid ratio of 7 (6 + 1
extra to remain dissolved), a feasible overrun of 600 % cannot be achieved for a
cream flow rate lower than 60 l/h.
Figure 3.5 shows that for the cream flow rates of 30 and 40 l/h, at the lower

gas:liquid ratios (≤ 10), the measured overruns agree very well with the calculated lines. This indicates that, for these situations, the overrun of whipped cream produced with the ACS is determined by the amount of gas dissolved in the cream. At higher gas:liquid ratios and for the cream flow rates of 50 and 60 l/h, the feasible overruns are higher than the measured data. Moreover, an increase in cream flow rate from 50 to 60 l/h does not significantly affect the measured foam properties. Note that the feasible overruns start to deviate from the measured values after the optimal quality of the foams is achieved (gas:liquid ratio > 10).

Two different factors might explain the deviation between the measured and calculated values of the overruns. Firstly, the presence of not dissolved gas (bubbles) in the cream might disturb the foam formation process and affect the initial foam properties. This was also observed in experiments performed with the aerosol can (figure 2.14). The presence of bubbles, caused by shaking the can, negatively affected the overrun. It is assumed that at the lower gas:liquid ratios in the ACS the gas is completely dissolved; bubbles will be present at higher ratios. The disturbing influence is determined by the amount and size of the bubbles. The effect will be larger when more and larger bubbles are present. It is difficult to estimate how the amount of bubbles is affected by the conditions in the ACS. When the gas:liquid ratio increases probably more bubbles will be present. For a similar ratio but at a higher cream flow rate, the amount of not dissolved gas will be less because of the higher pressure. Whether this is accompanied by the presence of less bubbles and/or smaller bubbles is not known. It is also difficult to estimate the bubble size at the varying conditions. In general, bubbles will be smaller at a higher cream flow rate due to the larger shearing forces in the static mixer. Although, because of the higher pressure drop they will expand more when flowing through the nozzle. Nevertheless, the disturbing effect of bubbles will become more important when the amount of not dissolved gas is larger. This occurs at lower pressures and thus at lower cream flow rates. Figure 3.5 however shows that the deviation between calculation and experiment becomes larger with increasing cream flow rate. Apparently, bubbles are not the main disturbing factor.

A second factor that might affect the initial overrun is the pressure drop over the nozzle. At higher pressure drops the mechanical forces acting upon the bubbles become larger. This negatively influences the initial overrun. The effect was already observed in results obtained with the aerosol can (figure 2.15). In the ACS the pressure drop over the nozzle, and consequently the mechanical forces, will become larger with increasing gas:liquid ratio and increasing cream flow rate. This agrees with the results in figure 3.5. The magnitude of the mechanical forces indeed plays an important role in determining the initial foam properties. Note that the destructive effect of the mechanical forces was visible in the appearance of the

edges of the blob (at gas:liquid ratios > 10).

It can be concluded that there is a correlation between the amount of gas dissolved in the cream in the ACS and the overrun of the produced foam. In the determination of the initial foam properties, the presence of bubbles might form some mechanical disturbance. More importantly, the mechanical forces resulting from the pressure drop over the nozzle, strongly affect the initial overrun of the whipped cream. At the higher pressure drops, an increase in forces acting upon the gas bubbles in the nozzle results in an increase of 'blow by'.

The initial foam properties at varying gas and liquid flow rates were also characterised by measurements of the firmness. Because of the overlapping results, these experimental data were added to the firmness measurements performed at the foams obtained with a varying nozzle geometry (described next). The combined results are plotted in figure 3.7 and will be discussed there.

Nozzle geometry

Analogous to the experiments performed with aerosol cans, the geometry of the holes in the nozzle did not show a significant effect on the initial properties of foam produced with the ACS. Increasing the length of the nozzle tube however did affect the overrun of the product. This is plotted in figure 3.6. The mean values of the overruns obtained at a gas:liquid ratio of 10 (at atmospheric conditions) are given as a function of the tube length. Differences measured between the triplicates of the overruns were less than 10 % (relatively). At a flow rate of 60 l/h the pressure before the nozzle with a tube longer than 5 cm became so high that the pressure inside the ACS exceeded the maximum allowed value of 15 bar. Consequently, no foams could be produced and no overruns were determined.

At a cream flow rate of 30 l/h the overrun remains more or less the same as the tube length varies. For the higher cream flow rates the graph shows a decreasing trend in the overrun with increasing tube length. As was expected, this trend becomes more pronounced as the cream flow rate, and thus the magnitude of the shear forces in the tube, becomes larger.

Comparing the results for the cream flow rate of 50 l/h in figure 3.6 with the results obtained with the aerosol can (figure 2.16), shows a slightly lower decrease in overrun for the ACS results. The flow rate out of an aerosol can decreases with increasing tube length. However, the flow rate out of the ACS is constant and on average higher than the flow rate out of the aerosol can. This indicates that the shear forces in the nozzle on the ACS are larger than in the nozzle on an aerosol can. Contrary to the results, a stronger decrease in overrun with increasing tube length would be expected with the ACS.
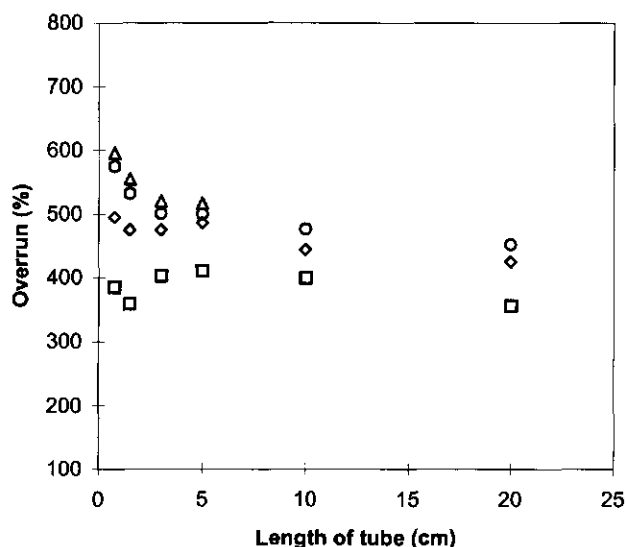
Figure 3.6   The overrun of aerosol whipped cream produced with the ACS as a function of the tube length of the nozzle at a cream flow rate of 30 l/h (□), 40 l/h (◊), 50 l/h (○) and 60 l/h (▵) and at a gas:liquid ratio of 10 (at atmospheric conditions).

In the ACS, the decrease in overrun due to extension of the nozzle tube is in fact larger than suggested by the results plotted in figure 3.6. An increasing tube length of the nozzle is namely accompanied with an increase in pressure before the nozzle (figure 3.4). At a higher pressure the amount of gas dissolved in the cream, and the feasible overrun of the foam, will be higher. Accounting for this effect, the decrease in the overruns of the foams produced with the ACS will be more pronounced. At a cream flow rate of 30 l/h, the feasible overrun of the foam increases from 370 % to 670 % for a tube length of respectively 0.75 and 20 cm. The measured overrun is however more or less constant. Therefore, in fact there is a decreasing trend in the overrun with longer tube length. Moreover, the decrease in overrun at a cream flow rate of 50 l/h will indeed be stronger with the ACS than for the foams out of an aerosol can.

At a lower gas:liquid ratio, the decreasing trend of the overrun with the tube length was only slightly visible. At a higher gas:liquid ratio the decreasing trend became more pronounced. This might be explained by the magnitude of the shear forces, becoming larger as the ratio increases. Obviously, the overrun of the foams out of the ACS depends on the cream flow rate. It is however worth noting, that the overrun out of the longer tubes (L > 5 cm), in which the shear forces have more time to affect the foam, is more or less the same for the different gas:liquid ratios. A

similar trend was visible in figure 3.5 where, at the higher shear forces, the overrun seemed to reach a plateau value for the higher gas:liquid ratios.

The firmness of the whipped creams out of the ACS is plotted against the overrun in figure 3.7. Note that these are the combined results of the variation in gas and liquid flow (previous experiment) and the different nozzle geometries.
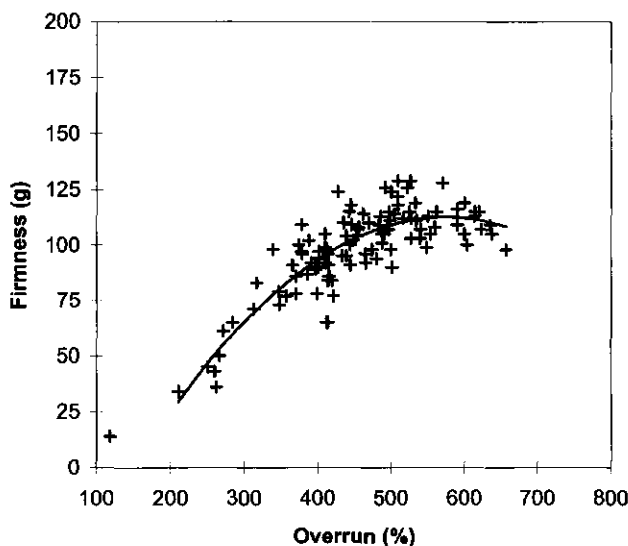
Figure 3.7   The firmness of aerosol whipped cream out of the ACS versus the overrun.

This figure shows a similar relation between the firmness and overrun of the foams as was found for the results obtained with the aerosol can (figure 2.17). Again, the firmness initially increases with the overrun, because the gas bubbles become more closely packed in the foam. At larger overruns the firmness reaches a plateau value. Here, the maximum packing between the bubbles is achieved, resulting in a polyhedral foam (§ 2.5.3).

Gas composition

The effect of addition of nitrogen to the nitrous oxide flow in the ACS on the initial overrun is presented in figure 3.8. The graph shows the mean value of the overrun of the produced foams versus the amount of nitrogen added relative to the amount of nitrous oxide. The triplicates of the overrun results varied less than 10 % (relatively).
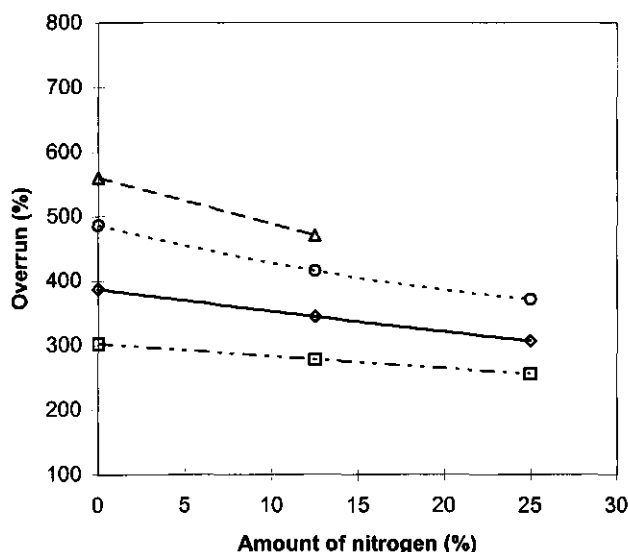
Figure 3.8   The initial overrun versus the amount of nitrogen added relative to the amount of
nitrous oxide at a cream flow rate of 30 l/h (□), 40 l/h (◊), 50 l/h (o) and 60 l/h (△)
and a nitrous oxide:cream ratio of 10 (at atmospheric conditions).

The presented results were obtained at a nitrous oxide:liquid ratio of 10 (at
atmospheric conditions). Similar trends were obtained for the other ratios. Due to
the pressure limitation in the ACS only two data points could be determined for the
cream flow rate of 60 l/h.

Figure 3.8 clearly shows the effect of addition of nitrogen. When more nitrogen is
added, the overrun becomes lower. This decrease is somewhat stronger at the
larger cream flow rates. The influence on the overrun is probably the result of two
effects which were both mentioned before. Firstly, the nitrogen is present in the
form of bubbles because it hardly dissolves in the cream. Bubbles were already
shown to negatively affect the initial overrun. Secondly, the addition of nitrogen to
the laughing gas induces an increase in the pressure before the nozzle.
Consequently, the mechanical forces acting upon the foam while flowing through
the nozzle are larger. This is also known to induce a decrease of the overrun. It
can be concluded that, although addition of a less soluble gas can improve the
stability against disproportionation, experiments with the ACS showed that it
negatively affects the initial overrun.

The relation between the firmness and overrun of the produced foams is affected
by addition of nitrogen in the ACS. This can be seen in figure 3.9.
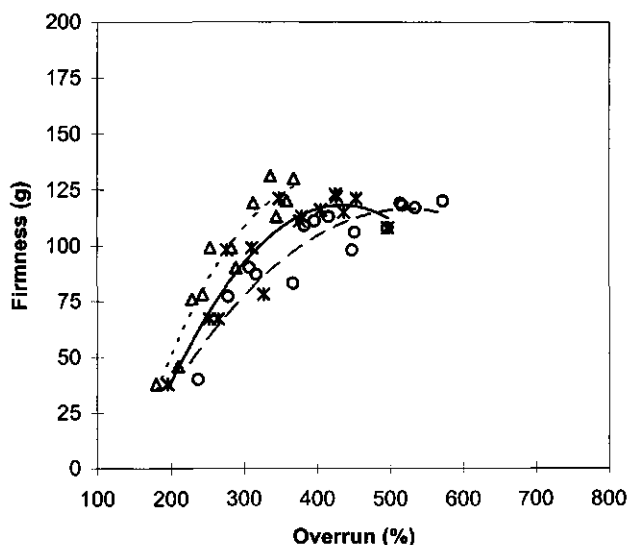
Figure 3.9   Effect of addition of 0 % (o), 12.5 % (x) and 25 % (Δ) nitrogen on the relation between firmness and overrun of whipped creams produced with the ACS.

It was assumed that the relation between firmness and overrun is a product characteristic, being independent of the addition of nitrogen. A decrease in overrun, induced by addition of nitrogen (figure 3.8), was expected to result in a lower firmness (figure 3.7). The results however showed that, despite of the lower overrun, the firmness did not change significantly. This is expressed in figure 3.9. Although there is large scatter in the data, the trend is apparent.

As was mentioned before, the addition of nitrogen results in a larger amount of not dissolved gas in the ACS. Furthermore, the mechanical forces acting upon the foam while it leaves the nozzle, increase. Despite of the resulting decrease in overrun, the texture of the foam, expressed in the firmness, does not seem to be significantly affected. It can be speculated that in the absence of nitrogen, the process of disproportionation proceeds faster. This results in a more broad bubble size distribution. Formation of a polyhedral foam would therefore be induced at a higher volume fraction of gas than in the presence of nitrogen. Consequently, if nitrogen is added the firmness will be higher at a lower overrun. Within the time scale of the experiment (approximately a minute) it is however not very likely that this effect is so pronounced.

An other possible explanation for the observed effect is that the decrease in overrun is mainly the result of destruction of foam bubbles near the nozzle walls. If

bubbles break down, cream films remain at the outside of the foam. Assuming that these films do not spread into the center of the foam, this will not damage the internal foam structure. The effective firmness will thereby not be influenced. The effect of mechanical forces, which is stronger than the effect of bubbles on the overrun (figure 3.5), will indeed dominantly take place at the walls of the nozzle tube.

If the latter explanation holds, the effect of mechanical forces on the relation between foam firmness and overrun would also have to be visible in other experiments where the forces are large enough to affect the properties. It was shown before that the effect of mechanical forces on the overrun became significant at conditions where the initial overrun was larger than 400-500 % (figure 3.5). Here, the effect on firmness could not be noticed. If it occurs, the effect would vanish in the large cloud of data at the higher overruns.

3.6   Conclusions

An important result from this research is the development of an apparatus, the Aerosol Can Simulator, which is able to produce aerosol whipped cream with properties comparable to the foam produced with an aerosol can. The static mixer in the apparatus realised optimal dissolution of the gas in the cream and is essential for the foam formation process. The ACS has proved to be a good tool to study the process of instant foam formation.

The main difference in the working of the ACS and the aerosol can is the regulating parameter. In the ACS the positioned flow rates of the gas and the cream determine the pressure before the nozzle whereas in an aerosol can the pressure before the nozzle determines the flow rate. A crucial similarity is that the process of foam formation in both methods is determined by choking conditions in the nozzle. Because of this, the relation between the different parameters is independent of the method and similar in both situations. The flow conditions and properties of foam out of an aerosol can and out of the ACS may therefore directly be related to each other.

The experiments performed with the ACS confirmed the important role of the amount of gas dissolved in the cream in the production of aerosol whipped cream. In order to obtain the desired overrun, it has to be assured that the necessary amount of gas can dissolve in the cream. The pressure before the nozzle, and thus the flow rate through the nozzle, has to be high enough.

The initial foam overrun was experimentally verified to be negatively affected by the presence of large shearing forces and, to a lesser extend, by bubbles present in

the cream. These factors also explain the effect of addition of nitrogen to the N_2O flow on the initial overrun. Although a less soluble gas can have a positive effect on the stability of foam against disproportionation, addition of nitrogen showed to have a negative effect on the overrun. The presence of extra N_2 results in higher pressures in the ACS and thereby larger shearing forces in the nozzle. Additionally, more not dissolved gas (bubbles) will be present in the cream.

Analogous to the findings with the aerosol can, the nozzle geometry showed to affect the flow properties in the nozzle of the ACS. Extension of the nozzle tube caused an increase in pressure before the nozzle. These findings correspond with theoretical calculations on the flow of foam through a tube. A longer tube, at a similar mass flow rate, results in an increase of frictional resistance against flow. This gives a larger pressure in and before the nozzle. Furthermore, the decrease in initial overrun found by extension of the tube of the nozzle on an aerosol can, was experimentally confirmed with the ACS.

For foams produced with nitrous oxide the relation between firmness and overrun was found to be similar to the results obtained with the aerosol cans. Addition of nitrogen to the gas flow, however, showed to affect this relation. The presence of N_2 negatively affected the overrun, whereas the firmness of the products did not change significantly. It is speculated that the larger shearing forces in the nozzle in the presence of extra gas, cause destruction of the foam near the nozzle walls without affecting the foam structure in the center of the flow.

3.7   References

-       Berge, L.I., 1990. Dissolution of Air Bubbles by the Resistive Pulse and the Pressure Reversal Technique. Journal of Colloid and Interface Science. 134 (2), 548-562.

-       Bird, R.B., Steward, W.E. and Lightfoot, E.N., 1960. Transport Phenomena. John Wiley & Sons, inc. Singapore.

-       Bisperink, C.G.J. and Prins, A., 1994. Bubble Growth in Carbonated Liquids. Colloids and Surfaces A: Physicochemical and Engineering Aspects, 85, 237-253.

-       Ergun, S., 1952. Fluid Flow through Packed Columns. Chemical Engineering Progress, 48(2), 89-94.

- Hirasaki, G.J. and Lawson, J.B., 1985. Mechanisms of the Foam Flow in Porous Media: Apparent Viscosity in Smooth Capillaries. Society of Petroleum Engineers Journal, april 1985, 176-190.
- Hsieh, D.Y., 1965. Some Analytical Aspects of Bubbles Dynamics. Journal of Basic Engineering, dec 1965, 991-1005.
- Jansen, L.P.B.M. and Warmoeskerken, N.M.C.G., 1987. Transport Phenomena Data Companion. Edward Arnold (Publishers) Ltd, London, Delftse Uitgevers Maatschappij bv, Delft.
- Kemblowski, Z. and Michniewics, M., 1979. A New Look at Laminar Flow of Power Law Fluids Through Granular Beds. Rheology Acta 18, 730-739.
- Kroezen, A.B.J., 1988. Flow Properties of Foam in Rotor-Stator Mixers and Distribution Equipment. Ph.D. Thesis, University of Twente, The Netherlands.
- Lemmen, J.T.E., 1991. Foam Finishing Technology: The Interaction of Foam with Stagnant and Moving Substrates in Foam Application. Ph.D. Thesis, University of Twente, The Netherlands.
- Mehta, D. and Hawley, M.C., 1969. Wall Effect in Packed Columns. Ind. Eng. Chem., Process Design and Development, 8 (2), 280-282.
- Nevers, N. de, 1991. Fluid Mechanics for Chemical Engineers. Second Edition. McGraw-Hill, Inc., New York.
- Prins, A., 1988. Principles of Foam Stability. In: Advances in Food Emulsions and Foams, Dickinson E. and Stainsby, G. (eds.), Elsevier Applied Science, England, 91-122.
- Ronteltap, A.D., 1989. Beer Foam Physics. Ph.D. Thesis, Wageningen Agricultural University.
- Ronteltap, A.D., 1990a. The Role of Surface Viscosity in Gas Diffusion in Aqueous Foams, part 1: Theoretical. Colloids and Surfaces, 47, 269-283.
- Ronteltap, A.D., 1990b. The Role of Surface Viscosity in Gas Diffusion in Aqueous Foams, part 2: Experimental. Colloids and Surfaces, 47, 285-298.
- Rosner, D.E. and Epstein, M., 1972. Effects of Interface Kinetics, Capillarity and Solute Diffusion on Bubble Growth Rates in Highly Supersaturated Liquids. Chemical Engineering Science, 27, 69-88.
- Ruckenstein, E. and Davis, E.J., 1970. Diffusion-Controlled Growth or Collapse of Moving and Stationary Fluid Spheres. Journal of Colloid and Interface Science, 34 (1), 142-158.
- Savins, J.G., 1969. Non-Newtonian Flow Through Porous media. Industrial and Engineering Chemistry, 61 (10), 18-47.
- Srinivas, B.K. and Chhabra, R.P., 1992. Effects of Particle to Bed Diameter Ratio on Pressure Drop for Power Law Fluid Flow in Packed Beds. International Journal of Engineering Mechanics, 5 (3), 309-327.
- Tao, L.N., 1978. Dynamics of Growth or Dissolution of a Gas Bubble. J. Chem. Phys. 69 (9), 4189-4194.
- Vries, A.J. de, 1958a. Foam Stability, part 2: Gas Diffusion in Foams, Recueil, 77, 209-223.
- Vries, A.J. de, 1958b. Foam Stability, part 3: Spontaneous Foam Destabilisation Resulting from Gas Diffusion, Recueil, 77, 283-296.
- Yung, C.N., de Witt, K.J., McQuillen, J.B. and Chai, A.T., 1989. A Numerical Study of Parameters Affecting Gas Bubble Dissolution. Journal of Colloid an Interface Science, 127 (2), 442-452.

Chapter 4

The foam stability of aerosol whipped cream

4.1   Introduction

As has been mentioned in the previous chapters, aerosol whipped cream destabilises rather fast. In this chapter the (in)stability of the foam is characterised in more detail. The stability of foam is affected by several processes which all contribute to the loss of overrun and firmness of the product on ageing. Firstly, some theoretical aspects on the main destabilisation processes will be described and their relevance for the stability of aerosol whipped cream will be discussed.
The properties of a foam are for a large part obtained from the properties of the surfaces in that foam. Consequently, the surface rheological properties of the liquid from which the foam is produced largely affect the different mechanisms that determine the foam stability. Some surface rheological techniques have been applied to aerosol whipping cream. The surface rheological measurements and observations will be presented and their importance will be discussed in relation to the stability of the whipped product.
The structure of a foam, resulting from the foam formation process, determines the properties and stability of that foam. Important structural elements in aerosol whipped cream are the gas bubbles, including the bubble surfaces, fat globules and protein particles. The latter were not studied in the present research. To obtain more information of the foam (micro)structure, some theoretical considerations on the bubble surface coverage will be given. The presence, size and location of the structural elements was studied in more detail by means of two microscopical techniques. Because the firmness of foam is strongly related to its structure, measurements of the firmness in time are finally presented to illustrate this aspect of foam stability.

4.2   Foam stability

An optimum stability of aerosol whipped cream is obviously an advantage. The stability of foam is largely determined by the contribution of different destabilisation phenomena, of which three important processes are drainage, coalescence and disproportionation (Prins, 1986). These processes are quite extensively described

by Ronteltap (1989) and recently by Bisperink (to be published).

4.2.1 Drainage of foam

Drainage of foam is the flow of liquid from that foam. In a polyhedral foam, like aerosol whipped cream (see figure 4.7), a distinction can be made between drainage from the Plateau borders and drainage from the thin films between the gas bubbles. The Plateau borders are the liquid edges in the foam where the films of three bubbles meet (de Vries, 1958a). Drainage from Plateau borders proceeds until the capillary suction equals the hydrostatic pressure of the liquid, or (Prins, 1986; Prins, 1988):

$$\frac{\gamma}{r} = \rho g h \qquad (4.1)$$

here γ is the surface tension and r the radius of curvature of the cylindrical shaped Plateau border, ρ the liquid density, g the acceleration due to gravity and h the hydrostatic height.

Drainage from a thin liquid film is driven by gravity which acts directly on the liquid in a non-horizontal film and indirectly through Plateau border suction (Prins, 1988). The presence of surface active components, like proteins, can stabilise the liquid films. The shear strain exerted by the flowing liquid on the film surfaces expands the top of the film. This results in an increase in surface tension because there is not enough surfactant present in the film to restore the original adsorption at the surface. At the same time the compression at the bottom of the film induces a lower surface tension. Consequently, a surface tension gradient is created from the bottom to the top. This gradient introduces a shear stress and can eventually compensate for the weight of the film. As a result, the film surfaces remain almost motionless (Prins, 1990).

Considering the film surfaces to be motionless, the time t needed for the drainage to a certain film thickness is given by (Prins, 1986; Walstra, 1989):

$$t(\delta) = \frac{6\eta l}{\rho g \delta^2} \qquad (4.2)$$

where η the liquid viscosity and l and δ respectively the height and the thickness of the film. Equation (4.2) illustrates that the drainage time depends strongly upon the film thickness. Additionally, drainage can be importantly slowed down through a higher liquid viscosity. This has experimentally been shown by several authors as mentioned by Bikerman (1973) and Halling (1981). The draining process can be

completely stopped when the liquid has a certain yield value (Prins, 1986; Walstra, 1989). Furthermore, the presence of a large number of particles in the films may greatly retard the process, especially when the particles aggregate in some manner and form a continuous network. This is known as the Pickering mechanism (Prins, 1988). In whipped fresh cream the fat globule network indeed contributes to the foam stability.

Besides viscous flow, a process called marginal regeneration can contribute to film drainage. Marginal regeneration consists of exchange of thicker and thinner film parts with the film surrounding the Plateau border; the thinner parts are drawn out of the border and thicker parts are sucked into it (Prins, 1995). Generally, protein stabilised films are too rigid with respect to shearing and to dilational deformation, to exhibit this process (Prins, 1986). Since milk proteins are known to adsorb at bubbles in cream (chapter 1), it is not expected that marginal regeneration will play an important role in aerosol whipped cream. More information on this process is described by Lucassen (1981) and Prins (1988).

In the present research no specific study was made on the role of drainage in the stability of aerosol whipped cream. However, the effect is estimated to be small compared to other destabilisation processes. Cream has a relatively high viscosity, especially at small shear rates (appendix II). The flow of cream out of the foam will therefore not proceed very fast (equation (4.2)). Moreover, the presence of fat globules in the liquid phase may also retard the drainage process. Although syneresis, which is a result of drainage, was not observed during the first period after the production of aerosol whipped cream, some loss of serum has occasionally been observed after a longer time (more than an hour).

The absence of drainage, or rather the capillary suction which counteracts the drainage process (equation (4.1)), is thought to be responsible for the initial 'dry' appearance of aerosol whipped cream (§ 3.5.3). The deterioration of the foam which is clearly visible within the first 15 minutes after foam production (figure 1.2) is expected to be primarily induced by other mechanisms than drainage.

4.2.2 Coalescence of gas bubbles

Coalescence is the merging of two bubbles as a result of rupture of the film between the bubbles. This process is therefore determined by the stability of the liquid films between the bubbles. The smaller the film thickness, the more liable the film is to rupture (de Vries, 1958a). The mechanisms that determine the (in)stability of a liquid film are very different when the film is young and thick than later when it is old and thin after drainage (Lucassen, 1981; Walstra, 1989). The stability of thin foam films, with a thickness of a few tens of nanometers, strongly depends on the

presence of disjoining pressure and surface-active material. More information on this topic is given by Lucassen (1981). The films in aerosol whipped cream are in the order of 1 µm, as will be visualised in § 4.4.3, and are not expected to become much thinner due to drainage (§ 4.2.1). The stability of relatively thick films will be considered in more detail.

Thinner places in a foam film, caused by for example a sudden disturbance, make the film more susceptible to rupture. In the presence of surface-active material in the liquid film, local thinning can be resisted by the Gibbs-Marangoni mechanism (Dickinson, 1992). At a thinner spot, the surface is locally enlarged and consequently has a higher surface tension than the undisturbed area. The resulting surface tension gradient causes the film surface to move towards the thinner spot. Simultaneously, film liquid is dragged along by viscous forces in the same direction and thereby prevents the film to break (Bikerman, 1973).

Rupture of a liquid film between two bubbles can be induced by the presence of either hydrophobic or spreading particles or by evaporation of liquid from the films (Prins, 1988). The latter is not important in the time scales relevant for the destabilisation of aerosol whipped cream, even more because there is a saturated atmosphere inside the foam and additionally a relatively low temperature (10 °C).

When a hydrophobic particle is present in a liquid film between the bubbles and bridges the film, the surfaces next to the particle are curved because of the poor wetting properties. This locally induces a higher Laplace pressure, causing the liquid to flow away from the particle to a lower pressure in the film. The process continues until the contact between the particle and the liquid is broken and the film ruptures (Prins, 1988; Ronteltap, 1989; Walstra, 1989). In aerosol whipped cream, the fat globules may act as disturbing particles. Although the interior of the globules is hydrophobic, the surrounding membrane contains more polar components (Mulder and Walstra, 1974). Therefore, it seems not likely that the fat globules act as a hydrophobic particle.

The collapse of a film can also be induced by the presence of particles from which surface-active material spreads over the film surface. The original stabilising surfactant may be replaced by the spreading material, which in turn is not able to retain the film stability (Prins, 1988). More importantly, when the spreading of the material causes the film to move away from the particle, viscous forces effect radial movement of the liquid underneath in the same direction (Ronteltap 1989). Because the amount of available film liquid is limited, this results in a local thinning of the film. Ultimately, film breakage can occur (Prins, 1989).

In order for the spreading particle mechanism to occur, the particle has to reach the film surface. This means that the film between the particle and the surface has to rupture. A milk fat globule will more readily reach the surface if fat crystals are

present (Walstra, 1989). Additionally, it is essential for the spreading that the surface tension of the film liquid γ_l is high enough (Prins, 1988; Prins,1989):

$$\gamma_l > \gamma_m + \gamma_{ml} \tag{4.3}$$

where γ_m and γ_{ml} are respectively the surface tension of the spreading material and the interfacial tension between that material and the liquid. This indicates that the spreading process will be promoted when the film surfaces are expanded. Prins (1986, 1988, 1989) assumes that the spreading mechanism is related to the penetration depth of the spreading motion. Consequently, a higher liquid viscosity and a larger spreading particle will be associated with a lower film stability.

Literature reports that the foam of milk is destabilised by spreading of fat globules (Anderson and Brooker, 1988; Mulder and Walstra, 1974; Prins, 1986). The spreading particle mechanism only leads to film rupture if the process proceeds long enough. In a system like aerosol whipped cream the amount of fat globules, which may spread at a film surface, is very high. If a considerable number of these particles simultaneously cause thinning of the film, the different processes may counteract each other. Furthermore, the surface area of a bubble at which the spreading can occur is limited. In such a situation, one may wonder whether the individual thinning processes can proceed long enough for film breakage to occur.

4.2.3   Disproportionation of gas bubbles

Disproportionation, also known as Ostwald ripening, is the growth of larger bubbles at the expense of smaller ones resulting from gas diffusion between bubbles of different size in the foam and between bubbles and the atmosphere. The driving force for disproportionation, restricted to the case that only one gas is present, is the Laplace pressure difference ΔP_L over the bubble surface (de Vries, 1958b; Lucassen, 1981):

$$\Delta P_L = \frac{2\gamma}{R_b} \tag{4.4}$$

where R_b is the radius of the bubble. This results in a higher pressure inside a smaller bubble. According to Henry's law the amount of gas dissolved is proportional to the pressure (§ 2.2.1). Consequently, the gas concentration in the liquid surrounding a smaller bubble will be higher than in the liquid surrounding a larger one. The existing gas concentration gradient in the liquid in between causes transport of gas from the smaller to the larger bubble. If the process proceeds, the smaller bubbles eventually disappear (Prins, 1986).

In § 3.3.1 different aspects of the dissolution (shrinking) of gas bubbles in the surrounding liquid were already mentioned. These can directly be related to the process of disproportionation. Evidently, the process is strongly promoted by a better solubility of the dispersed gas in the surrounding liquid. The gas composition in the bubble is therefore significant. Furthermore, the diffusion distance of the gas between the bubbles is an important factor (de Vries, 1958b).

In general, disproportionation is a self-accelerating process because the decrease in bubble radius during the shrinking process results in an increase of the driving force (equation (4.4)). The shrinking is, however, also accompanied by compression of the smaller bubble surface which causes the surface tension to decrease. Consequently, the Laplace pressure difference is lower and gas transport is slowed down. The surface rheological properties of the liquid therefore play a significant role in the disproportionation process.

An important property considering the stability against disproportionation is the surface dilational modulus E (Lucassen and van den Tempel, 1972):

$$E = \frac{d\gamma}{d\ln A} \tag{4.5}$$

This property relates to surface rheological behaviour close to equilibrium. Most surfaces of practical systems show visco-elastic behaviour. For these surfaces E depends on the frequency of the applied deformation ω. In this case, the modulus is composed of an elastic part, the storage modulus or surface dilational elasticity E_d, and a loss modulus, $\omega\eta_d$ (Lucassen-Reynders, 1981):

$$|E| = \sqrt{E_d^2 + (\omega\eta_d)^2} \tag{4.6}$$

Visco-elastic surface behaviour may slow down the process of disproportionation but will not completely stop it (Prins, 1988). Lucassen (1981) found that the process of disproportionation can be stopped when, over a relevant time scale, the bubble surface is *purely* elastic and the surface dilational elasticity E_d is larger than half the surface tension:

$$E_d \geq \frac{\gamma}{2} \tag{4.7}$$

Pure elastic behaviour appears in the absence of relaxation processes.

Because a bubble surface is continuously compressed during the shrinking process, it may be more relevant to consider deformation far from equilibrium. The relation between the compression of the bubble surface A and the lowering of the

surface tension γ in the stationary state is now given by the surface dilational viscosity η_s^d (Prins, 1986):

$$\eta_s^d = \frac{\Delta\gamma}{d\ln A/dt} \qquad (4.8)$$

where $\Delta\gamma$ is the decrease in surface tension due to the compression and $d\ln A/dt$ the compression rate of the bubble surface. Strictly speaking, the expansion of the larger bubble during the process has to be accounted for as well. The expansion rate of this bubble is, however, much smaller than the compression rate of the smaller one. Consequently, the effect on the gas transport process is much smaller and may even be neglected (Prins, 1986).

Prins (1988, 1990) describes that for practical systems like milk and beer, the surface dilational viscosity depends strongly on the compression rate. This behaviour can be described by a power law equation:

$$\log\eta_s^d = m \log\left|\frac{d\ln A}{dt}\right| + n \qquad (4.9)$$

where m and n are constants. For most practical systems, including aerosol whipping cream, m is close to -1, at least at room temperature. Thus, when the compression rate becomes very small, η_s^d becomes very high. The higher η_s^d, the higher the resistance of the surface to compression. If it would be possible to slow down $d\ln A/dt$ during the shrinkage, η_s^d would increase, thereby reinforcing the deceleration of the shrinking process.

The effect of the surface dilational viscosity on the disproportionation rate can be significant, as was shown by Ronteltap (1990 a,b). Disproportionation can, however, only be stopped by purely elastic surface behaviour. This corresponds to an infinitely large surface dilational viscosity (Prins et al., 1996) and therefore, according to equation (4.9), to an infinitely small compression rate. If the bubbles contain a well soluble gas, as in aerosol whipped cream, the shrinking will go fast. A large compression rate results. In this case, the surface dilational viscosity will be relatively low and disproportionation will not be slowed down significantly. Moreover, for a self-accelerating shrinking process, η_s^d decreases further as the process proceeds and the acceleration of the disproportionation is reinforced.

Several factors result in the formation of a 'rigid' surface and thereby help to stop disproportionation. The surface active-material present in the liquid may form some kind of network around the bubble, like an insoluble layer of protein (Prins et al., 1996) or a gel phase (Westerbeek, 1989). Also when the bubble surface becomes fully covered with solid particles, the shrinking process can be stopped. This occurs

for example in whipped fresh cream, although it may be questioned whether this is caused by surface or bulk properties. Finally, the presence of a high enough yield stress (Prins, 1986) or biaxial stress (Kokelaar, 1994) in the continuous bulk phase around the bubbles can stop disproportionation.

Aerosol whipped cream is expected to be susceptible to disproportionation because of the high solubility of nitrous oxide in the cream (Wijnen and Prins, 1995). The study presented in this chapter therefore mainly focuses on the role of this process in the destabilisation of the foam.

4.3   Surface rheology

4.3.1 Theory

Rheology is defined as the science of the deformation and flow of matter (Whorlow, 1980). Surface rheology or two-dimensional rheology, studies the relation between the *strain* (amount of deformation) of a surface, the *force* operating in the surface and the *time* scale. A review on surface rheology is given by van den Tempel (1977). In the majority of surface rheological measurements, a dilational deformation is applied to the surface and the resulting change in surface tension is taken as a reflection of the force acting in that surface. This section gives some rheological surface properties and describes various measurements used in practice to study these properties.

Surface rheological properties
One of the basic parameters in the surface rheology is the surface tension γ. The surface tension is the free energy required to increase the surface area by unit amount (Dickinson, 1992). It is a characteristic property of a system which depends on temperature and pressure and is greatly affected by the presence of surface-active material (Prins, 1990). Adsorption of surfactant at a surface causes lowering of the surface tension with $d\gamma$ according to Gibbs:

$$d\gamma = -RT\, \Gamma\, d\ln a \qquad (4.10)$$

where Γ is the surfactant adsorption per unit area and a the activity of the surfactant in solution. The equation indicates that the more surface active material is present in the surface as well as in the bulk solution, the lower the surface tension will be.

When a surface is expanded or compressed, the adsorption per unit surface area

will change. Consequently, the surface tension will be affected. Deformation of a surface results in behaviour which can have elastic and viscous characteristics. If a surface behaves purely elastic, the energy stored in the surface during deformation is recoverable afterwards. No relaxation processes occur during the time scale of deformation. Viscous behaviour reflects the loss of energy through relaxation processes. Relaxation occurs for example by diffusion of surface-active material to the surface or rearrangement of adsorbed molecules within the surface (Lucassen-Reynders, 1993). In practice, most products show visco-elastic behaviour with both a viscous and an elastic component.

Surface rheological parameters that are relevant for the present study are the surface tension, both during surface expansion and in equilibrium, and the surface dilational moduli. These parameters were already introduced in § 4.2. The surfaces studied in this research are considered to be homogeneous. For numerous real systems, including cream, the surfaces are actually non-uniform. Lucassen (1992a,b) described that the presence of particles or droplets in a surface can significantly affect its rheological behaviour. The dilational modulus of such a composite surface depends on the fractions and the moduli of the composing surfaces. In the presence of droplets, the tensions of the curved surfaces involved additionally play a role (Lucassen, 1992b). Even in the absence of surface-active material it is possible that a surface covered with particles will resist deformation (Lucassen; 1992a).

Surface rheological measurements

Surface rheological measurements involve surface deformation. Three types of deformations can be distinguished: dilational, shearing and bending deformations. During dilational deformations the surface area increases or decreases whereas the shape of the liquid surface remains the same. Shearing deformations involve a constant area and a changing shape of the liquid surface. (Lucassen-Reynders, 1993). Bending of a surface changes a flat surface into for example a cylindrical or spherical one. This type of deformation, which will not be considered further, becomes important when the radius of curvature is of molecular dimensions. The present study mainly focuses on dilational deformation.

Prins (1995) described some of the methods that are used in practice to determine surface rheological properties. These properties can be studied by deforming the surface either close to equilibrium using a dynamic measurement, or far from equilibrium in a stationary (steady) state measurement. Surface dilational behaviour close to equilibrium can be studied with the ring trough method (§ 4.3.2), first described by Kokelaar et al. (1991). The measured properties are in particular relevant in relation to disproportionation (Prins, 1995).

Techniques that deform a surface far from equilibrium are for example the overflowing cylinder (Bergink-Martens, 1993) and the falling film apparatus (Ronteltap, 1989). These techniques, which will be described in § 4.3.2, both supply information of expanded surface behaviour. The falling film apparatus studies the susceptibility of an expanded liquid film to breakage, due to the presence of particles (§ 4.2.2). This is relevant for the process of coalescence. It is known that surface expansion negatively affects the stability of liquid films. The film stability strongly depends on the amount of surface-active material that can be supplied to the expanding surface (Prins, 1995). With the overflowing cylinder the ability of a solution to supply surface-active material to an expanding surface can be measured.

The techniques mentioned deform in pure dilation. The resulting changes in surface tension are measured by means of the Wilhelmy plate technique (Padday, 1957). In this chapter a relatively new method, the canal technique, is described. Deformation in this method is not free from shear. In an open rectangular canal a liquid surface is continuously compressed far from equilibrium. Under these circumstances some kind of network may be formed in the surface. Surface rheological properties are determined without a Wilhelmy plate. The observed behaviour can be related to the stability against disproportionation.

To characterise the surface rheological properties of aerosol whipping cream, several surface rheological techniques were applied. The measured properties will be discussed in relation to the effect they will have on the stability of aerosol whipped cream.

4.3.2 Experimental

Aerosol whipped cream is usually formed out of cream with a low temperature (5 °C). Due to the insulating properties of the gas, the temperature in the foam remains below 10 °C during the first 15 minutes. Within this period the main foam destabilisation takes place (figure 1.2). Therefore, most of the surface rheological measurements were performed at temperatures of 5-10 °C.

The overflowing cylinder technique
The overflowing cylinder technique, extensively studied by Bergink-Martens (1993), is used to study the rheological properties of an expanded surface in a situation far from equilibrium. In this apparatus, represented in figure 4.1, the liquid is pumped upwards through a vertical cylinder where it is allowed to flow over the top rim. This causes the liquid surface to expand continuously in a radial manner and a steady state situation is accomplished (Bergink-Martens et al., 1990, 1994).
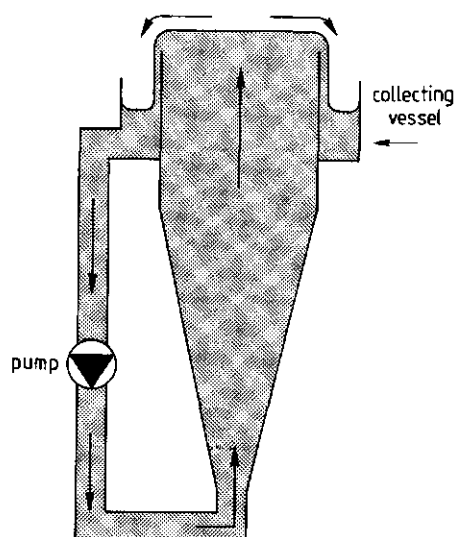
Figure 4.1 The overflowing cylinder technique (from Bergink-Martens et al., 1994).

The overflowing cylinder technique was applied to determine the dynamic surface tension γ_d of the expanded surface of aerosol whipping cream using the Wilhelmy plate technique. The glass Wilhelmy plate was roughened to ensure optimal wetting with the liquid. Dynamic measurements were performed in a cylinder with a diameter of 4 cm. The dynamic surface tension depends on the surface expansion rate. This expansion rate is influenced by the liquid flow rate and the height of the falling liquid film at the outside wall of the cylinder (Bergink-Martens, 1993). Experimental conditions were chosen in such a way that the highest γ_d value possible was obtained, at a liquid flow rate of 120 l/h. Additional measurements of the equilibrium surface tension γ_e were performed at zero flow.

Because the fat globules in the cream may affect the surface rheological properties, creams with a varying fat content of 0, 10, 20, 30 and 38 % w/w, were studied. Measurements were performed at a temperature of 10 °C. It was not possible to measure at lower temperatures since the pump produced some heat that was transferred to the cream. All the data presented are averages of at least duplicates.

The falling film apparatus

The falling film apparatus, schematic represented in figure 4.2, gives qualitative information about the susceptibility of a liquid film for rupture. The liquid under

cylinder technique, a small fat layer attaches to the Wilhelmy plate. This will affect the measurement (see § 4.3.3). Unfortunately, no better alternative was available. The surface dilational properties of cream with a fat content of 32 % w/w were measured at different angular velocities between 0.013 and 1.3 rad/s. This corresponds to a time scale of 1-100 s. The cream temperature was 6 °C. For an accurate measurement it is necessary to deform the surface area within the linear region where the surface dilational properties do not depend on the magnitude of the applied deformation. In the experiments the relative deformation of the surface area was 1.6 %.

The canal technique

The canal technique was developed to study the surface rheological behaviour of a liquid during continuously deformation, in the absence of a Wilhelmy plate. The present study focuses on the behaviour of a compressed part of the surface. It has been observed that during compression some kind of network may be formed in the surface. Prins et al. (1996) studied the skin formation of an aqueous egg-white solution with this technique. The method consists of an open rectangular canal through which liquid is pumped. Viscous forces exerted by the flowing liquid on the surface induce a stress on that surface. This stress can be compensated by means of a surface tension gradient, by the presence of a more or less coherent layer on the surface or by both phenomena. An almost motionless surface may result. A schematic presentation of the canal is given in figure 4.4.
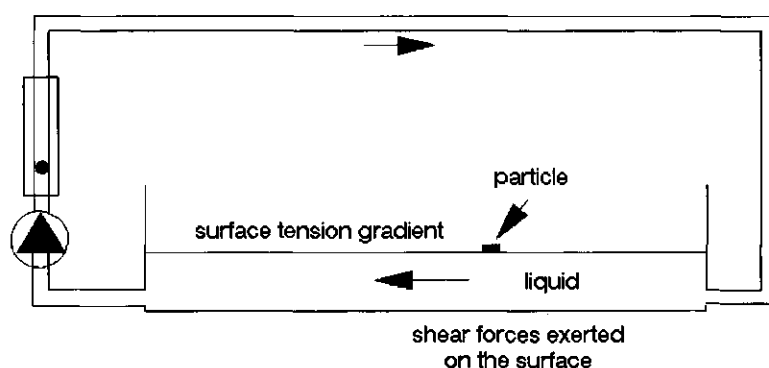

Figure 4.4   Schematic representation of the canal method (from Prins et al, 1996).

When the surface is completely motionless its behaviour is purely elastic. The canal can now be approximated as a rectangular canal with four walls. The stress σ exerted on the motionless liquid surface of a square canal is given by (appendix VII):

$$\sigma = 3.89\eta Q\frac{b+h}{(bh)^2} \qquad (4.11)$$

with η is the liquid viscosity, Q the volumetric flow rate of the liquid and b and h respectively the width and the height of the wetted part of the canal.

A change of the flow rate results in a change of the applied stress and a movement of the surface. This movement can be measured with a cathetometer as the displacement of an aluminium particle positioned on that surface. A surface dilational modulus E can now be estimated (appendix VII):

$$E = \frac{l d\sigma}{d\ln l} \qquad (4.12)$$

here, l is the length of the motionless surface between the particle and the wall of the canal and dl the displacement of the particle on the surface as a result of a change $d\sigma$ in applied stress. The stress is changed by changing the liquid flow. It has to be noted that in the derivation of the equation for E several assumptions and simplifications are made. The values of E should therefore only be used as an order of magnitude estimation.

In the present study the canal method was used to study the surface behaviour of cream in compression. Experiments were performed at 5-10 °C using aerosol whipping cream with a fat content of 30 % w/w and fresh whipping cream with a fat content of 35 % w/w. The width of the canal was 5 cm, the height of the liquid in the canal was 2.5 cm. The cream flow rate was varied between 20 and 80 l/h, resulting in stresses in the order of 10^{-1}-10^{-2} N/m^2 for cream.

4.3.3 Results and discussion

The overflowing cylinder technique

The dynamic and equilibrium surface tension of aerosol whipping cream were measured in the overflowing cylinder. In figure 4.5 the data of the dynamic surface tension γ_d and the surface tension in the equilibrium situation γ_e are represented as a function of the fat content of the cream at a temperature of 10 °C. The duplicates of the measurements differed less than 5 % in the dynamic situation and up to 10 % in the equilibrium situation. The deviations could be twice as high between

different batches of cream. The measurements of the equilibrium surface tensions showed more scattering because it was difficult to determine when the previously expanded surfaces had reached an equilibrium situation. The data of γ_e were taken as soon as a stable value seemed to be established. Although, sometimes the surface tension slightly kept decreasing during several hours afterwards.
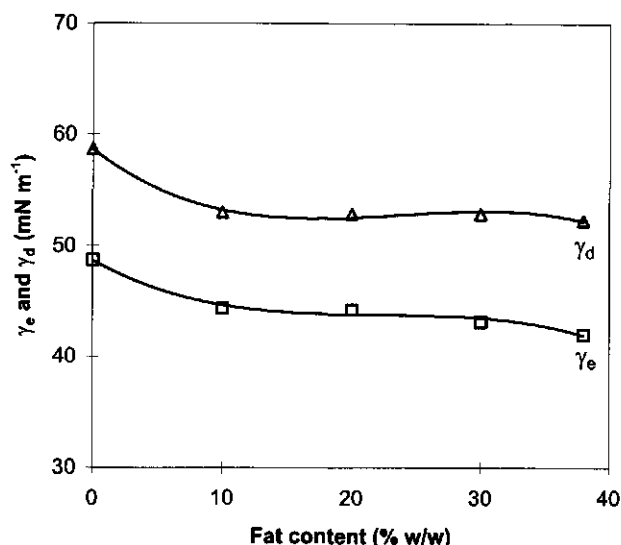
Figure 4.5 γ_d (△) and γ_e (□) of aerosol whipping cream as a function of the fat content at 10 °C.

These data show that, since γ_d is larger than γ_e, the surface active compounds in cream are not able to establish the level of equilibrium surface tension during expansion. Consequently, surface tension gradients can be created during expansion of the liquid films in the foam. An important finding from figure 4.5 is furthermore that the presence of fat globules affects the surface properties of the liquid. Both γ_d and γ_e show a decreasing trend with increasing fat content. The fat globules probably adsorb at the surface and additionally may even spread some surface active components and/or liquid fat over it. Finally, it can be marked that the difference between γ_d and γ_e seems to be independent of the fat content of the cream. This indicates that the surface properties, both in equilibrium and in dynamic situation, are mainly determined by the milk proteins.

It is difficult to predict from the measurements in the overflowing cylinder if aerosol whipped cream is susceptible to coalescence. In order for film rupture to occur a

triggering factor is needed. Considering aerosol whipping cream, the fat globules might act as spreading particles (§ 4.2.2).

The falling film apparatus

The falling film apparatus was used to study the spreading of surface active components and/or liquid fat out of the fat globules on the aerosol cream surface. In addition, the film stability was studied as a function of the fat content of the cream. Experiments were performed at room temperature (± 20 °C). Although the data were not very reproducible in a quantitative way, the trends following from the data were apparent. Qualitatively, the following relations were clearly observed.

*   The creams studied, with varying fat content, all showed sparkling light spots. This demonstrates that material is present that can spread under certain conditions at the film surface and thereby may induce coalescence. In this respect it has to be noted that in cream with a fat content of 0 % w/w (skim milk) also a small amount of fat is present. The amount of sparkling light spots increased with an increasing cream fat content. Apparently, the fat globules provide the spreading material.
*   The number of holes formed per unit time in the films of aerosol whipping cream increased as the fat content became higher. Obviously, the film stability is related to the number of fat globules and thereby the amount of spreading material present.
*   The volumetric flow rate at which a film with a certain length ruptured was lower as the fat content of the cream was lower. This means that cream with a low fat content is able to form a stable film at a flow rate where no stable film can be formed under similar conditions in the presence of more fat. Accordingly, the length of a stable film that could be formed at a certain volumetric flow rate decreased with increasing fat content. The flow rate corresponds to the film thickness. At a same flow rate, the thickness of a shorter film is on average larger than the thickness of a longer film. Cream with a lower fat content is therefore able to form a thinner stable film than cream with a higher fat content.

These results all lead to the conclusion that, under certain conditions, aerosol whipping cream is susceptible to film rupture caused by the presence of fat globules. The film stability is obviously related to the amount of fat present in the cream, showing a decreasing stability with an increasing fat content of the cream.

Despite the observations, it is not expected that the process of coalescence plays an important role in the destabilisation of aerosol whipped cream. The above relations were observed at room temperature and may be related to processes occurring at the outside of a blob of aerosol whipped cream, placed at room

temperature. At lower temperatures inside the blob, it is however likely that spreading, especially of liquid fat, will happen less or not at all. Furthermore, the surface area of a bubble is much more limited than that of the falling film. In addition, the amount of globules in the film between two bubbles is so high that the distance between the globules at the surface will be relatively small. As was already explained in § 4.2.2 it is questionable whether thinning of the film, resulting from the spreading particle mechanism, is able to proceed long enough under these conditions for rupture to occur.

The ring trough method
The surface dilational elasticity (storage modulus) and the loss modulus of aerosol whipping cream were measured to determine whether they are capable of stopping the process of disproportionation. The results are presented in figure 4.6. To see if the requirement for the stability against disproportionation is fulfilled, $E_d \geq \gamma/2$ (equation (4.7)), the value for $\gamma/2$ is plotted as well.
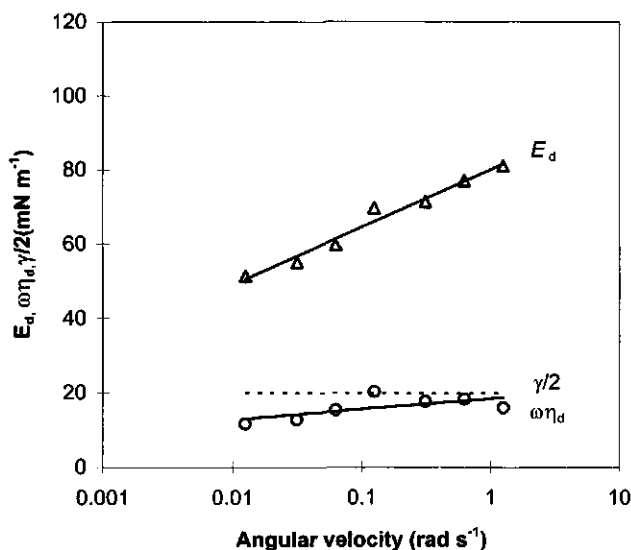
Figure 4.6   The surface dilational elasticity E_d (△), the loss modulus $\omega\eta_d$ (○) and half the surface tension $\gamma/2$ (- - -) of aerosol whipping cream as a function of the angular velocity; $\mathrm{dln}A = 1.5$ %; $T = 6$ °C (from Wijnen and Prins, 1995).

The graph shows that aerosol whipping cream does not behave purely elastic in this dynamic measurement close to equilibrium; the loss modulus is larger than zero. Consequently, according to the Lucassen condition (see § 4.2.3),

disproportionation can not be stopped by the surface rheological properties of aerosol whipping cream within the time scales measured (1-100 s). The surface dilational elasticity is however always larger than half the surface tension. As a result, disproportionation might be slowed down.

It is important to note that the magnitude of the moduli plotted in figure 4.6 is questionable. The measurements were performed at a surface having more or less constant properties in time. However, additional research has shown that very often the surface dilational modulus of aerosol whipping cream significantly changes in time, especially at higher temperatures. A fresh cream surface shows a modulus slightly smaller or comparable to the moduli plotted in figure 4.6. Within a few hours the surface dilational modulus can however increase by a factor 5-10. It is speculated that some kind of network may be formed at the surface. In this case, it is difficult to perform reliable measurements with the ring trough method, since the surface properties strongly depend on the history of the surface.

In addition, the surface properties in the ring trough seemed to be affected by the presence of the Wilhelmy plate. During the experiments a small fat layer became attached to the plate, thereby disturbing optimal wetting of the plate and affecting the measurements. Cleaning and repositioning of the plate in between the measurements sometimes resulted in a decrease of the moduli measured afterwards. It is possible that this procedure locally disrupted the network present at the surface.

It can be concluded that it is difficult to perform reliable measurements of surface properties of cream with the ring trough method since the properties often strongly depend on the history of the surface. Moreover, the reliability of using a Wilhelmy plate can be questioned. Although the magnitude of the moduli in figure 4.6 might not be completely correct, the conclusions following from these results are not affected by the shortcomings of the method applied to aerosol whipping cream. Purely elastic behaviour was never observed and the surface dilational elasticity always exceeded half the surface tension. Disproportionation will therefore not be stopped by the surface rheological properties of aerosol whipping cream but it might be slowed down.

The canal technique

The ring trough technique studies surface rheological behaviour in dilation close to equilibrium. In a foam produced with a good soluble gas, bubbles may shrink fast during disproportionation. Consequently, the bubble surfaces deform rather far from equilibrium. It seems therefore more obvious to study surface rheological behaviour under these circumstances.

As pointed out before, purely elastic surface behaviour is a prerequisite to stop the

shrinking process. Prins et al. (1996) demonstrated that it depends on the method used whether or not pure elastic behaviour is observed. An aqueous egg white solution showed visco-elastic behaviour in the ring trough technique, whereas pure elastic behaviour was found in the canal technique. The difference was explained by assuming that the surface layer is an elastic gel filled with water. In a dynamic measurement water can flow through the layer, causing viscous effects. During continuous compression, when the transport of water has come to an end, only the elastic properties of the network are measured.

In the present study the canal technique was used to study if aerosol whipping cream is able to show pure elastic behaviour during continuous compression far from equilibrium. A plus of this method, compared to the ring trough, is that no Wilhelmy plate is used. In the beginning of the canal a small falling film was introduced to apply an expansion followed by a compression to the surface. This mechanical treatment is known to induce a more rigid surface for several surfactants (Kokelaar, 1994; Prins et al., 1996).

During experiments performed in the ring trough some kind of skin was visible at the surface of aerosol whipping cream. It was therefore expected that skin formation would also be seen in the canal technique. Aerosol whipping cream was pumped through the canal at a temperature of 5-10 °C. Indeed a skin was formed at the liquid surface. The skin seemed mainly composed of fat globules since it showed more yellow than the underlying liquid. Although the skin was attached to the walls of the canal, the rest of the skin rippled, also at small liquid flows. The liquid surface was not motionless and did not show purely elastic behaviour. Consequently, it has to be concluded that the surface rheological properties of aerosol whipping cream in the canal during compression far from equilibrium are not able to stop the process of disproportionation.

For comparison, the experiment was repeated with fresh whipping cream. This product was able to form a motionless surface within a few minutes. This was probably due to partial coalescence of the fat globules, resulting in network formation. The movement of a particle at the surface was measured. Changing the flow between 20 and 80 l/h resulted in displacements of approximately $2 \cdot 10^{-2}$ cm. The length of the motionless surface between the particle and the canal wall was estimated at 25 cm. To calculate the stress on the liquid surface (equation (4.11)), the plateau value of the viscosity of aerosol whipping cream was used (0.04 Pas, appendix II). It has to be noted that unhomogenised fresh cream in practice has a lower viscosity than the homogenised aerosol cream (Mulder and Walstra, 1974). On the other hand the shear rates in the channel are relatively low (1-10 s^{-1}) and consequently the apparent viscosity will be higher (appendix II). With the mentioned parameters the surface dilational modulus (equation (4.12)) was estimated to be in

the order of 10^4-10^5 mN/m, which is at least 100 times larger than measured for other practical systems (Kokelaar, 1994; Prins et al., 1996). From this it is to be expected that whipped fresh cream, produced with laughing gas, will be more stable against disproportionation.

4.4   Foam structure

4.4.1 General considerations

The properties and stability of a foam are obviously related to the foam structure. Important structural elements in aerosol whipped cream are the gas bubbles, the surrounding liquid films and the fat globules. It is known that in whipped fresh cream the fat globules adsorb at the bubble surfaces and form a continuous network which stabilises the foam (§ 1.4). The surface structure of bubbles is therefore very important in relation to the foam stability.

Also in aerosol whipped cream, interaction between fat globules can contribute to the stability of gas bubbles. To accomplish this, it helps when the fat globules are adsorbed at the bubble surfaces. Moreover, they have to be in contact with neighbouring globules. The extent of the contact between the fat globules depends on the ratio between the total bubble surface and the surface that can effectively be covered by the adsorbed fat globules.

The microstructure of aerosol whipped cream can be studied with cryo scanning electron microscopy (cryo-SEM) (Anderson and Brooker, 1988; Brooker et al., 1986). Images obtained with this technique give information about the bubble size distribution and the position of the fat globules in the foam. This information can be related to the foam stability.

The bubble size distribution also gives insight into the foam structure. Moreover, measurements in time supply information on destabilisation processes occurring in the foam. Drainage results in a decrease of the volume fraction of gas in the foam in time. Coalescence, the merging of bubbles, induces a decrease in the number of bubbles but an increase of the bubble size. The process of disproportionation results in an increase of the number of both smaller and larger bubbles.

Finally, the foam firmness in a way reflects its structure. The firmness of aerosol whipped cream seems to be related to its overrun and average bubble diameter, as described in § 2.5 and § 3.5. Studying the firmness in time reflects changes in these parameters and therefore gives an indication for the amount of destabilisation taking place.

4.4.2 Experimental

Bubble surface coverage

Interaction between fat globules at a bubble surface is maximal when the surface is completely covered. The ratio between the total bubble surface and the total effective surface of the fat globules determines whether or not the globules may realise a close-packed bubble surface. The total bubble surface area A_t available for coverage per volume of foam equals:

$$A_t = \frac{\alpha_g 4\pi R_b^2}{4/3\pi R_b^3} = \frac{3\alpha_g}{R_b} \qquad (4.13)$$

where α_g is the volume fraction gas in the foam and R_b the volume/surface average bubble radius.

When a spherical globule adsorbs on a surface it covers an area which at the most equals its cross-section πR_d^2, with R_d being the radius of the fat droplet. Maximum coverage of a surface with globules is achieved when the globules are close-packed. In this case, each fat globule effectively covers a hexagonal, which encloses the globule, with a surface of $2\sqrt{3}R_d^2$ (Princen, 1979). The total surface A_{ef} that can effectively be covered by the present fat globules per volume of foam is thereby limited to:

$$A_{ef} = \frac{\alpha_d 2\sqrt{3}R_d^2}{4/3\pi R_d^3} = \frac{3\sqrt{3}\,\alpha_d}{2\pi R_d} \qquad (4.14)$$

where α_d is the volume fraction of fat globules in the foam.

Consequently, it is possible that the gas bubble surfaces are close-packed with fat globules when $A_{ef} \geq A_t$. It has to be noted though that some fat globules may adsorb on more gas bubbles at the same time whereas other globules will not make contact with a bubble surface.

Cryo-SEM (Scanning Electron Microscopy)

Cryo-SEM can be used to study the microstructure of a product. The general application of electron microscopy in the analysis of food structure is described by Heertje and Pâques (1995). Anderson and Brooker (1988) and Brooker et al. (1986) applied the method for the investigation of aerosol whipped cream.

In the present study aerosol whipped cream (fat content 35 % w/w, overrun $\approx$ 600 %) was produced using an aerosol can. A small amount of the foam was put on a specimen holder, quickly frozen by plunging it into liquid nitrogen and

transferred to an Oxford Instruments CT 1500 HF cryo transfer unit in which the foam was cryo-fractured and coated with 2 nm platinum. If desired, the sample was also freeze-dried for a few minutes at -95 °C in this unit before the coating step. Finally, the specimen was observed in a JEOL 6300 F field emission cryo SEM at - 170 °C at 2 kilovolt, which was connected with the Oxford Instruments cryo transfer unit. Samples were studied at different magnifications: 300 and 7000 times.

Bubble size distribution

There are several methods to measure the bubble size distribution in a foam, which gives insight into the foam structure. A review on these methods is given by Bisperink et al. (1992). Most of these techniques are however not able to distinguish between the processes drainage, coalescence and disproportionation. A method that can be used to characterise the different destabilisation processes is the Foam Analyser (Bisperink et al., 1992). This method works accurate and relatively fast but unfortunately can not detect bubbles smaller than approximately 20 μm. Simple microscopic research showed that aerosol whipped cream contains smaller bubbles, the amount of which will increase if shrinking of bubbles occurs during destabilisation. The Foam Analyser is therefore not suited to study this product.

It was chosen to study the susceptibility of aerosol whipped cream to the different destabilisation processes with the Leica Q500MC Image Analysis System. This method uses a reversed microscope and a video camera to sample the images. The camera generates an electronic signal proportional to the local intensity of illumination. Bubbles show a bright inside and a darker edge. The surrounding liquid has an intermediate illumination. Because of these differences in brightness, the images can be analysed.

A small sample of aerosol whipped cream (fat content 35 % w/w; overrun approximately 600 %) was put on a glass plate and additionally slightly spread to ensure a thin enough sample for the light to go through. The equipment contains a computer with which the bubble size distribution can be calculated. In order to obtain a reliable distribution, a few hundred bubbles are needed (Bisperink et al., 1992). Because aerosol whipped cream contains some small bubbles (10 μm), a relatively large magnification was needed to study the sample. Moreover, in order to analyse the images, the bubbles have to be distinguished as separate elements. This needs a certain distance between the bubbles and therefore a certain magnification. Because of this magnification, the amount of bubbles per image was not very large and the different processes could not be analysed quantitatively.

The occurrence of the different destabilisation processes in aerosol whipped cream was studied qualitatively by visually following images of a group of gas bubbles as

a function of time. Changes in number and size of the different bubbles as time proceeds, are an indication for the susceptibility towards the different mechanisms. The images were followed for a few minutes.

Firmness
The firmness of aerosol whipped cream was measured as a function of time to illustrate the destabilisation of the foam. The method to measure the firmness of aerosol whipped cream was already described in § 2.5.2. For each measurement a different bowl with foam is necessary. With the ACS (Aerosol Can Simulator) foams with similar properties were produced at a cream flow rate of 50 l/h and a gas flow rate being 6, 8 and 14 times larger than the cream flow rate, at atmospheric conditions. A gas:liquid ratio of 6 gives a soft foam, a ratio of 8 supplies a very nice foam, whereas a ratio of 14 results in products which are clearly 'over the top'. The firmness of the foams was studied over a period of 15 minutes after foam production.

4.4.3 Results and Discussion

Bubble surface coverage
The surface coverage of the gas bubbles in aerosol whipped cream is estimated by comparing the total bubble surface available with the surface that can effectively be covered by the present fat globules (§ 4.4.2). For aerosol whipped cream with an overrun of 600 %, the volume fraction of gas α_g equals 0.86. The average bubble diameter in the foam is estimated to be 50 µm (see also figure 4.7). Consequently, the total bubble surface area A_t available per volume foam equals (equation (4.13)) $1 \cdot 10^5$ m²/m³.

If the fat content of the cream is 35 % w/w, the volume fraction of fat in the cream can be derived from equation (2.6). At a temperature of 5 °C, the volume fraction of fat globules is 0.37. In the foam the volume fraction α_d is thus $(1-\alpha_g) \cdot 0.37 = 0.052$. The average fat globule diameter is taken to be 1.5 µm. The total surface that can effectively be covered with fat globules per volume foam now follows from equation (4.14): $A_{ef} = 6 \cdot 10^4$ m²/m³.

The ratio between A_{ef} and A_t gives information about the probability that the fat globules can form some kind of network to help stabilising the foam. For the conditions assumed above, A_{ef} is calculated to be smaller than A_t. It is therefore not expected that the present fat globules will form a close-packed conformation at the bubble surface. However, at a low overrun or for a higher average bubble diameter A_{ef} can be somewhat larger than A_t. The possibility of a close-packed surface can thus not be ruled out. Although some globules may adsorb on more bubbles at the

same time, there will also be fat globules present in the liquid films and plateau borders without adsorbing at a surface. Of course it is possible that a structure will form in a less than close-packed configuration. An open structure is however likely to supply less firmness to a surface than a more packed structure.

Cryo-SEM

The microstructure of aerosol whipped cream, having an overrun in the order of 300-400 %, was already studied using cryo-SEM by Anderson and Brooker (1988) and Brooker et al. (1986). Their results indicated that the bubbles in the foam are deformed by each other. In the present research, this was also observed with cryo-SEM at a magnification of 300 times. Because of the high volume fraction of gas in the aerosol whipped cream ($\geq$ 0.8), the bubbles are pressed against one another, resulting in a polyhedral foam (figure 4.7).

100 µm
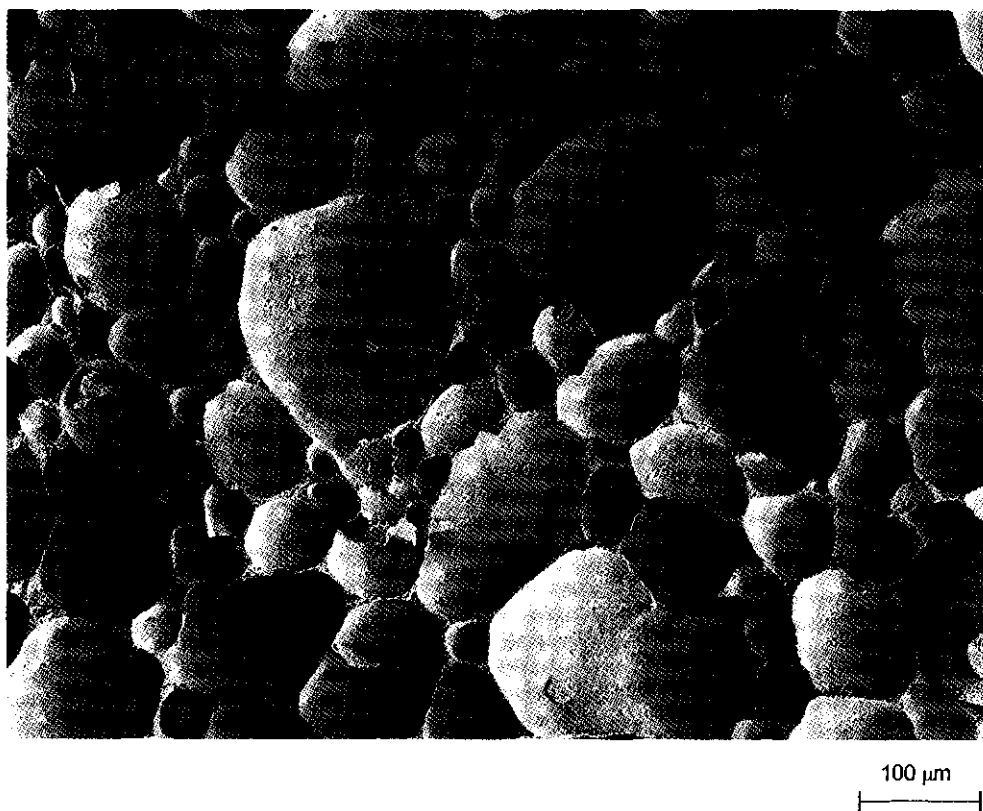
Figure 4.7   The microscopic structure of aerosol whipped cream; magnification 300 times.

This picture indicates the bubble size distribution of the foam. The gas bubbles in aerosol whipped cream are in the order of 10-100 µm.

The microstructure of aerosol whipped cream studied at a magnification of 7000 times is presented in figure 4.8. This magnification is higher than the magnification of the images presented by the authors mentioned.

10 µm
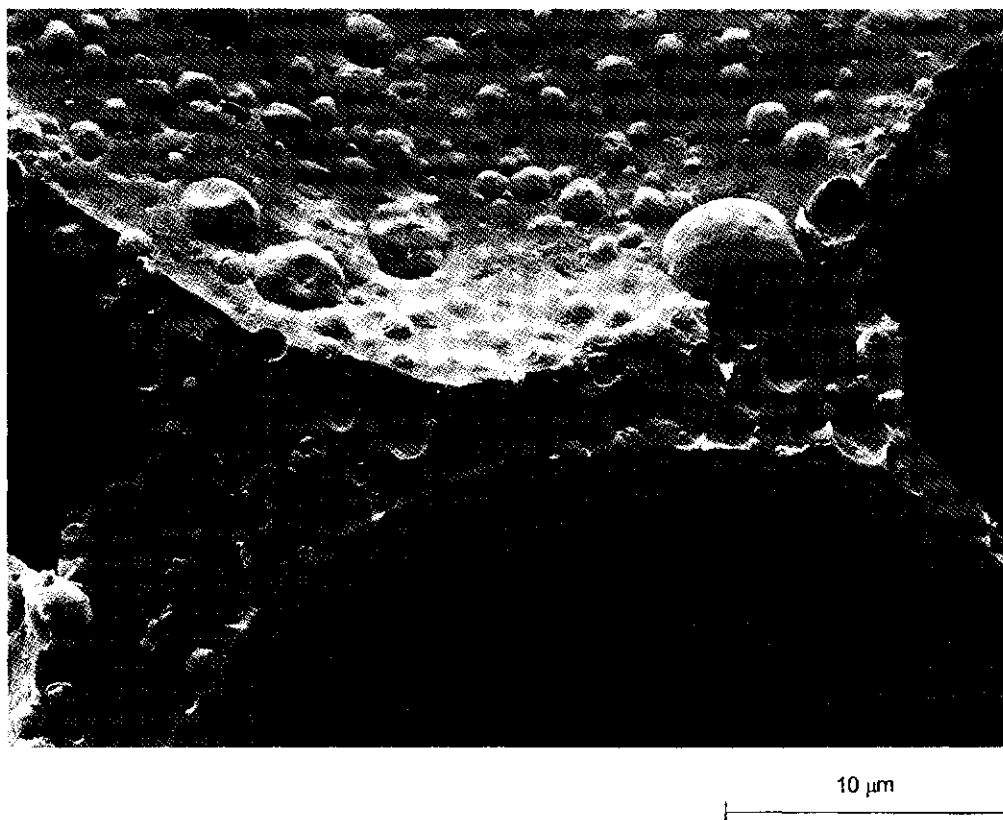
Figure 4.8   The microstructure of aerosol whipped cream; magnification 7000 times.

Figure 4.8 shows two curved gas bubble surfaces and part of the liquid film in between. It clearly follows from this image that the major amount of the spherical fat globules is adsorbed at the bubble surfaces. Additionally, some globules are positioned inside the liquid film between the bubbles. These findings agree with literature (Anderson and Brooker, 1988; Brooker et al.; 1986). The bubble surfaces are not completely covered with the globules. Moreover, no sign of the presence of some kind of network between the fat globules is visible. The globules therefore do

not seem to be capable of providing stability to the foam.

Bubble size distribution

An impression of the bubble size distribution in aerosol whipped cream can be obtained from figures 4.9.a, 4.9.b and 4.9.c.

100 µm

Figure 4.9   The bubble size distribution of aerosol whipped cream of fresh foam (a), after 1 minute (b) and after 2.5 minutes (c).

Figure 4.9.a shows a relatively fresh foam (picture taken within 30 seconds after production). The next image is taken after 1 minute and figure 4.9.c gives the situation after 2.5 minutes.

Firstly, it has to be noted that the images indicate a spherical foam instead of a polyhedral one. Considering the overrun of the foam (± 600 %) this is not very likely. Moreover, cryo-SEM pictures showed that similar aerosol whipped cream was polyhedral (figure 4.7). The preparation of the sample in the presented technique is of course far from ideal. The foam was most likely mechanically damaged due to the spreading of the foam. Furthermore, the sample is very thin so that gas diffusion to the surroundings will probably proceed fast. In addition, because the surroundings and the equipment have a higher temperature (± 20 °C) the foam slightly heats up. This will affect the destabilisation. All these factors may contribute to the transition into a spherical foam. The method can therefore only be used to get insight into the occurrence of different processes and should not be applied in a quantitative manner for aerosol whipped cream.

Studying the images in figure 4.9 shows shrinking of most of the bubbles in time. In the central top two very tiny bubbles, which are positioned against a large one, even completely disappear within 2.5 minutes. The massive shrinking of the bubbles is due to gas diffusion through the large exchanging interface of the sample to the surroundings. Occasionally, some growth of a bubble was observed as well. This is for example visible when the larger bubbles in the left top of figure 4.9.a and 4.9.b are compared. The observations support the picture that aerosol whipped cream is susceptible to disproportionation. Sporadically, coalescence between bubbles was also observed. This was unfortunately not captured in a picture.

The firmness
The firmness is one of the parameters that can be distinguished in the complex property called foam stability. Figure 4.10 shows the firmness of aerosol whipped cream as a function of time. The data of the three series measured show a similar trend. The strong decrease in the firmness illustrates that the foam destabilises fast as time proceeds. The main drop in firmness occurs within the first 5-10 minutes after foam production. Note that a change in gas:liquid ratio hardly has any effect on the firmness. As followed from figure 3.7, the firmness of aerosol whipped cream with an overrun larger than 400 % seemed to reach a plateau value and is thus not significantly affected by the overrun.
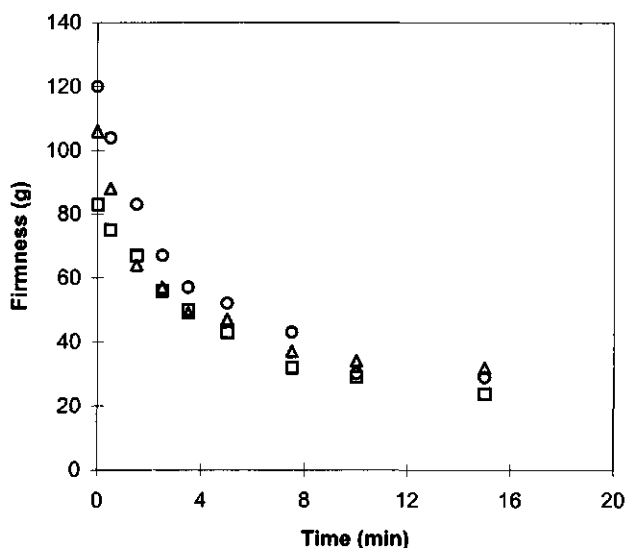
Figure 4.10   The firmness of aerosol whipped cream as a function of time; foams produced with
the ACS at a cream flow rate of 50 l/h and a gas:liquid ratio of 6 ($\square$), 8 (o) and 14
($\triangle$) (at atmospheric conditions), with an overrun of approximately 400, 450 and
500 % respectively.

In chapters 2 and 3 it was illustrated that the firmness of aerosol whipped cream is
related to its overrun. Considering this polyhedral foam, the resistance against
deformation furthermore seemed to correspond to the Laplace pressure difference
over the surface of the bubbles. The observed decrease in firmness may simply
result from a decrease in overrun, giving the bubbles more space to move around
during deformation. Additionally, the destabilising processes occurring in the foam
may very well result in an increase of the average bubble size. This will result in a
lower Laplace pressure inside the bubbles (equation (4.4)), and therefore a lower
firmness. It is difficult to distinguish whether the decrease in firmness observed in
figure 4.10 is due to a decrease in overrun or an increase in gas bubble diameter.
Probably, both processes contribute.

4.5   Conclusions

Aerosol whipped cream destabilises rather fast. The results presented in this
chapter clearly indicate that the foam is susceptible to disproportionation. This is
thought to be caused by the high solubility of laughing gas in cream. From a

surface rheological point of view the process of disproportionation can only be stopped completely when the bubble surface behaves purely elastic. Surface rheological properties of aerosol whipping cream measured in the ring trough (close to equilibrium) and with the canal technique (during continuous compression far from equilibrium) both showed visco-elastic behaviour. Disproportionation will therefore not be stopped completely. However, the surface dilational elasticity showed to exceed half the surface tension. This indicates that, according to the Lucassen condition (equation (4.7)), the process of disproportionation might be slowed down.

Disproportionation in a foam can be greatly retarded in the presence of some kind of rigid network at the bubble surfaces. It was shown with the canal technique that aerosol whipping cream is not able to form a pure elastic network at its surface during continuous compression. Although it was not possible to conclude from calculations whether or not the fat globules are able to form a close-packed structure at the bubble surface, cryo-SEM pictures showed no sign of a fat network at the surface which might help to stabilise the foam. These results indicate that disproportionation will probably occur in aerosol whipped cream. Images of the bubble size distribution in time showed that bubbles in the foam indeed disproportionate in practice.

Occasionally, some coalescence was observed in aerosol whipped cream as well. This process is related to expanding surface behaviour. The dynamic surface tension during expansion in an overflowing cylinder was measured to be higher than the equilibrium surface tension. Consequently, surface tension gradients can be created during film expansion. The surface tension showed a decreasing trend with an increasing amount of fat present in the cream. This indicates that fat globules may adsorb at the surface, which indeed was observed in cryo-SEM images. In order for coalescence to occur, a triggering factor is needed. In aerosol whipped cream, the fat globules may act as a spreading particle. Observations in the falling film apparatus indeed showed that spreading of material, provided by the fat globules, can be seen at the cream surface under certain conditions. The amount of globules is, however, so large that the distance between them in the foam films is relatively small. In addition, the surface area of a bubble is limited. Thus, it becomes questionable whether the thinning of liquid films caused by the spreading particles can proceed long enough for film rupture to occur. For this reason, it is expected that coalescence is not that important in the stability of aerosol whipped cream.

It is not easy to measure surface rheological properties of aerosol whipping cream. The Wilhelmy plate may disturb the measurement, in particular in a situation close to equilibrium. Moreover, the cream surface sometimes showed to change

significantly in time. This introduces a history dependence of the surface properties, which can trouble the experiments and therefore has to be accounted for.

Finally, the sharp decrease in firmness as a function of time reflected the fast destabilisation of aerosol whipped cream. It is believed that the decrease in firmness is a result of a decrease in overrun and an increase in average bubble size, both caused by destabilisation processes.

4.6   References

- Anderson, M. and Brooker, B.E., 1988. Dairy Foams. In: Advances in Food Emulsions and Foams. Dickinson, E. and Stainsby, G. (eds.), Elsevier Applied Science, London, 221-255.
- Bergink-Martens, D.J.M., 1993. Interface Dilation. The Overflowing Cylinder Technique. Ph.D. Thesis, Wageningen Agricultural University.
- Bergink-Martens, D.J.M., Bos, H.J., Prins, A. and Schulte, B.C., 1990. Surface Dilation and Fluid Dynamical Behaviour of Newtonian Liquids in an Overflowing Cylinder. I Pure Liquids. Journal of Colloid and Interface Science, 138 (1), 1-9.
- Bergink-Martens, D.J.M., Bos, H.J. and Prins, A., 1994. Surface Dilation and Fluid Dynamical Behaviour of Newtonian Liquids in an Overflowing Cylinder. II Surfactant Solutions. Journal of Colloid and Interface Science, 165, 221-228.
- Bikerman, J.J., 1973. Foams. Springer-Verlag, New York, Inc..
- Bisperink, C.G.J. The Influence of Spreading Particles on the Stability of Thin Liquid Films. Ph.D. Thesis, Wageningen Agricultural University, to be published.
- Bisperink, C.G.J., Ronteltap, A.D. and Prins, A., 1992. Bubble-size Distributions in Foams. Advances in Colloid and Interface Science, 38, 13-23.
- Brooker, B.E., Anderson, M. and Andrews, A.T., 1986. The Development of Structure in Whipped Cream. Food Microstructure, 5, 277-285.
- Dickinson, E., 1992. An Introduction to Food Colloids. Oxford University Press, Oxford.
- Halling, P.J., 1981. Protein Stabilised Foams and Emulsions. Crit. Rev. Food. Sci. Nutr., 15(2), 155-203.
- Heertje, I. and Pâques, M., 1995. Advances in Electron Microscopy. In: New Physico-Chemical Techniques for the Characterisation of Complex Food Systems, Dickinson, E. (ed.), Chapmann & Hall, Cambridge University Press, 1-53.
- Kokelaar, J.J., 1994. Physics of Breadmaking. Ph.D. Thesis, Wageningen Agricultural University.
- Kokelaar, J.J., Prins, A. and de Gee, M., 1991. New Method for Measuring the Surface Dilational Modulus of a Liquid. Journal of Colloid and Interface Science, 146, 507-511.

- Lucassen, J., 1981. Dynamic Properties of Free Liquid Films and Foams. In: Anionic Surfactants, Lucassen-Reynders, E.H. (ed.), Marcel Dekker Inc., New York, 217-265.
- Lucassen, J., 1992a. Capillary Forces Between Solid Particles in Fluid Interfaces. Colloids and Surfaces, 65, 131-137.
- Lucassen, J., 1992b. Dynamic Dilational Properties of Composite Surfaces. Colloids and Surfaces, 65, 139-149.
- Lucassen, J. and van den Tempel, M., 1972. Dynamic Measurements of Dilational Properties of a Liquid Interface. Chemical Engineering Science, 27, 1283-1291.
- Lucassen-Reynders, E.H., 1981. Surface Elasticity and Viscosity in Compression/Dilation. In: Anionic Surfactants, Lucassen-Reynders, E.H. (ed.), Marcel Dekker Inc., New York, 173-216.
- Lucassen-Reynders, E.H., 1993. Interfacial Viscoelasticity in Emulsions and Foams. Food Structure, 12, 1-12.
- Mulder, H. and Walstra, P., 1974. The Milk Fat Globule; Emulsion Science as Applied to Milk Products and Comparable Foods. Centre for Agricultural Publishing and Documentation, Wageningen, the Netherlands.
- Padday, S.F., 1957. A Direct Reading Electrically Operated Balance for Static and Dynamic Surface-Tension Measurement. Proceedings International Congress Surfactant Activity, London, vol. 1, 1-6.
- Princen, H.M., 1979. Highly Concentrated Emulsions. I. Cylindrical Systems. Journal of Colloid and Interface Science, 71(1), 55-66.
- Prins, A., 1986. Some Physical Aspects of Aerated Milk Products. Netherlands Milk and Dairy Journal, 40, 203-215.
- Prins, A., 1988. Principles of Foam Stability. In: Advances in Food Emulsions and Foams, Dickinson E. and Stainsby, G. (eds.), Elsevier Applied Science, England, 91-122.
- Prins, A., 1989. Foam Stability as Affected by the Presence of Small Spreading Particles. In: Surfactants in Solution, vol. 10. Mittal, K.L. (ed.), Plenum Press, New York, 361-380.
- Prins, A., 1990. Liquid Flow in Foams as Affected by Rheological Surface Properties: a Contribution to a Better Understanding of the Foaming behaviour of Liquids, 1990. In: Hydrodynamics of Dispersed Media, Hulin, J.P., Cazabat, A.M., Guyon, E. and Carmona, F. (eds.), Elsevier Science Publishers B.V, 5-15.
- Prins, A., 1995. Dynamic Surface Tension and Dilational Interfacial Properties. In: New Physico-Chemical Techniques for the Characterisation of Complex Food Systems, Dickinson, E. (ed.), Chapmann & Hall, Cambridge University Press, 214-239.
- Prins, A., Jochems, A.M.P., Kalsbeek, H.K.A.I., Boerboom, F.J.G., Wijnen, M.E. and Williams, A., 1996. Skin Formation on Liquid Surfaces under Non-Equilibrium Conditions. Progr. Colloid Polym Sci, Steinkopf Verlag, 100, 321-327.
- Ronteltap, A.D., 1989. Beer Foam Physics. Ph.D. Thesis, Wageningen Agricultural University.
- Ronteltap, A.D., 1990a. The Role of Surface Viscosity in Gas Diffusion in Aqueous Foams, part 1: Theoretical. Colloids and Surfaces, 47, 269-283.
- Ronteltap, A.D., 1990b. The Role of Surface Viscosity in Gas Diffusion in Aqueous Foams, part 2: Experimental. Colloids and Surfaces, 47, 285-298.
- Tempel, van den, M., 1977. Surface Rheology. Journal of Non-Newtonian Fluid Mechanics, 2, 205-219.

- Vries, A.J. de, 1958a. Foam Stability, Part 1: Structure and Stability of Foams, Recueil, 77, 81-91.
- Vries, A.J. de, 1958b. Foam Stability, Part 2: Gas Diffusion in Foams. Recueil, 77, 209-223.
- Walstra, P., 1989. Principles of Foam Formation and Stability. In: Foams: Physics, Chemistry and Structure, Wilson, A.J. (ed.), Springer Verlag, London, 1-15.
- Westerbeek, J.M.M., 1989. Contribution of the α-gel Phase to the Stability of Whippable Emulsions. Ph.D. Thesis, Wageningen Agricultural University.
- Whorlow, R.W., 1980. Rheological Techniques. Ellis Horwood Limited, England.
- Wijnen, M.E. and Prins, A., 1995. Disproportionation in Aerosol Whipped Cream. In: Food Macromolecules and Colloids, Dickinson, E. and Lorient, D. (eds.), Royal Society of Chemistry, 309-311.

Chapter 5

Concluding remarks

5.1 Introduction

The aim of this study was to obtain more knowledge of the physical phenomena that are important in the formation and stability of instant foams. The results of the research, which mainly focused on aerosol whipped cream, helped to enlarge the insight into the physics of instant foam behaviour. The development of the Aerosol Can Simulator (ACS) significantly contributed to improve this insight. Using the findings obtained with aerosol cans made it possible to understand and optimise the working of the instant foam apparatus (chapter 3). In this last chapter the general conclusions of the thesis and some final considerations on the research are given.

5.2 General conclusions

In order to outline the most important findings of this study, the instant foam behaviour of aerosol whipped cream is divided into four different stages: the situation in the aerosol can or the ACS before the nozzle, the behaviour of the two-phase flow in the nozzle, the initial foam properties and the foam behaviour at longer time scales. The behaviour in each of these four stages is determined by different parameters. Table 5.1 gives an overview of the important parameters per stage. The parameter that is thought to be most important is represented bold.

The situation in the aerosol can/ACS
Considering the situation in the aerosol can or ACS before the nozzle, the most relevant parameter for instant foam behaviour, as studied in this thesis, is the amount of gas that is dissolved in the cream (chapter 2 and 3). It is essential to ensure optimal dissolution of the gas in the cream before it enters the nozzle, because the amount of dissolved gas determines the initial overrun of the produced foam. A large amount of dissolved gas results in a high initial overrun of aerosol whipped cream. Dissolution of the gas is stimulated by good solubility properties of the gas, a high pressure, phase equilibrium in the aerosol can and a large exchanging interface between gas and cream in the ACS. Before the cream enters the nozzle it is, however, desired that the amount of not dissolved bubbles is

minimal because the presence of these bubbles may disturb the foam behaviour in the following stages of the process.

Table 5.1   Overview of important parameters that determine the instant foam behaviour in the aerosol can/ACS before the nozzle, the foam behaviour in the nozzle, the initial foam properties and the foam behaviour at longer time scales. The main parameter per stage is represented bold.

Stages in instant foam behaviour	Important parameters
In the aerosol can/ACS	**amount of dissolved gas in the cream**
	gas solubility
	pressure
	state of the phase equilibrium (aerosol can)
	exchanging interface between gas and cream (ACS)
In the nozzle	**choking conditions**
	the presence of not dissolved bubbles
	nozzle geometry
Initial foam properties	**amount of dissolved gas in the cream**
	pressure
	the presence of not dissolved bubbles
	nozzle geometry
	surface rheological properties
Foam stability	**gas solubility**
	surface rheological properties
	bubble size distribution

The situation in the nozzle

A major conclusion in this thesis is that the flow properties of aerated cream through the nozzle are regulated by choking conditions, indicating that the velocity in the smallest opening of the nozzle, the holes, is limited to the speed of sound (chapter 2). These choking conditions determine apart from the velocity also the density, pressure and temperature of the aerated cream in the nozzle. The whole process of instant foam formation is thus controlled by the physics of choking.

Experiments showed that the formation of bubbles occurs in the holes of the nozzle. They are probably formed at sites, such as small cracks, in the walls of the holes. Considering the volume fraction of gas present in the cream while flowing through these holes, the gas bubbles present at this stage will be spherically shaped (chapter 2).

Additionally, it was found that the presence of bubbles that are in the cream before it enters the nozzle, disturbs the flow process through the nozzle and induces sputtering of the product. This disturbing effect is determined by the amount and

size of the bubbles. Furthermore, the nozzle geometry affects the flow properties. In particular extension of the nozzle tube may result in a situation where choking does no longer occur (chapter 2 and 3).

The initial foam properties

The high initial overrun of the instant foams produced in this research results from the amount of gas dissolved in the cream. This high overrun of aerosol whipped cream is important because it provides the firmness to the foam. The volume fraction of gas in the foam is so high that the gas bubbles are closely packed and deform each other. Consequently, the bubbles are no longer spherical but polyhedrical of shape.

There is an optimum in the relation between the initial overrun of the foam and the pressure (thus the amount of dissolved gas) before the nozzle. If the pressure is too high, it results in breakdown of the foam during flow through the nozzle. This is expressed in a lower initial overrun of the foam. Furthermore, the presence of not dissolved bubbles negatively affects the initial overrun (chapter 2 and 3).

The nozzle geometry can also affect the initial foam properties. Extension of the nozzle tube is accompanied by an increase in the shear forces acting upon the bubbles while flowing through the nozzle. It is believed that because of these shear forces the bubbles in the foam coalesce, resulting in an increase of 'blow by' and consequently a decrease of the initial overrun of the foam.

Obviously, the initial foam properties of aerosol whipped cream will be related to the surface rheological properties of the cream. This relation was, however, not studied in the present research.

The foam stability

The high solubility of laughing gas in cream leads to a large amount of gas dissolved in the cream at the higher pressures before the nozzle. This obviously plays an important role in the process of instant foam formation. Unfortunately, the high solubility of the gas makes the aerosol whipped cream susceptible to disproportionation. The surface rheological properties of cream showed not to be suitable to stop this process. Since it is expected that coalescence will not play an important role in aerosol whipped cream, the fast destabilisation of the foam is very likely the result of disproportionation (chapter 4). This foam destabilisation is expressed in a fast decrease of the firmness as a function of time.

Disproportionation would not occur in a monodisperse foam. The broad bubble size distribution (in the order of 10-100 μm) of aerosol whipped cream apparently triggers the destabilisation. It is not unlikely that, especially as a result of gas diffusion out of the foam, the gas bubbles will regain a spherical shape again.

5.3   Final considerations

Before this research started there was a lack of fundamental knowledge about the physics of instant foam behaviour. Now it can be concluded that some insight into the physical mechanisms relating to the formation and stability of instant foams has been gained. There is a better understanding of the parameters that regulate these mechanisms. With the obtained knowledge, it is possible to produce an instant foam with required initial properties.

A problem is the poor stability of the aerosol whipped cream after it has been made. Looking ahead, an obvious question is what the possibilities are to improve the foam stability. Although in this thesis not much attention has been paid to that problem, some recommendations on this topic can be made. The stability of aerosol whipped cream can be improved by slowing down the process of disproportionation. It is not easy to accomplish this because several compromises are involved:

*   Using a less soluble gas for the foam production will decrease the rate of disproportionation. However, the amount of gas dissolved in the cream before the nozzle and thereby the initial overrun of the foam will be lower. Consequently, the initial firmness may be less. The bulk properties of the cream, for example in the presence of a network in the foam lamellae, can compensate this loss of firmness.

*   The stability against disproportionation of aerosol whipped cream is also improved by purely elastic surface behaviour (chapter 4). This can result from the presence of some kind of network in the bubble surfaces. Formation of a network has to be induced by forces acting upon the cream while flowing through the nozzle. Additional research on the possibility of creating a pure elastic surface within such a short time scale is recommended. However, if a network is able to form within a very short time, it is likely that the cream will already destabilise to some extent in the can during storage and thus has a poor physical stability (chapter 1).

*   Producing a foam with small bubbles of similar size would slow down the disproportionation process. It is however very complicated, if not impossible, to regulate the size of the formed bubbles and thereby the bubble size distribution. The gas bubbles are formed at various times and at sites with different size and shape in the walls of the nozzle. Consequently, they will differ in their final size and gas diffusion between bubbles will result.

It has to be concluded that, although the physics of instant foam behaviour seems to be well understood after the presented study, additional research is required to improve the stability of aerosol whipped cream.

List of symbols

Roman symbols

a	activity of the surfactant in solution	mol m^{-3}
$a_{j,k}$	constant characteristic of the jk binary pair	-
A	area	m^2
b	width of the canal	m
$b_{j,k}$	empirical coefficient of the jk binary pair	mol m^{-3}
c	speed of sound	m s^{-1}
C	concentration	mol m^{-3}
C_P	specific heat capacity at constant pressure	J kg^{-1} K^{-1}
C_V	specific heat capacity at constant volume	J kg^{-1} K^{-1}
D	diameter of the tube	m
D_p	mean diameter of the glass beads	m
$\mathbb{D}$	diffusion coefficient	m^2 s^{-1}
e_v	friction loss factor	-
$e_{v,area}$	friction loss factor for the change in flow area	-
$e_{v,rem}$	remaining friction loss factor	-
E	surface dilational modulus	N m^{-1}
E_d	surface dilational elasticity	N m^{-1}
f	friction factor	-
f_i	fugacity of component i	N m^{-2}
g	acceleration due to gravity	m s^{-2}
G_s	mass of gas dissolved in the cream	kg
h	height	m
$H_{i,j}$	Henry's constant for gas i in the pure solvent j	N m^{-2}
$H_{i,k}$	Henry's constant for gas i in the pure solvent	N m^{-2}
$H_{i,m}$	Henry's constant for gas i in the mixture of the solvents	N m^{-2}
k	ratio of mass flow gas to mass flow cream	-
K	bulk modulus	N m^{-2}
l	length	m
L	length of the tube	m
m	mass of flow	kg
m	power law constant	-
$\dot{m}$	mass flow rate	kg s^{-1}
M	number of moles gas (gas transport)	mol
M_g	molar weight of gas	kg mol^{-1}
n	number of moles	mol
n	power law constant	-

O	overrun of foam	%
O_f	feasible overrun	%
p	rheological constant	N m^{-2} s^n
p_i	partial pressure of component i in the gas phase	N m^{-2}
P	pressure	N m^{-2}
P_i^s	vapor pressure of pure liquid i at the temperature of the solution	N m^{-2}
ΔP_{area}	pressure drop induced by the change in flow area	N m^{-2}
ΔP_{ev}	pressure drop induced by the presence of a fitting	N m^{-2}
ΔP_L	Laplace pressure difference over the bubble surface	N m^{-2}
ΔP_m	pressure drop over the static mixer	N m^{-2}
q	plasticity factor	-
Q	volumetric flow rate	m^3 s^{-1}
r	radius of curvature of the Plateau border	m
R	gas constant	J mol^{-1} K^{-1}
R_b	bubble radius	m
R_c	radius of cylinder	m
R_d	radius of fat droplet	m
R_h	hydrodynamic radius	m
Re	Reynolds number	-
s	entropy	J K^{-1}
S	gas solubility	kg kg^{-1} Pa^{-1}
S'	apparent gas solubility	kg kg^{-1} Pa^{-1}
S_c	gas solubility corrected for the presence of other gases	kg kg^{-1} Pa^{-1}
S_t	total geometric surface area of the solid particles	m^2
t	time	s
T	temperature	K
v_i	molar volume of pure "liquid" i (fictitious)	m^3 mol^{-1}
v_j^∞	partial molar volume of i in the liquid phase at infinite dilution	-
v	velocity	m s^{-1}
v_0	superficial velocity in static mixer	m s^{-1}
v_e	velocity downstream of fitting	m s^{-1}
V	volume	m^3
w	mass of medium present in the can	kg
W_i	mass of fixed volume of unaerated cream	kg
W_f	mass of fixed volume of aerated cream	kg
x	mass fraction fat in the cream	-
x_i	solubility (mole fraction) of the gas in the liquid	-
x_j	mole fraction of solvent j in the mixture	-
x_k	mole fraction of solvent k in the mixture	-
Δx	thickness of the diffusion layer	m

Greek symbols

α	volume fraction of gas in the foam	-
δ	thickness of the film	m
ε	void fraction in static mixer	-
γ	ratio of specific heats at constant pressure and constant volume C_P / C_V (gas expansion)	-
γ	surface tension	N m^{-1}
γ_m	surface tension of spreading material	N m^{-1}
γ_{ml}	interfacial tension between spreading material and liquid	N m^{-1}
$\dot{\gamma}$	shear rate	s^{-1}
Γ	two-phase isentropic exponent	-
Γ	surfactant adsorption	mol m^{-2}
η	viscosity	N s m^{-2}
η^*	apparent viscosity	N s m^{-2}
η_d	surface dilational viscosity (dynamic measurements)	N s m^{-1}
η_s^d	surface dilational viscosity (continuous expansion/compression)	N s m^{-1}
κ	isothermal compressibility	m^2 N^{-1}
ρ	density	kg m^{-3}
ρ_s	mass of gas dissolved in the cream	kg m^{-3}
σ	stress	N m^{-2}
τ	shear stress	N m^{-2}
ϕ	flux over bubble surface	mol m^{-2} s^{-1}
ϕ_j	the volume fraction of solvent j	-
ϕ_k	the volume fraction of solvent kj	-
ω	radial frequency	rad s^{-1}

Subscripts

a	air		0	position in the can
c	aerosol can		1	position in the holes of the nozzle
d	dynamic		2	position at the entrance of the
e	equilibrium			nozzle tube
ef	effectively covered		3	postion at the end of the nozzle tube
f	foam			
g	gas (nitrous oxide)			
h	headspace in aerosol can			
l	cream		atm	atmospheric conditions
o	fat		,t	time
s	dissolved in the cream			
t	total			
w	skim milk			

Solubility properties of nitrous oxide

Solubility of nitrous oxide in water

Table I.1   Solubility properties of N_2O in water; data taken from literature.

T (°C)	H_{lit}[1] atm mol⁻¹mol	S_{lit}[1] at 1 atm g l⁻¹	S_{lit}[2] at 1 atm l l⁻¹	S_{lit}[3] at 1 atm l l⁻¹	S_{lit}[4] at 1 bar l l⁻¹
0				1.297	1.3
5	1170		1.14		1.17
10	1410	1.705	0.948		1.05˙
15	1660		0.789		0.92˙
20	1980		0.665		0.79
25	2250	1.211	0.561	0.588	0.66˙
30	2590		0.472		0.54˙
35	3020				0.41˙
40			0.358		0.28˙

H_{lit} and S_{lit} are respectively the Henry constant and the gas solubility taken from literature. Note that the dimensions differ per column.

˙ calculated through interpolation with formula given in the literature [4]

[1] Perry, 1963

[2] Marshall, 1976

[3] Braker and Mossman, 1980

[4] Ahlberg, 1985

Solubility of nitrous oxide in oil

Table I.2   Solubility properties of N_2O in different oils at 20 °C and 1 atm.

Solvent	Bunsencoefficient m³ m⁻³
Corn oil	1.96
Olive oil	1.40
Soybean oil	1.90

Data taken from Marshall, 1976.

References

- Ahlberg, K., 1985. AGA Gas Handbook.
- Braker, W. and Mossman, A.L., 1980. Matheson Gas Data Book, Matheson, USA.
- Marshall, N., 1976. Encyclopedie des Gaz. Division Scientifique, Elsevier, Amsterdam.
- Perry, J.H., 1963. Chemical Engineers Handbook. Mc Graw-Hill, Inc., New York.

Physical properties of cream

Density of milk plasma and milk fat as a function of the temperature

Table II.1   Density of milk plasma and fat as a function of temperature.

T (°C)	ρ Milk Plasma (kg m^{-3})	ρ Milk Fat (kg m^{-3})	T (°C)	ρ Milk Plasma (kg m^{-3})	ρ Milk Fat (kg m^{-3})
5	1035.9	959	40	1026.1	902
10	1035.2	951	50	1019.8	898
15	1034.4	938	60	1016.6	889
20	1033.3	916	70	1011.2	882
25	1031.9	912	80	1005.0	876
30	1030.0	909			

Data taken from Walstra and Jennes, 1984

Viscosity of cream

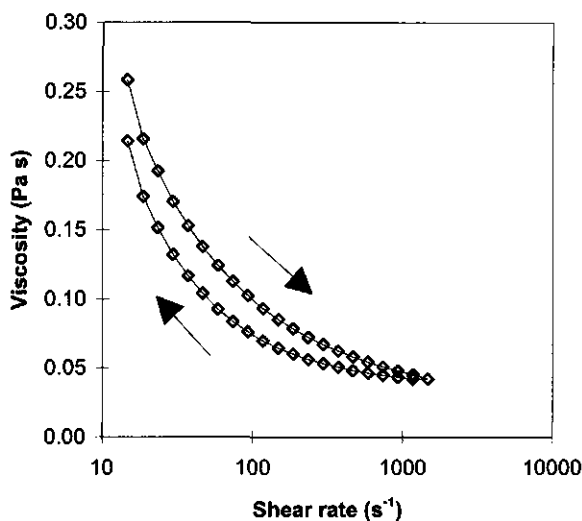**Figure II.1**   The viscosity of aerosol whipping cream; fat content 35 % w/w, T = 5 °C
Measured with the VOR Reometer using concentric cylinders.

Reference
-       Walstra, P. and Jennes, R., 1984. Dairy Chemistry and Physics. John Wiley & Sons, Inc., USA.

The speed of sound in aerosol whipped cream

The speed of sound in the gas phase c_g can be calculated using:

$$c_g = \left(\frac{\gamma RT}{M}\right)^{1/2}$$

The gas constant R = 8.314 J/mol/K, the molar weight of nitrous oxide M_g = 44.013*10^{-3} kg/mol and γ = 1.303 for triatomic gases. At T = 278.15 K :

$$c_g = 262 \text{ m/s}$$

It is more difficult to estimate the speed of sound in cream. Using ultrasound Kloek (to be published) measured the speed of sound in an 20 % w/w emulsion of fully hydrogenated palm oil in a 2 % w/w sodium caseinate solution as a function of the temperature. At a temperature of 278.15 K the extrapolated value for c is 1500 m/s at a fat crystallisation of 100 %. Considering cream with a higher fat content (35 % w/w) would result in a higher value for c at this temperature. The lower percentage of solid fat in the cream (approximately 50 %, Mulder and Walstra, 1974) will result in a lower value for the speed of sound. Assuming these effects counterbalance each other results in an estimated speed of sound in the cream c_l of:

$$c_l = 1500 \text{ m/s}$$

Specific heat capacities

Cream:	C_P = 3.333.10^3 J/kg/K [*]
N_2O:	C_P = 0.878.10^3 J/kg/K [**]
N_2O:	C_V = 0.674.10^3 J/kg/K [**]

[*] at 20 °C and 1 atm; C_P will be much higher at lower T; extrapolated from Walstra and Jennes, 1984.

[**] at 25 °C and 1 atm; Braker and Mossman, 1980.

References

- Braker, W. and Mossman, A.L., 1980. Matheson Gas Data Book, Matheson, USA.
- Kloek, W. Crystallisation of Fats in Relation to their Mechanical Properties. Ph.D Thesis, Wageningen Agricultural University, The Netherlands, to be published.
- Mulder, H. and Walstra, P., 1974. The Milk Fat Globule; Emulsion Science as Applied to Milk Products and Comparable Foods. Centre for Agricultural Publishing and Documentation, Wageningen, the Netherlands.
- Walstra, P. and Jennes, R., 1984. Dairy Chemistry and Physics. John Wiley & Sons, Inc., USA.

Derivation of velocity using the momentum equation

The velocity in the holes v_1 can be calculated using the momentum equation. The assumption of frictionless behaviour appears to be acceptable:

$$vdv = -\frac{dP}{\rho_f} \rightarrow v_1 = \sqrt{-2\int_0^1 \frac{dP}{\rho_f}} = \sqrt{-2\int_0^1 \frac{dP}{\alpha\rho_g+(1-\alpha)(\rho_s+\rho_l)}} \tag{IV.1}$$

where ρ_f is the density of the foam.
Assuming adiabatic expansion of the gas ($P.\rho_g^{-\Gamma}$ = constant = c) gives:

$$P = c\rho_g^{\Gamma} \tag{IV.2}$$

The amount of gas dissolved in the liquid ρ_s equals $P.S$, or:

$$P = \frac{\rho_s}{\rho_l S_c} \tag{IV.3}$$

Combining equations IV.2 and IV.3 results in:

$$\rho_s = c\rho_l S_c \rho_g^{\Gamma} \tag{IV.4}$$

From equation IV.2 it follows that:

$$dP = c\Gamma\rho_g^{\Gamma-1}d\rho_g \tag{IV.5}$$

Substituting equations IV.4 and IV.5 in IV.1 gives:

$$\int_0^1 \frac{1}{\rho_f}dP = \int_0^1 \frac{c\Gamma\rho_g^{\Gamma-1}d\rho_g}{\alpha\rho_g+(1-\alpha)(c\rho_l S_c\rho_g^{\Gamma}+\rho_l)} \tag{IV.6}$$

Since the mass flow of the gas and liquid (kg/s) does not change during flow through the nozzle, the ratio of the mass flow of the components is constant. Both components move with the same velocity v through the same area A. Therefore the ratio of the mass flows equals the ratio of the densities of the components:

$$\frac{\alpha\rho_g+(1-\alpha)\rho_s}{(1-\alpha)\rho_l} = \frac{\alpha\rho_g+(1-\alpha)c\rho_l S_c\rho_g^{\Gamma}}{(1-\alpha)\rho_l} = \text{constant} = k \tag{IV.7}$$

or

$$\alpha = \frac{-c\rho_l S_c\rho_g^{\Gamma}+k\rho_l}{\rho_g-c\rho_l S_c\rho_g^{\Gamma}+k\rho_l} \quad , \quad 1-\alpha = \frac{\rho_g}{\rho_g-c\rho_l S_c\rho_g^{\Gamma}+k\rho_l} \tag{IV.7'}$$

Substituting equations IV.7' in equation IV.6 gives:

$$\int_0^1 \frac{dP}{\rho_f} = \int_0^1 \frac{c\Gamma\rho_g^{\Gamma-1}d\rho_g}{\left(\dfrac{(-c\rho_l S_c\rho_g^{\Gamma}+k\rho_l)\rho_g}{\rho_g-c\rho_l S_c\rho_g^{\Gamma}+k\rho_l} + \dfrac{\rho_g(c\rho_l S_c\rho_g^{\Gamma}+\rho_l)}{\rho_g-c\rho_l S_c\rho_g^{\Gamma}+k\rho_l}\right)} \approx c\Gamma\int_0^1 \frac{(\rho_g-c\rho_l S_c\rho_g^{\Gamma}+k\rho_l)\rho_g^{\Gamma-1}d\rho_g}{(k\rho_l\rho_g+\rho_l\rho_g)}$$

or

$$\int_0^1 \frac{dP}{\rho_f} = \frac{c\Gamma}{(k+1)\rho_l}\int_0^1 \rho_g^{\Gamma-1}d\rho_g + \frac{c\Gamma k}{(k+1)}\int_0^1 \rho_g^{\Gamma-2}d\rho_g - \frac{c^2 S_c\Gamma}{(k+1)}\int_0^1 \rho_g^{2\Gamma-2}d\rho_g \qquad (IV.8)$$

Integration gives:

$$\int_0^1 \frac{dP}{\rho_f} = \frac{c}{(k+1)\rho_l}\left[\rho_g^{\Gamma}\right]_0^1 + \frac{c\Gamma k}{(\Gamma-1)(k+1)}\left[\rho_g^{\Gamma-1}\right]_0^1 - \frac{c^2 S_c\Gamma}{(2\Gamma-1)(k+1)}\left[\rho_g^{2\Gamma-1}\right]_0^1 \qquad (IV.9)$$

Since c in equation IV.9 equals $P\cdot\rho_g^{-\Gamma}$ this results in

$$\int_0^1 \frac{dP}{\rho_f} = \frac{1}{(k+1)\rho_l}\left[P\right]_0^1 + \frac{\Gamma}{\Gamma-1}\frac{k}{(k+1)}\left[\frac{P}{\rho_g}\right]_0^1 - \frac{\Gamma}{2\Gamma-1}\frac{S_c}{(k+1)}\left[\frac{P^2}{\rho_g}\right]_0^1 \qquad (IV.10)$$

Substituting equation IV.10 in equation IV.1 gives:

$$v_1 = \sqrt{2\left[\frac{P_0-P_1}{(k+1)\rho_l} + \frac{\Gamma}{\Gamma-1}\frac{k}{(k+1)}\left(\frac{P_0}{\rho_{g,0}}-\frac{P_1}{\rho_{g,1}}\right) - \frac{\Gamma}{2\Gamma-1}\frac{S_c}{(k+1)}\left(\frac{P_0^2}{\rho_{g,0}}-\frac{P_1^2}{\rho_{g,1}}\right)\right]} \qquad (IV.11)$$

Since

$$P_0\rho_{g,0}^{-\Gamma} = P_1\rho_{g,1}^{-\Gamma} \quad -\rho_{g,1} = \left(\frac{P_1}{P_0}\right)^{\frac{1}{\Gamma}}\rho_{g,0}$$

$\rho_{g,1}$ can be eliminated from equation IV.11 resulting in:

$$v_1 = \sqrt{2\left[\frac{P_0-P_1}{(k+1)\rho_l} + \frac{\Gamma k}{(\Gamma-1)(k+1)}\left(\frac{P_0}{\rho_{g,0}}-\frac{P_1}{\rho_{g,0}}\left(\frac{P_0}{P_1}\right)^{\frac{1}{\Gamma}}\right) - \frac{\Gamma S_c}{(2\Gamma-1)(k+1)}\left(\frac{P_0^2}{\rho_{g,0}}-\frac{P_1^2}{\rho_{g,0}}\left(\frac{P_0}{P_1}\right)^{\frac{1}{\Gamma}}\right)\right]} \qquad (IV.12)$$

or,

$$v_1 = \sqrt{2\left[\frac{P_0-P_1}{\rho_l(k+1)} + \frac{\Gamma k}{(\Gamma-1)(k+1)}\frac{P_0}{\rho_{g,0}}\left(1-\left(\frac{P_1}{P_0}\right)^{\frac{\Gamma-1}{\Gamma}}\right) - \frac{\Gamma S_c}{(2\Gamma-1)(k+1)}\frac{P_0^2}{\rho_{g,0}}\left(1-\left(\frac{P_1}{P_0}\right)^{\frac{2\Gamma-1}{\Gamma}}\right)\right]} \qquad (IV.12')$$

where P_0 is the pressure and $\rho_{g,0}$ the gas density inside the can.

Derivation of the relations between dL, dα, dP and dv

Assuming isothermal expansion the relation between the pressure and the gas density is given by:

$$\frac{P}{\rho_g} = \text{constant} = c \qquad (V.1)$$

Differentiation of equation V.1 gives:

$$d\rho_g = \frac{dP}{c} = \frac{\rho_g}{P}dP \qquad (V.1')$$

From equation IV.7 it follows:

$$\frac{\alpha\rho_g + (1-\alpha)\rho_s}{(1-\alpha)} = k\rho_l \qquad (V.2)$$

Differentiation of equation V.2 gives:

$$\frac{\rho_g}{(1-\alpha)^2}d\alpha + \frac{\alpha}{(1-\alpha)}d\rho_g + d\rho_s = 0 \qquad (V.2')$$

Since $\rho_s = \rho_l.P.S$, $d\rho_s = \rho_l.S.dP$. Combining equations V.1' and V.2' results in the relation between dα and dP:

$$d\alpha = -\left(\frac{\alpha(1-\alpha)}{P} + \frac{(1-\alpha)^2\rho_l S_c}{\rho_g}\right)dP = -\left(\alpha(1-\alpha) + (1-\alpha)^2\frac{\rho_s}{\rho_g}\right)\frac{dP}{P} \qquad (V.3)$$

The equation of continuity for flow through a tube is ($\rho_f Av$ = constant, A = constant):

$$\rho_f Adv + Avd\rho_f = 0 \qquad (V.4)$$

The density of the foam ρ_f is:

$$\rho_f = \alpha\rho_g + (1-\alpha)(\rho_s + \rho_l) \qquad (V.5)$$

Differentiation of equation V.5 gives:

$$d\rho_f = \alpha d\rho_g + \rho_g d\alpha + (1-\alpha)d\rho_s - (\rho_s + \rho_l)d\alpha \qquad (V.5')$$

Substituting equations V.1'and V.3 in equation V.5' gives:

$$d\rho_f = \left[\frac{\alpha\rho_g}{P} + (1-\alpha)\rho_l S_c - (\rho_g - \rho_s - \rho_l)\left(\frac{\alpha(1-\alpha)}{P} + \frac{(1-\alpha)^2\rho_l S_c}{\rho_g}\right)\right]dP = \left(\frac{\alpha}{P} + \frac{(1-\alpha)\rho_l S_c}{\rho_g}\right)\rho_f dP$$

(V.5")

Combining equation V.4 with equation V.5" results in a relation between dv, dA and $d\alpha$:

$$\rho_f A dv - Av\left(\frac{\alpha}{P} + \frac{(1-\alpha)\rho_l S_c}{\rho_g}\right)\rho_f \ dP = 0$$

or,

$$dv = -\left(\frac{\alpha}{P} + \frac{(1-\alpha)\rho_l S_c}{\rho_g}\right)v \ dP = -\left(\frac{\alpha\rho_g + (1-\alpha)\rho_s}{\rho_g P}\right)v \ dP$$

(V.6)

Considering the flow through the tube, the friction in the tube cannot be neglected. The equation of momentum is:

$$\rho_f A v dv + A dP + f\rho_f \frac{v^2}{2}\pi D dL = 0$$

(V.7)

Substituting equation V.6 in equation V.7 results in an equation for dP:

$$-\rho_f A v^2\left(\frac{\alpha}{P} + \frac{(1-\alpha)\rho_l S_c}{\rho_g}\right)dP + A dP + f\rho_f\frac{v^2}{2}\pi D dL = 0$$

or,

$$dP = \frac{\rho_g P\left(f\rho_f\dfrac{v^2}{2}\pi D dL\right)}{\rho_f A v^2(\alpha\rho_g + (1-\alpha)P\rho_l S_c) + \rho_g P} = \frac{2}{D}\frac{f\rho_g\rho_f P v^2 dL}{\rho_f v^2(\alpha\rho_g + (1-\alpha)\rho_s) - \rho_g P}$$

(V.8)

The dissolution of a spherical gas bubble

Bisperink and Prins (1994) developed a model based on Fick's first law to calculate bubble growth at a model cavity. This model has been adapted for the dissolution of a spherical bubble in the surrounding liquid. The driving force for the dissolution of the gas bubble is the concentration difference ΔC_i between the bubble surface and the liquid bulk at time $t = i$:

$$\Delta C_i = \frac{P_{b,i}}{H} \rho - C_{g,i} \tag{VI.1}$$

where $P_{b,i}$ is the pressure in the bubble at time $t = i$, H Henry's law constant, ρ the density of the liquid and $C_{g,i}$ the concentration of gas in the liquid bulk at time $t = i$, being lower than concentration at the bubble surface.

The model calculates the time interval needed for a very small decrease of the bubble radius. The shrinking bubble is schematically represented in figure VI.1.
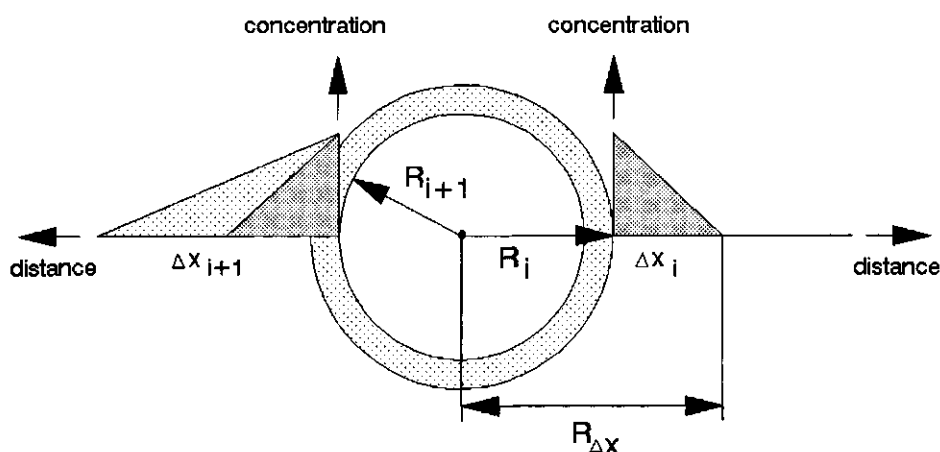

Figure VI.1   Schematic drawing of a shrinking bubble with the various parameters used in the presented theory for the calculation of the bubble shrinking rate.

When a bubble with radius R_i shrinks to radius R_{i+1}, the number of moles gas $\Delta M_{i \to i+1}$ that leaves the bubble in time interval $i + 1$ equals:

$$\Delta M_{i-i+1} = \frac{\Delta V_{b,i-i+1}}{MV} \tag{VI.2}$$

with $\Delta V_{b,i \to i+1}$ ($= 4/3\pi R_{i+1}^3 - 4/3\pi R_i^3$) being the volume change in time interval $i + 1$ and MV the molar volume of the gas in the gaseous phase at bubble pressure $P_{b,i}$ ($MV = RT/P_{b,i}$, where R is the gas constant and T the temperature).

This amount of gas diffuses into the boundary layer that is wrapped around the bubble (figure VI.1). Consequently, the number of moles that leaves the bubble equals the number that enters the boundary layer in the same time interval. Assuming that the concentration gradient in this layer remains linear during the shrinkage of the bubble (figure VI.1), the number of moles gas $\Delta M_{i \to i+1}$ that enters the boundary layer in time interval $i + 1$ equals:

$$\Delta M_{i-i+1} = \frac{1}{2}\Delta C_i V_{1,i+1} - \frac{1}{2}\Delta C_i V_{1,i} = \frac{1}{2}\Delta C_i V_{1,i-i+1} \qquad (VI.3)$$

where $V_{1,i}$ and $V_{1,i+1}$ are the volume of the boundary layer respectively at time i and $i + 1$ and $V_{1,i \to i+1}$ is the change in volume of the layer in time interval $i + 1$. Combining equations (VI.2) and (VI.3) gives for $V_{1,i+1}$:

$$V_{1,i+1} = V_{1,i} + V_{1,i-i+1} = V_{1,i} + \frac{2P_{b,i}\,\Delta V_{b,i-i+1}}{RT\Delta C_i} \qquad (VI.4)$$

The volume of the boundary layer, and thereby its thickness, increases in time because of the penetration of the concentration gradient into the liquid. The thickness of the diffusion layer Δx_i results from the difference in the radius of the bubble plus the diffusion layer $R_{\Delta x,i}$ and the bubble radius R_i (figure VI.1):

$$\Delta x_i = R_{\Delta x,i} - R_i = \left(\frac{3V_{1,i+1}}{4\pi} + R_i^3\right) - R_i \qquad (VI.5)$$

The surface compression of the bubble during the shrinking process results in contraction of the boundary layer and therefore effects a further increase of the layer thickness.
According to Fick's law the flux $\phi_{i \to i+1}$ over a bubble surface in time interval $i+1$ can now be calculated using the concentration difference ΔC_i and the thickness of the diffusion layer Δx_i:

$$\phi_{i-i+1} = D\left(\frac{\Delta C_i}{\Delta x_i}\right)MV \qquad (VI.6)$$

where D is the diffusion coefficient of the gas in the liquid.
The time $\Delta t_{i \to i+1}$ needed for the bubble to shrink from radius R_i to R_{i+1} finally follows from the change in bubble volume $\Delta V_{b,i \to i+1}$, the flux $\phi_{i \to i+1}$ and the area of the bubble:

$$\Delta t_{i-i+1} = -\frac{\Delta V_{b,i-i+1}}{4\pi R_i^2 \phi_{i-i+1}} \qquad (VI.7)$$

Reference
-        Bisperink, C.G.J. and Prins, A., 1994. Bubble Growth in Carbonated Liquids. Colloids and Surfaces A: Physicochemical and Engineering Aspects, 85, 237-253.

Determination of *E* in the canal method

The stress σ exerted by a flowing liquid on a motionless liquid surface is given by (Bird et al, 1960):

$$\sigma = f \frac{1}{2} \rho v^2 \qquad (VII.1)$$

where ρ is the liquid density and *v* the average flow velocity. The friction factor *f* for a rectangular canal with a height to width ratio of 0.5 is (Sissom and Pitts, 1974):

$$4f = \frac{62.19}{Re} \qquad (VII.2)$$

The average flow velocity *v* follows from the volumetric liquid flow rate *Q* and the cross-section of the liquid stream. The Reynolds number *Re* equals $4\rho v R_h/\eta$. Here, η is the liquid viscosity and R_h the hydraulic radius, being the cross section of the stream divided by the wetted perimeter of the liquid. For the canal having a width *b* and a height of the wetted part *h* the hydraulic radius equals $(b \cdot h)/(2b + 2h)$. Consequently, for a rectangular cross section with h/b = 0.5:

$$\sigma = 3.89 \eta Q \frac{b+h}{(bh)^2} \qquad (VII.3)$$

Considering a motionless surface, the shear stress exerted on the surface by the streaming liquid, which is a function of *Q*, is compensated by a surface tension gradient:

$$\sigma = \frac{d\gamma}{dl} \qquad (VII.4)$$

where *l* is the length coordinate in the upstream direction. Integration of equation (VII.4) gives, for *Q* = constant:

$$\gamma = l\sigma + \gamma_0 \qquad (VII.5)$$

with γ_0 being the surface tension at *l* = 0. Changing the liquid flow rate results in a change in applied shear stress dσ. According to equation (VII.5) this is related to a change in surface tension dγ and the resulting movement d*l* of the surface which can be studied by the position of a particle:

$$d\gamma = l\frac{d\sigma}{dQ}dQ + \sigma dl \qquad (VII.6)$$

where *l* is the length of the motionless surface between the particle on the surface and the down stream wall of the canal. It can be noted that the value of σd*l* is small compared to *l*dσ for the conditions considered, or:

$$d\gamma = l\frac{d\sigma}{dQ}dQ \tag{VII.7}$$

The area of the motionless surface A equals $b \cdot l$. Since b is constant, dA is:

$$dA = bdl \tag{VII.8}$$

so,

$$d\ln A = \frac{dA}{A} = \frac{bdl}{bl} = d\ln l \tag{VII.9}$$

The surface dilational modulus of the liquid surface now follows from equations (VII.7) and (VII.9):

$$E = \frac{d\gamma}{d\ln A} = \frac{ld\sigma}{d\ln l} \tag{VII.10}$$

The derivation of this equation was recently published by Prins et al. (1996).

References

- Bird, R.B., Steward, W.E. and Lightfoot, E.N., 1960. Transport Phenomena. John Wiley & Sons, Inc., Singapore.
- Prins, A., Jochems, A.M.P., Kalsbeek, H.K.A.I., Boerboom, F.J.G., Wijnen, M.E. and Williams, A., 1996. Skin Formation on Liquid Surfaces under Non-Equilibrium Conditions. Progr. Colloid Polym Sci, Steinkopf Verlag, 100, 321-327.
- Sissom, L.E. and Pitts, D.R., 1974. Elements of Transport Phenomena. McGraw-Hill, Inc., USA.

Summary

Instant food products are products which are prepared relatively quick and easy. An example of such a product is aerosol whipped cream. This product can be seen as an instant substitute for whipped fresh cream. Aerosol whipped cream is characterised by a high overrun (400-600 %). The firmness of the foam is relatively low because, unlike in whipped fresh cream, the gas bubbles are not surrounded by a fat globule network. Destabilisation of the product becomes visible within 15 minutes after foam formation. The aim of this study was to obtain more knowledge about the physics of the formation and stability of instant foams. Although the study focuses on aerosol whipped cream, the various phenomena that are discussed in this thesis are more broadly applicable.

Two methods were used to produce aerosol whipped cream. The first method is the aerosol can. Due to the high pressure in the can (5-10 bar), the propellant nitrous oxide, also known as laughing gas, is for the larger part dissolved in the cream. When the product leaves the can, gas will come out of solution because of the pressure decrease and a foam is formed. During spraying, the pressure inside the can also decreases, which affects the flow properties out of the can and thereby the foam properties.

The second method, the Aerosol Can Simulator (ACS), was developed as a standardised and controllable method for the production of instant foam. In this apparatus an adjustable flow of gas and cream are mixed in a static mixer where gas is dissolved in the cream. At the end of the ACS the flow is forced through a nozzle, similar to the nozzle used on the aerosol can. This results in a foam. With this continuous method of producing instant foam, the effects of different parameters on the foam properties can be studied.

Results obtained using the ACS generally confirmed the findings obtained with the aerosol can. An important conclusion is that the flow of foam through the nozzle is controlled by choking conditions; the velocity in the smallest opening of the nozzle (the holes) is limited to the speed of sound. The speed of sound in a liquid containing gas bubbles is much lower than the speed of sound in the gas or liquid phase separately. Because the velocity in the holes corresponds to the speed of sound in foam, the foam formation apparently occurs in the holes of the nozzle.

The flow through the nozzle of an aerosol can is hindered by the presence of relatively large bubbles. Large bubbles can be present in the aerosol can after shaking the can before use. In the ACS they are present when not all the gas is dissolved in the cream. When a bubble fills a hole in the nozzle cone for a large part, the flow will locally be dominated by gas flow phenomena, thereby disturbing

the homogeneous two-phase flow. This leads to a decrease in mass flow rate out of the can and to sputtering of the foam while leaving the nozzle. The effect was less pronounced in experiments performed with the ACS.

The geometry of the nozzle influences the flow properties of the foam. Extension of the nozzle tube results in an increase of frictional resistance against flow and eventually choking conditions in the holes of the nozzle can no longer be reached. By increasing the flow area of the holes in the nozzle, the mass flow rate is increased (aerosol can) and the pressure before the nozzle (ACS) decreased. However, the effect was measured to be less than expected. In the presence of more or larger holes the flow properties might be less favourable. Moreover, the nozzle with the larger flow area showed to be susceptible to the mechanical force applied for opening the nozzle, especially when being used in the ACS. This negatively affected the flow area during pressing the nozzle.

The solubility of the gas in the cream plays a central role in the process of foam formation. Nitrous oxide is more soluble in the fat phase than in the 'skim milk phase' of the cream. This is caused by the bond character of the interacting molecules of the gas and the liquid phases. The initial overrun of aerosol whipped cream is determined by the amount of N_2O dissolved in the cream. The amount of dissolved gas was varied by temperature-fat content combinations of the cream and by shaking the can. In a not shaken aerosol can there are no bubbles present in the cream and therefore the establishment of phase equilibrium between the gas dissolved in the cream and the gas present in the headspace of the can is impeded. Consequently, more gas will remain dissolved in the cream in the can during spraying. This was expressed in a higher initial overrun of the foam.

Experiments performed with the ACS stressed the importance of the mass of gas dissolved in the cream for the initial overrun. In order to obtain the desired overrun, it has to be assured that the necessary amount of gas is dissolved in the cream. It is not sufficient to simply add the required amount of gas to the cream. In addition, the pressure before the nozzle, and thus the mass flow rate through the nozzle, has to be high enough for the gas to dissolve.

The initial overrun can be negatively affected by mechanical forces in the nozzle. These forces increase with increasing pressure before the nozzle or increasing mass flow rate through the nozzle. The decrease in overrun becomes stronger at longer tube lengths of the nozzle. Mechanical forces might induce coalescence (merging) of bubbles in the foam. Coalescence is promoted when longer nozzle tubes are used. The resulting relatively large bubbles will not remain stable when flowing out the nozzle. This is probably the cause of 'blow by'.

For aerosol whipped cream produced with nitrous oxide there is a link between the overrun and firmness at overruns < 400 %. At higher volume fractions of gas the

foam will be polyhedral and maximal firmness is achieved. This firmness seems to correlate with the resistance of individual bubbles against deformation, following from the Laplace pressure difference over the surface of the bubbles. When nitrogen is added extra to the mixture of N_2O and cream in the ACS, a decrease in overrun results without affecting the firmness. It is speculated that in the presence of extra gas the larger shearing forces in the nozzle cause foam destruction near the nozzle walls without affecting the foam structure in the center of the flow.

Because of the high solubility of nitrous oxide in the cream, aerosol whipped cream is susceptible to disproportionation, the shrinkage of smaller bubbles due to gas transport to larger bubbles. This destabilisation process can be stopped when the bubble surfaces behave purely elastic and the surface dilational elasticity exceeds half the surface tension. Surface rheological properties of the cream measured in the ring trough (close to equilibrium) and in the canal technique (during continuous compression far from equilibrium) showed visco-elastic behaviour. However, the surface dilational modulus was larger than half the surface tension. This indicates that disproportionation may be slowed down.

In addition, disproportionation can be greatly retarded when the bubble surfaces are fully covered with particles. Cryo-SEM observations, however, indicated that the bubble surfaces are not completely covered with fat globules. Moreover, no sign of a network between the fat globules that can stabilise the bubbles was visible. Images of the bubble size distribution in time confirmed that the bubbles in aerosol whipped cream disproportionate.

The foam stability can also be affected by the process of coalescence. Coalescence can be induced by the presence of spreading particles. Under certain conditions in the falling film apparatus spreading of material, provided by fat globules, was visible at a film of aerosol whipping cream. The amount of fat globules in aerosol whipped cream is however so large that the distance between them in the foam films will be relatively small. In addition, a bubble has a limited surface area. Therefore, it is questionable whether the thinning of liquid films can proceed long enough for rupture to occur. Although some coalescence has been observed occasionally, it is expected that this process is not that important in the deterioration of aerosol whipped cream.

This study improved the insight into the physical parameters and mechanisms that determine the formation process of instant foam and its stability. With the obtained knowledge, it is possible to adjust and thereby optimise the initial foam properties. However, additional research is necessary to improve the stability of aerosol whipped cream.

Samenvatting

Instant levensmiddelen zijn producten die relatief snel en makkelijk kunnen worden bereid. Een voorbeeld van deze producten is spuitroom. Dit product kan worden gezien als instant substituut voor opgeklopte slagroom. Het schuim wordt gekarakteriseerd door een hoge opslag (400-600 %) en heeft een relatief lage stevigheid omdat de gasbellen, in tegenstelling tot in opgeklopte slagroom, niet omringd zijn door een vetbolletjesnetwerk. Bovendien destabiliseert het product al zichtbaar binnen 15 minuten na schuimvorming. Het doel van deze studie was het verkrijgen van meer kennis over de fysica van de vorming en stabiliteit van instant schuimen. Ondanks het feit dat de studie zich richt op spuitroom, zijn de diverse verschijnselen die in dit proefschrift worden besproken breder toepasbaar.

Er zijn twee methoden gebruikt om spuitroom te produceren. De eerste methode is de spuitbus. Door de hoge druk in de bus (5-10 bar), is het drijfgas distikstofmonoxide, ook bekend als lachgas, voor het grootste gedeelte opgelost in de room. Wanneer het product de bus verlaat, zal vanwege de drukverlaging gas uit oplossing komen en wordt een schuim gevormd. Tijdens het spuiten daalt de druk in de bus. Dit beïnvloedt het stromingsgedrag door de spuitmond (ventiel) en daarmee de kwaliteit van het schuim.

De tweede methode, de spuitbussimulator (ACS), is ontwikkeld als een gestandaardiseerde en gecontroleerde methode voor de productie van instant schuim. In dit apparaat worden een ingestelde gas- en roomstroom gemengd in een statische menger, waar het gas wordt opgelost in de room. Aan het uiteinde van de ACS wordt het mengsel door een spuitmond geforceerd, welke identiek is aan de spuitmond die op de spuitbus zit. Dit resulteert in een schuim. Op deze manier kan instant schuim continu worden geproduceerd en kunnen de effecten van bepaalde factoren op de producteigenschappen worden bestudeerd.

Resultaten verkregen met de ACS bevestigden over het algemeen de bevindingen verkregen met de spuitbus. Een belangrijke conclusie is dat de stroming van schuim door het ventiel gecontroleerd wordt door 'choking' condities; de snelheid in de kleinste opening van het ventiel (de gaatjes) is gelimiteerd tot de geluidssnelheid ter plekke. De geluidssnelheid in een vloeistof die gasbelletjes bevat is veel lager dan de geluidssnelheid in het gas of de vloeistof afzonderlijk. Aangezien de snelheid in de gaatjes overeenkomt met de geluidssnelheid in schuim vindt de vorming van schuim plaats in de gaatjes van het ventiel.

De stroming door de spuitmond van een spuitbus wordt verstoord door de aanwezigheid van relatief grote bellen. Deze grote bellen kunnen in de spuitbus aanwezig zijn door het schudden van de bus voor gebruik. In de ACS kunnen ze aanwezig zijn wanneer niet al het gas is opgelost. Wanneer een bel een gaatje in

de kegel van het ventiel voor een groot deel vult, zal de stroming lokaal worden bepaald door de gasfase. Hierdoor wordt de homogene twee-fasestroming verstoord. Dit resulteert in een afname van de massastroomsnelheid uit de bus en het spetteren van de room tijdens het verlaten van de spuitmond. Dit effect was minder zichtbaar in de experimenten uitgevoerd met de ACS.

De geometrie van het ventiel beïnvloedt de stromingseigenschappen van het schuim. Verlenging van het ventielpijpje heeft een toename van de wrijvingsweerstand tegen stroming tot gevolg, zodat uiteindelijk 'choking' condities niet meer kunnen worden bereikt. Door vergroting van het doorstroomoppervlak van de gaatjes in het ventiel stijgt de massastroomsnelheid door de spuitmond (spuitbus) en daalt de druk voor de spuitmond (ACS). Het gemeten effect is echter minder groot dan verwacht. Bij aanwezigheid van meer of grotere gaatjes zijn de stromingscondities mogelijk minder gunstig. Bovendien was de plastic ventielkegel met het grotere doorstroomoppervlak gevoelig voor de mechanische kracht die nodig was om het ventiel te openen, vooral tijdens toepassing in de ACS. Dit had een negatief effect op het doorstroomoppervlak wanneer er op het ventiel werd gedrukt.

De oplosbaarheid van het gas in de room speelt een centrale rol in het proces van instant schuimvorming. Lachgas is beter oplosbaar in de vetfase dan in de 'ondermelkfase' van de room. Dit komt door het bindingskarakter tussen de moleculen van de gas- en vloeistoffasen. De beginopslag van spuitroom wordt bepaald door de hoeveelheid N_2O die is opgelost in de room. De hoeveelheid opgelost gas is gevarieerd door temperatuur-vet combinaties van de room en door het al dan niet schudden van de bus. In een ongeschudde bus zijn geen bellen aanwezig in de room. Het instellen van het fase-evenwicht tussen het gas opgelost in de room en het gas aanwezig in de kopruimte van de bus verloopt daardoor traag. Er blijft meer gas opgelost in de room in de bus tijdens het spuiten. Dit komt tot uiting in een hogere beginopslag van het schuim.

Experimenten uitgevoerd met de ACS hebben het belang van de massa opgelost gas in de room voor de beginopslag benadrukt. Om de gewenste beginopslag te verkrijgen is het noodzakelijk dat de benodigde hoeveelheid gas is opgelost in de room. Het volstaat niet om eenvoudigweg de benodigde hoeveelheid gas aan de room toe te voegen. Daarnaast moet ook de druk voor de spuitmond, en daarmee de massastroomsnelheid door de spuitmond, voldoende hoog zijn om het gas te laten oplossen.

De beginopslag kan negatief worden beïnvloed door mechanische krachten in de spuitmond. Deze krachten zullen toenemen met toenemende druk voor de spuitmond of toenemende massastroomsnelheid door de spuitmond. De afname van de opslag wordt sterker bij langere ventielpijpjes. Mechanische krachten

veroorzaken mogelijk coalescentie, of samenvloeien, van bellen in het schuim. Het coalescentieproces wordt bevorderd door het gebruik van langere ventielpijpjes. De resulterende relatief grote bellen zullen niet stabiel blijven tijdens het stromen uit de spuitmond. Dit is waarschijnlijk de oorzaak van 'blow by'.

Voor spuitroom geproduceerd met lachgas bestaat er een verband tussen de opslag en stevigheid bij een opslag < 400 %. Bij hogere volumefracties gas zal het schuim polyedrisch zijn en is de maximale stevigheid bereikt. Deze stevigheid lijkt gecorreleerd te zijn met de weerstand tegen vervorming van individuele bellen, welke volgt uit het Laplacedrukverschil over het oppervlak van de bellen. Wanneer stikstof extra wordt toegevoegd aan het mengsel van N_2O en room in de ACS, daalt de opslag zonder dat de stevigheid wordt beïnvloed. Er wordt gespeculeerd dat in de aanwezigheid van extra gas, de grotere afschuifkrachten in de spuitmond het schuim afbreken aan de spuitmondwand zonder dat de schuimstructuur in het centrum van de stroom wordt aangetast.

Vanwege de goede oplosbaarheid van lachgas in room, is spuitroom gevoelig voor disproportionering, het krimpen van kleinere bellen als gevolg van gastransport naar grotere bellen. Dit destabilisatieproces kan worden gestopt wanneer de oppervlakken van de bellen zich zuiver elastisch gedragen en bovendien de oppervlaktedilatatiemodulus groter is dan de helft van de oppervlaktespanning. Oppervlaktereologische eigenschappen van de room gemeten in de ringtrog (dicht bij evenwicht) en met de kanaaltechniek (tijdens continue compressie ver van evenwicht) toonden visco-elastisch gedrag aan. De oppervlaktedilatatiemodulus was echter groter dan de helft van de oppervlaktespanning. Dit geeft aan dat disproportionering mogelijk kan worden vertraagd.

Disproportionering kan ook voor een groot deel worden vertraagd wanneer de beloppervlakken geheel bedekt zijn met deeltjes. Cryo-SEM opnames hebben laten zien dat de beloppervlakken niet geheel bedekt zijn met vetbolletjes. Er was bovendien geen netwerk tussen de vetbolletjes zichtbaar dat de bellen zou kunnen stabiliseren. Beelden van de bellengrootteverdeling in de tijd hebben bevestigd dat de bellen in spuitroom disproportioneren.

De schuimstabiliteit kan ook worden beïnvloed door coalescentie. Dit proces is kan worden geïnduceerd door spreidende deeltjes. Onder bepaalde omstandigheden bij bestudering van een vrij vallende roomfilm, was het spreiden van materiaal, afkomstig van vetbolletjes, aantoonbaar. De hoeveelheid vetbolletjes in spuitroom is echter zo groot dat de afstand tussen de vetbolletjes in de schuimfilmpjes relatief klein zal zijn. Bovendien heeft een bel een begrensd oppervlak. Het is daarom de vraag of het dunner worden van de vloeistoffilms lang genoeg kan doorgaan om filmbreuk te veroorzaken. Hoewel coalescentie sporadisch is waargenomen, wordt verwacht dat dit proces niet zo belangrijk is voor het schuimgedrag van spuitroom.

Deze studie heeft het inzicht verbeterd in de fysische parameters en mechanismen die het vormingsproces en de stabiliteit van instant schuim bepalen. Met de verkregen kennis is het mogelijk om de begineigenschappen van het schuim aan te passen en daarmee te optimaliseren. Echter, verder onderzoek is noodzakelijk om de schuimstabiliteit van spuitroom te verbeteren.

Nawoord

Bijna is het dan zover... Het proefschrift is geschreven, een datum is geprikt, receptie en feest zijn geregeld. Ik kan met plezier terugkijken op een leerzame periode van veel spuitroom spuiten, computeren, schrijven, doorzetten, ups en downs, maar vooral van erg veel gezelligheid. Kortom, een tijd die ik niet had willen missen. Dit dankzij vele anderen die hierbij hun steentje hebben bijgedragen.

Allereerst wil ik graag mijn promotor Albert Prins bedanken. Vele uren hebben we ons samen gebogen over de mysteries die bij het onderzoek naar boven kwamen. Zijn enthousiasme en optimisme voor het onderzoek en zijn uitdagende, stimulerende manier om mij te motiveren, hebben me laten zien hoe leuk onderzoek kan zijn. Door de samenwerking met co-promotor Hans Bos zijn we heel anders tegen het spuitproces aan gaan kijken. Zijn inbreng was onmisbaar voor het verloop van het onderzoek. Ik heb erg veel van onze samenwerking geleerd.

Stagiare Judith Kobessen (IAH-Larenstein) en doctoraalstudenten Jeroen Tahey en Angèle Jochems (LUW) hebben een belangrijke bijdrage geleverd aan het tackelen van het probleem van de spuitroom. Het was erg leuk om met jullie samen te werken. Bedankt voor jullie positieve inzet!

Het onderzoek is opgestart op initiatief van Zuivelcoöperatie Coberco UA. De samenwerking met hun heb ik als bijzonder prettig ervaren. Geert Verhoeven was altijd bereid me te helpen wanneer nodig (ook op computergebied...) en heeft ook vele nuttige suggesties voor het onderzoek gedaan. Daarnaast heeft hij het proefschrift grondig doorgenomen en van commentaar te voorzien. Vandaar dat hij welverdiend naast me op het podium mag staan. Ook de belangstelling van Cor van den Boogaard, Alie van Schouwenburg, Daniël Abts, Marleen Vanrusselt en Dominique Craninx tijdens de projectbesprekingen heb ik erg op prijs gesteld. Verder hebben vele andere medewerkers van Coberco hun steentje bijgedragen aan dit onderzoek door het maken van spuitroom, het vullen van bussen, het altijd beschikbaar stellen van middelen en informatie, het leveren van discussie en vooral het tonen van belangstelling.

De prettige samenwerking met de medewerkers van de werkplaats in het Biotechnion hebben het onderzoek zeer zeker bevorderd. Ik wil jullie allemaal hartstikke bedanken voor de vele creatieve uurtjes die jullie aan het project hebben besteed. Naast het bouwen van de spuitbussimulator (ACS), waar met name Andre Sanders heel wat tijd in heeft gestoken, stonden jullie ook altijd klaar om 'even snel' een apparaatje in elkaar te draaien. Daarnaast wil ik graag de medewerkers van de voormalige tekenkamer bedanken voor alle hulp, met name Mees Schimmel die de ACS op papier heeft gezet. Ook bedank ik de medewerkers van MediaService voor het maken van foto's en andere hulp.

Alle medewerkers van de sectie Zuivel en Levensmiddelennatuurkunde (tegenwoordig GLF geheten), bedankt voor jullie hulp, belangstelling en vooral voor het creëren van een goede werksfeer! Katja Grolle en Aliza de Groot hebben enthousiast, accuraat, vol overgave en vooral erg gezellig meegeholpen bij de uitvoering van vele spuitexperimentjes. Martin Bos heeft de moeite genomen het proefschrift te lezen en me van vele bruikbare tips voorzien. Cor van den Berg leverde nuttige discussie tijdens projectbijeenkomsten. Henk Jansen stond altijd klaar om computerproblemen op te lossen. Yvonne Smolders heeft vooral de laatste weken druk meegeholpen om dit proefschrift uit de printer te krijgen, van plaatjes te voorzien en door de kopieermachine te krijgen. Ik ben blij dat je paranimf wilt zijn.

Ook buiten mijn werkkring om hebben vele mensen me geholpen om dit onderzoek tot een goed einde te brengen. Allereerst wil ik mijn ouders bedanken voor hun stimulerende belangstelling. Lieve paps en mams, het voelt goed te weten dat jullie er altijd voor me zijn.

Andere familieleden en vrienden hebben, ieder op hun manier, geholpen dit proefschrift tot stand te brengen. Bedankt allemaal. Bert Groeneveld heeft heel wat uurtjes met me achter het beeldscherm gezeten om tot het uiteindelijke ontwerp van de omslag van dit proefschrift te komen. Je bijdrage mag gezien worden!

Tot slot, Mees, gelukkig weet je zelf wat het inhoudt om een promotieonderzoek tot een goed eind te willen brengen. Ik waardeer het dat ook jij mijn proefschrift kritisch hebt doorgelezen. Daarnaast wil ik je vooral bedanken voor je voortdurende steun, de vele bekers koffie en al je vrije tijd die je op velerlei manieren hebt besteed aan 'de spuitroom'. Door jou is het hele promotiegebeuren een stuk makkelijker verlopen!

Marlies

Curriculum Vitae

Maria Elisabeth (Marlies) Wijnen werd geboren op 12 mei 1967 in Groningen. In 1985 behaalde zij het Atheneum-B diploma aan het Stella Maris college te Meerssen. Daarna begon ze aan de studie Gezondheidswetenschappen aan de Rijksuniversiteit van Maastricht. Na het behalen van haar propedeutisch diploma aldaar begon ze in 1986 haar studie Levensmiddelentechnologie aan de Landbouwuniversisteit te Wageningen. Ze koos voor de afstudeervakken Wiskunde en Levensmiddelennatuurkunde. Aan het eind van haar studie liep ze stage bij Unilever Colworth House in Engeland. In maart 1992 slaagde ze met lof voor het doctoraalexamen.

Van april 1992 tot april 1996 was ze aangesteld als Assistent in Opleiding bij de sectie Zuivel en Levensmiddelennatuurkunde, die tegenwoordig Geïntegreerde Levensmiddelentechnologie en Fysica heet. In deze periode werd het in dit proefschrift beschreven onderzoek uitgevoerd.

Vanaf 30 september 1996 is ze werkzaam als onderzoeksleidster bij Coberco Research te Deventer, binnen de groep Levensmiddelennatuurkunde.